CHEMICAL INTERACTION OF NITRIC OXIDE AND HUMAN HEMOGLOBIN

by

Benjamin Peter Luchsinger

A dissertation submitted in partial fulfillment
of the requirements for the degree

of

Doctor of Philosophy

in

Chemistry

MONTANA STATE UNIVERSITY
Bozeman, Montana

April 2004

© COPYRIGHT

by

Benjamin Peter Luchsinger

2004

All Rights Reserved

APPROVAL

of a dissertation submitted by

Benjamin Peter Luchsinger

This (dissertation) has been read by each member of the thesis (dissertation) committee and has been found to be satisfactory regarding content, English usage, format, citations, bibliographic style, and consistency, and is ready for submission to the College of Graduate Studies.

David J. Singel

Approved for the Department of Chemistry and Biochemistry

Paul Grieco

Approved for the College of Graduate Studies

Bruce McLeod

STATEMENT OF PERMISSION TO USE

In presenting this dissertation in partial fulfillment of the requirements for a doctoral degree at Montana State University, I agree that the Library shall make it available to borrowers under rules of the Library. I further agree that copying of this dissertation is allowable only for scholarly purposes, consistent with "fair use" as prescribed in the U.S. Copyright Law. Requests for extensive copying or reproduction of this dissertation should be referred to Bell & Howell Information and Learning, 300 North Zeeb Road, Ann Arbor, Michigan 48106, to whom I have granted "the exclusive right to reproduce and distribute my dissertation in and from microform along with the non-exclusive right to reproduce and distribute my abstract in any format in whole or in part."

Benjamin Peter Luchsinger

April 19, 2004

ACKNOWLEDGMENTS

"If I have seen a little further it is by standing on the shoulders of Giants."-- Isaac Newton

I acknowledge the help of Dr. Joseph Boneventura for early training in tonometer methods and in working with hemoglobin during a brief visit to Duke University Medical School. Doing experiments with Andrew J. Gow, of the Stamler lab at Duke, while he visited MSU was very stimulating. Hemoglobin used in this work was a generous gift of Apex Biochemicals (North Carolina) and was received with the help of Tim McMahon of the Stamler laboratory. I acknowledge the valuable experience of mentoring undergraduates from MSU and visitors through the NSF REU program including Jason Roach, Eric Rich, Elizabeth Williams, Lisa Lee, and Jay Stringer.

I acknowledge Melanie Rogers, Doreen Brown, and many others, from the Dooley group, for helping me get started on my biochemistry skills. I acknowledge assistance in some EPR experiments and in programming, and in valuable discussion with members of the Singel group from Dr. Dwight Schwartz, Eric Walter, and Elizabeth Williams.

I acknowledge my mother, Mary, for her loving kindness throughout the years. I acknowledge Leslie Babich for without him I may not have graduated from college or attended graduate school. I thank him very much.

A very big thanks to Elizabeth M. Williams for helping me with the text of my dissertation.

I want to thank Jonathan S. Stamler for involving me in the study of SNO-hemoglobin. I particularly want to thank David J. Singel for being a great scientist and attempting to pass on this greatness. Also, for letting me take research in the directions I was most interested in.

TABLE OF CONTENTS

1. INTRODUCTION 1

SNO-HEMOGLOBIN 1
DELIMITATION OF THESIS WORK 12
REFERENCES 14

2. THE OXYHEMOGLOBIN REACTION OF NITRIC OXIDE 17

ABSTRACT 17
INTRODUCTION 17
METHODS 20
Reaction Product Analysis. 20
NO Treatment of Hb. 22
Titration of Normoxic Hb with NO. 22
Measurements of S-Nitroso-, Iron Nitrosyl-, and Met-Hb. 23
EPR Analysis 23
Measurement of Oxygen Saturation. 23
Extinction Coefficients. 24
Modeling of UV-Visible Difference Spectra. 24
RESULTS AND DISCUSSION 25
REFERENCES 36

3. ROUTES TO S-NITROSO-HEMOGLOBIN FORMATION WITH HEME REDOX AND PREFERENTIAL REACTIVITY IN THE β-SUBUNITS 39

ABSTRACT 39
INTRODUCTION 40
MATERIALS AND METHODS 41
RESULTS 44
Reductive Nitrosylation Kinetic Analysis. 51
Additional SNO-Hb Producing Reactions. 53
DISCUSSION 58
ADDENDUM 60
REFERENCES 63

4. NITRIC OXIDE MIGRATION FROM CYS(β-93) TO β-HEME-IRON(II)NO 67

INTRODUCTION 67
MATERIALS AND METHODS 68
EXPERIMENTS AND RESULTS 69
EPR characterization of SNO-hemoglobin 69
Thiol-to-heme-transfer 70
Heme-to-thiol transfer 74
REFERENCES 79

APPENDICES 80

APPENDIX A 81
NITRIC OXIDE IN THE HUMAN RESPIRATORY CYCLE 81
APPENDIX B 89
UV/VIS DECOMPOSITION IN MATHEMATICA® 89
APPENDIX C 94
TARGET FACTOR ANALYSIS IN MATHEMATICA® 94

LIST OF FIGURES

Figure Page

2.1 Production of iron nitrosylHb by addition of NO to variously oxygenated hemoglobin 26
2.2 Production of metHb by reaction of NO is disfavored with increasing oxygen saturation 27
2.3 NO addition under normoxic conditions..... 29
2.4 S-nitrosoHb and iron nitrosylHb formed under various physiological air-oxygenated conditions..... 32
3.1 Visible absorption spectra of species involved in the reductive nitrosylation reaction 43
3.2 NO-group mass balance in the reductive nitrosylation of human met-Hb with NO 46
3.3 EPR spectra of Fe(II)NO obtained by reductive nitrosylation of met-Hb with NO 48
3.4 Kinetics of reductive nitrosylation in a deoxygenated solution 52
3.5 Conversion of heme-Fe(II)NO centers to heme-Fe(III) and SNO-Hb 55
3.6 EPR spectra from Fe(II)NO and Fe(III) hemes obtained by exposure of hemoglobin to nitrite 57
3.7 X-band EPR spectra of nitrosylhemoglobin spectral components..... 61
4.1 X-band EPR spectrum S-nitroso-nitrosylhemoglobin, $(SNO)_2$-Hb$(NO)_4$. 70
4.2 UV/Vis and EPR spectra of SNO-oxyhemoglobin 71
4.3 Tabulation of hemoglobin composition during slow transfer of -NO from hemoglobin thiol to heme 72
4.4 EPR characterization of subunit preference of slow transfer of -NO from hemoglobin thiol to heme.. 73
4.5 EPR spectra of hemoglobin incubated with nitritie during cycles of oxygenation and deoxygenation..... 77

.

ABSTRACT

In the past decade an entirely new areas of biomedical science have emerged with the recognition of the critical roles played by nitric oxide (NO) in biology. The discoveries of the role of NO in the cardiovascular systems, where it participates in regulating the tone of blood vessels and the flow of blood, raised an intriguing biochemical problem about the chemical interaction of NO and hemoglobin in blood. Historically, investigation of the interaction of NO and hemoglobin have suggested the formation of heme-Fe(II)NO hemoglobin and nitrate. Neither of these products is considered to exhibit NO-related bioactivity, thus the reaction of NO with hemoglobin was thought to quench the bioactive potential of NO. In this thesis we explore the idea that these are not the only two fates of NO in its interaction with hemoglobin. Product formation following encounters of NO and hemoglobin under various conditions of oxygenation, oxidation, and NO/heme ratios are analyzed by UV/Vis optical spectroscopy, EPR (electron paramagnetic resonance) spectroscopy, and colorimetric chemical analyses. This battery of methods enables quantification of the hemoglobin species: heme-Fe(II)NO (with distribution over the hemoglobin subunits) heme-Fe(III)NO, oxyhemoglobin, methemoglobin, deoxyhemoglobin, S-nitrosohemoglobin (SNO-hemoglobin). We present results that establish a previously unsuspected favoring of protein nitrosylation at heme and thiol positions in the reaction of oxyhemoglobin with NO. We demonstrate coupling of heme reduction/oxidation activity with thiol reactivity. We provide evidence for transfer of the NO group from heme to thiol and *vice versa*. We demonstrate unprecedented subunit selectivity of interactions of NO with hemoglobin. Finally, we present results that highlight the nitrite reductase activity of hemoglobin whereby nitrite, which has a significant concentration in blood, is converted to bioavailable forms of NO. Overall, the *in vitro* chemistry reported here provides for a complete basis for rationalizing the *in vivo* biochemistry required for the hemoglobin/NO system to serve as regulator of blood flow.

CHEMICAL INTERACTION OF NITRIC OXIDE AND HUMAN HEMOGLOBIN

Benjamin Peter Luchsinger 2004

INTRODUCTION

SNO-Hemoglobin

Nitric oxide (NO) was named "Molecule of the Year" by *Science* magazine in 1992 (1). In 1998, NO research earned Robert F. Furchgott, Louis J. Ignarro, and Ferid Murad the Nobel Prize in Physiology and Medicine. Though NO is structurally simple, it possesses rich reaction chemistry. NO, a gas at room temperature, is rapidly diffusing in solution, can be a neutral metal ligand, and has one unpaired electron. Adding an electron to NO generates the nitroxyl anion (NO^-) while removing an electron creates the nitrosonium ion (NO^+). Reactions involving these formal, redox-related species allow NO to perform chemistry unique to this molecule (2). Only in the last decade has it begun to be understood that this chemistry is central to a variety of diverse biological processes.

For decades, NO was thought to exhibit only toxic effects on biological systems. Certainly, excessive exposure to NO can have cytotoxic effects, and NO involvement in pathophysiology of Huntington's, Parkinson's, arthritis, and diabetes has been shown (3). Since the late 1980's, however, essential physiological roles for NO have been demonstrated (4). For instance, endogenous NO performs essential tasks in both neurotransmission and the immune response of humans (5). One of the most intriguing roles of NO in the body is that exhibited in the cardiovascular system. The 1998 Nobel Prize recognized the discovery that the "endothelium-derived relaxing factor" (EDRF) that participates in the regulation of blood vessel tone is in fact NO (6). Through earlier

studies involving nitroglycerin, it had been known that NO could act as vasodilatory agent; NO is a product of the breakdown of nitroglycerin and other vasorelaxant drugs (7). Identification of EDRF as NO, however, was the first evidence that NO is an endogenously produced substance. The subsequent elucidation of the enzymatic production of NO from L-arginine by NO-synthase (8) consolidated the current understanding that NO is an endogenous mediator of vascular tone.

Even before the identity of EDRF was established, it was known that NO could tightly bind the heme iron of hemoglobin (9). Hemoglobin was demonstrated as a functional antagonist of EDRF (NO) (6, 10). The antagonistic behavior was exploited in studies that demonstrated NO to be EDRF (6). Accordingly, the notion of a fundamental biological activity of NO in the cardiovascular system is challenged by the fact that the circulation and other biological environments contain numerous potential reactants, such as hemoglobin, that can transform or quench NO biological activity (2). These reactions primarily involve NO adduct formation with metal ions and reaction with oxygen species (11) or oxidative activation to form nitrites including peroxynitrite (12, 13), and nitrates (14, 15). Therefore, a primary question is: How can NO exert biological activity in the cardiovascular system without being quenched by hemoglobin? This question has been addressed on three complementary levels. Liao and co-workers have championed the idea that owing to the flow of blood, the large red blood cells tend to remain centered in the vessels and avoid the walls where NO is produced (16). Lancaster has shown that the cellular packaging of the hemoglobin further inhibits its reaction with NO (17, 18). Finally, and arguably most important is that the chemistry of NO includes the formation of thionitrites, which not only maintain bioactivity, but are among the most potent

vasodilatory compounds known. More importantly, they are also, by far, the most prevalent bioactive NO compounds in the blood, entailing both low-molecular weight nitrosthiols derivatives of cysteine and glutathione, but also S-nitrosylated proteins, such as S-nitrosalbumin (19).

Stamler and co-workers in 1996, discovered that, among the blood proteins that sustain S-nitrosylation is hemoglobin. Specific cysteine residues of hemoglobin form S-nitrsosthiols both in *vivo* and *in vitro* (20). In tetrameric human Hemoglobin, with two α- and two β-subunits, S-nitrosylation occurs at a highly conserved cysteine residue – Cys-β93 – in human hemoglobin. S-nitrosylated hemoglobin, or SNO-hemoglobin, has further been characterized by mass-spectrometry (21) and x-ray crystallography (22). Therefore, these observations provide direct evidence for a previously unsuspected NO/Hemoglobin reaction channel, via S-nitrosylation, that is evidently competitive with the Fe(II)-NO and nitrate forming reactions, *in vivo*. This observation again raises the question of how and why this competition works.

S-nitrosylation of hemoglobin has been observed to be linked to the quaternary state of hemoglobin. The NO is buried in the ligated R-state of hemoglobin, but exposed and readily lost by transnitrosation in the T-state structure. Stamler *et al.* also demonstrated the existence and variable nature of nitrosylated hemoglobin *in vivo* (20, 23). Micromolar concentrations of nitrosylated hemoglobin – SNO-hemoglobin and hemoglobin-Fe(II)NO – were found in blood with different distributions between the two in arterial *versus* venous blood. During the arterial/venous transit the total number of NO groups on hemoglobin (SNO-hemoglobin and hemoglobin-Fe(II)NO) remains approximately constant under normal physiological conditions, but the relative amounts

of each species shifts in favor of SNO-hemoglobin in the arteries and heme-Fe(II)NO in the veins. The reversible nature of SNO formation and release in this reaction maintains availability of NO for vasorelaxant action and blood flow regulation (20, 24).

This connection between vasodilatory potential and hemoglobin oxygenation seemed to be tailored made to answer a long-standing problem in human physiology. In the microcirculation, blood flow is regulated by position-to-position variations in O_2 content which are coupled to local vasodilation and vasoconstriction. Decreases and increases in the O_2 content of blood are, thus, coupled to increases and decreases in blood flow and *vice versa*. These responses, also known as hypoxic vasodilation and hyperoxic vasoconstriction, respectively, provide a means by which blood flow is precisely matched with the oxygen needs of the tissues (25-28). This autoregulation of blood flow is known to be exerted through local modulation of arteriolar tone, thus implicating a role for NO bioactivity. Until now, the detailed biochemical mechanism through which graded changes in O_2 content evoke the vascular responses remains a major unanswered question in vascular physiology. Hemoglobin would appear to be an ideal O_2 sensor in this regulatory process as ambient oxygen tension is rapidly reflected in the oxygen-saturation of hemoglobin, and especially since it is the O_2 saturation of blood, rather than the ambient pO_2, that determines blood flow (26). The discovery of SNO-hemoglobin and its allosterically controlled NO-bioactivity activity provides an attractive solution to this problem.

Prevailing ideas about the chemistry of the hemoglobin interaction with NO, however, present a conceptual roadblock for understanding the manner in which this signal transduction occurs. To regulate oxygen dependent blood flow, hemoglobin in its

encounters with NO, must avoid generating the ostensible dead ends of nitrate and unrecoverable heme-Fe(II)NO (29). There must be physiologically accessible routes to SNO formation and release. What are the important factors: that govern the maintaining of bioactivity in encounters of NO with hemoglobin; that steer reactions away from dead-ends such as nitrate and re-activate putative dead-ends such as nitrosylated hemes; and that enable the formation of SNO-hemoglobin? This thesis work is directed toward answering these questions. The chemical mechanisms of SNO-hemoglobin formation, as well as the cycling/interplay of NO between Cys-β93 and heme-Fe(II) *in vivo* remain to be clarified. This thesis work primarily consists of elucidating possible reaction pathways for the production and interchange between heme-Fe(II)NO, Cys-β93-NO, and heme-Fe(III)NO forms of adult human hemoglobin (Hemoglobin A_o). First, the reaction of oxyhemoglobin with NO is investigated. It is demonstrated that this reaction involves more than a simple competition between nitrate and heme-nitrosyl forming reaction channels. Bioavailable NO is not wholly consumed but is conserved, in part, through the formation of SNO-hemoglobin. Second, reductive nitrosylation reactions are explored to demonstrate and illuminate chemical mechanisms the establish connectivity between redox of the heme and nitrosylation of thiol groups within the hemoglobin molecule. We demonstrate that heme and NO redox work together in a variety of reactions to produce SNO-hemoglobin. Finally, I investigate the role of nitrite in hemoglobin reactions and demonstrate the preference for both heme and S-nitrosylation reactions on the β-subunits of hemoglobin. Overall, I describe results that support the role of hemoglobin-nitrosyl complexes as reservoirs, transporters, and producers of NO in the circulation.

The experiments described in Chapter 2, address one of the puzzling issues in NO hemoglobin chemistry. Historically, it was accepted that reactions between NO and normoxy-hemoglobin (>99% oxyhemoglobin) yield a vasorelaxation-impotent product, nitrate. Upon exposure to oxyhemoglobin, NO was found to react with the oxygen ligand to produce nitrate and methemoglobin (hemoglobin-Fe(III)), an EPR-detectable species (30, 31). Early studies focused on NO chemistry with the majority hemoglobin species (oxyhemoglobin > 99%), not on the minority species (deoxyhemoglobin<1%). Eq. 1.3. The reaction rates - near NO diffusion rate - of oxyhemoglobin/NO (3.7×10^7 $M^{-1}sec^{-1}$) (31) and deoxyhemoglobin/NO (2.5×10^7 $M^{-1}sec^{-1}$) (31) are very similar, It is expected that when oxy- and deoxyhemoglobin are both present with NO their respective reactions will compete.

$$\text{heme-Fe(II)}O_2 + NO \rightarrow \text{heme-Fe(III)} + NO_3^- \qquad [1.1]$$

$$\text{heme-Fe(II)} + NO \rightarrow \text{heme- Fe(II)NO} \qquad [1.3]$$

However, the reaction conditions of these experiments were not representative of the physiological condition. Previous experiments investigated NO:oxyhemoglobin > 1, while we use significantly lower NO:oxyhemoglobin ratios (≈1:100 for EPR and ≈1:1000 for chemiluminescence measurements). By using NO/hemoglobin ratios that are more physiologically relevant, and by studying the systematic trends over the full range of oxyhemoglobin/deoxyhemoglobin ratios, we find clear deviations from this simple competition behavior. Most significantly, we find that reactions 1.1 and 1.3 cannot account for all of the products. Additional products are formed, including SNO-

hemoglobin that maintain the bioavailability of NO in the presence of hemoglobin. The use of EPR and chemiluminescence in this study enables us to directly probe minority species that cannot be quantified by UV/Vis spectroscopy. In addition, we demonstrate that the reaction of NO with oxyhemoglobin/deoxyhemoglobin generates both SNO-hemoglobin and nitrosylhemoglobin. Formation of SNO-hemoglobin and nitrosylhemoglobin represent reaction channels that maintain NO bioavailability in the presence of large concentrations of hemoglobin, characteristic of the physiological situation. The notion that hemoglobin acts as a sink for NO *in vivo* is abrogated by the results of these experiments. Significant aspects of this work have subsequently been challenged by one group (32), but when performed under conditions analogous to ours, and with special attention to maintaining physiological conditions, our results were confirmed by others (33, 34).

To further investigate redox-induced formation of S-nitrosylated hemoglobin, a study of the reductive nitrosylation of human methemoglobin, reported in Chapter 3 of this thesis, was performed. Methemoglobin, the oxidized form of hemoglobin, occurs naturally in human circulation and accounts for approximately 1-3% of the total heme concentration. The reaction between methemoglobin and NO is as follows:

$$\text{heme-Fe(III)} + \text{NO(aq)} \leftrightarrows \text{heme-Fe(III)NO} \leftrightarrows \text{heme-Fe(II)NO}^{+} \quad [1.3]$$

α-heme:

$$\text{heme-Fe(II)NO}^{+} + \text{OH}^{-}\text{(aq)} \rightarrow \text{heme-Fe(II)} + \text{H}^{+}\text{(aq)} + \text{NO}_2^{-}\text{(aq)} \quad [1.4]$$

β-heme:

$$\text{heme-Fe(II)NO}^{+} + \text{Cys-b93-S}^{-}\text{(aq)} \rightarrow \text{heme-Fe(II)} + \text{Cys-b93-NO} \qquad [1.5]$$

Due to the low physiological concentration of methemoglobin in the blood, reductive nitrosylation of methemoglobin is admittedly not the most appealing mechanism for the principle route of *in vivo* SNO-hemoglobin production. Nevertheless, investigation of this reaction allows insight into the role of redox reactions in the formation of SNO-hemoglobin. Changes in heme iron oxidation state induce SNO-hemoglobin formation, which preferentially occurs over the formation of nitrite when NO is limiting and gradually introduced. Moreover, EPR data confirm that heme nitrosation occurs preferentially at the β-subunit. In addition, the reverse reaction of Eq. 1.3 involving mild oxidation by potassium ferricyanide led to the formation of SNO-hemoglobin verifying the reversibility of hemoglobin S-nitrosylation reactions:

$$\text{heme-Fe(II)NO} + [\text{Fe(CN)}_6]^{3-}\text{(aq)} \rightarrow \text{heme-Fe(III)NO} + [\text{Fe(CN)}_6]^{4-}\text{(aq)} \qquad [1.6]$$

$$\text{heme-Fe(III)NO} \leftrightarrows \text{heme-Fe(II)NO}^{+} \qquad [1.7]$$

$$\text{heme-Fe(II)NO}^{+} + \text{(Cys-}\beta\text{93)-S}^{-}\text{(aq)} \rightarrow \text{heme-Fe(II)} + \text{(Cys-}\beta\text{93)-SNO} \qquad [1.8]$$

The oxidative agent, potassium ferricyanide, has a reduction potential within the biological range.

Finally, reactions of deoxyhemoglobin and nitrite lead to the formation of Fe(II)NO primarily on the β-subunits as evidenced by EPR. Upon subsequent reoxygenation of these reaction products, SNO-hemoglobin is formed. Taken together, the results from

reductive and oxidative experiments demonstrate coupling between redox reactions of the heme and reactivity of the Cys-β93 residues of human hemoglobin.

Each of the reaction pathways [1.3] – [1.8] supports the transfer of NO from heme to thiol. This allows for an economical production of NO. It can bind to heme, without wasteful loss, but as temporary storage. Oxidative processing selectively on the β-subunits enables reconstitution of NO bioactivity.

A similar question of economy applies to the release of NO-bioactivity from SNO-hemoglobin. The relative destabilization of the SNO moiety in the deoxyhemoglobin (T-state) versus oxyhemoglobin (R-state) enables the dispensing of potent NO bioactivity in response to ambient oxygen levels. It must be noted, however, that SNO-hemoglobin concentrations are ~1 μM (19) *in vivo*, while vessels in bioassay are fully relaxed at concentrations of ~10 nM (20). Thus less than ~ 1% of the NO should be dispensed, even in constricted, hypoxic vessels. Therefore, what is the fate of the rest of the NO?

As detailed in Chapter 3, formation of nitrite by formal nitrosation of water/hydroxide would not represent an unrecoverable loss of NO bioactivity within the RBC owing to the nitrite reductase activity of hemoglobin. It is also reasonable to assume that any hemolytic loss of NO would quickly be collected by the heme to form heme-Fe(II)NO.

In Chapter 4 of this thesis we report observations of the latter process, namely NO transfer from thiol to heme. After preparation of SNO-oxyhemoglobin (a preparation which inevitably incorporates a small portion of methemoglobin in the sample), we probed for thiol-to-heme migration by monitoring EPR of heme Fe(II)NO species and loss of SNO by Greiss and Saville assays.

$$(SNO)_2\text{-}Hb(O_2)_3[Fe(II)] + e^- \rightarrow (SNO)\text{-}Hb(O_2)_3\ [Fe(II)NO] \qquad [1.9]$$

$$(SNO)_2\text{-}Hb[(\alpha\text{-}Fe(II)O_2)_2(\beta\text{-}Fe(II)O_2)(\beta\text{-}Fe(II))] + e^- \rightarrow$$

$$(SNO)\text{-}Hb[(\alpha\text{-}Fe(II)O_2)_2(\beta\text{-}Fe(II)O_2)(\beta\text{-}Fe(II)NO)] \qquad [1.10]$$

These measurements demonstrate proportionate loss of NO from thiol and gain at the heme. Because of the high background methemoglobin levels it is difficult to determine if there is a proportionate increase in methemoglobin, which would account for the formal NO-group reduction.

In addition to the above reactions of aqueous NO and S-nitrosothiol species with hemoglobin, we explored the interaction of hemoglobin with the nitrite anion (NO_2^-). Nitrite is a product observed in reductive nitrosylation experiments. Furthermore, the concentration of nitrite in the erythrocyte is far greater than that of aqueous NO. Therefore, we investigate the deoxyhemoglobin/nitrite reaction as a possible reaction adduct for NO bioactivity.

Experiments in which nitrite was added to deoxyhemoglobin in anaerobic conditions suggest the formation of a heme-Fe(II)NO^+ species.

$$\text{heme-Fe(II)} + H^+(aq) + NO_2^-(aq) \rightarrow \text{heme-Fe(II)}NO^+ + OH^-(aq) \qquad [1.11]$$

The heme-Fe(II)NO^+ species is in resonance with a nitrosylated methemoglobin species as indicated in Equation 1.12:

$$\text{heme-Fe(II)}NO^+ \leftrightarrow \text{heme-Fe(III)NO} \qquad [1.12]$$

The NO in the heme-Fe(III)NO species can undergo additional chemistry to create three different products: nitrite, (Cys-β93)-SNO, and heme-Fe(II)NO through mechanisms discussed in Chapter 4. These three products serve to create and preserve NO bioactivity from nitrite. We report additional experiments involving cycles of oxygenation/deoxygenation that demonstrate subunit selectivity. Each result presented in this chapter points to a potential role for nitrite in regulation of vascular tone through hemoglobin ligation intermediates.

In summary, the results presented in this doctoral thesis abolish the previously accepted notion of hemoglobin as an NO sink. We demonstrate the formation of S-nitrosylated hemoglobin – a species that maintains bioavailability of NO. We show that even direct exposure of oxyhemoglobin to NO results in substantial formation of SNO hemoglobin. We present results from experiments involving oxyhemoglobin, deoxyhemoglobin, methemoglobin, and nitrosohemoglobin species with NO. The chemistry we report herein possesses several novel features: a) the redox coupling between the thiol and heme NO chemistry; b) unprecedented β-subunit selective chemistry; and c) novel intra-molecular NO-group transfer chemistry. As a whole, the chemistry of NO/hemoglobin reactions observed *in vitro* suggests a possible role of NO and hemoglobin in regulation of vascular tone *in vivo*.

Delimitation of Thesis Work

The work reported in this thesis represents my contribution to a broader, collaborative project involving members of the Singel group at Montana State University, Bozeman, MT 59717 and the Stamler group at Duke University Medical Center, Durham, NC 27710, USA.

Chapter 2 is a copy of a published article: Gow AJ, Luchsinger BP, Pawloski JR, Singel DJ, Stamler JS. The oxyhemoglobin reaction of nitric oxide. Proc Natl Acad Sci U S A. 1999 Aug 3;96(16):9027-32. The bulk of the work reported in chapter 2, specifically the UV-Vis and EPR spectroscopy quantification of methemoglobin and heme-Fe(II)NO reaction products as a function of O_{sat} from 0 to ~85% was done by the author at Montana State University. Reactions at very low NO levels and higher oxygen saturations were done at Duke University Medical Center in the laboratory of Dr. Jonathan S. Stamler by Dr. Andrew J. Gow. Red blood cell experiments were done at Duke University Medical Center in the laboratory of Dr. Jonathan S. Stamler by Dr. John R. Palowski.

Chapter 3 is a copy with some elaboration of experimental methods of the publication: Luchsinger BP, Rich EN, Gow AJ, Williams EM, Stamler JS, Singel DJ. Routes to S-nitroso-hemoglobin formation with heme redox and preferential reactivity in the β-subunits. Proc Natl Acad Sci U S A. 2003 Jan 21;100(2):461-6. Some preliminary work for this article was conducted by Dr. Andrew J. Gow and Eric N. Rich at Duke University Medical Center. All of the measurements reported in detail were performed at Montana State University by the author with assistance from Eric N. Rich and Elizabeth

M. Williams. SNO measurements after nitrite incubation were performed at Duke University Medical Center.

All of the work summarized in Chapter 4 was performed at Montana State University by the author. Some of these spectra were introduced into the publication that forms an appendix to this thesis: McMahon TJ, Moon RE, Luchsinger BP, Carraway MS, Stone AE, Stolp BW, Gow AJ, Pawloski JR, Watke P, Singel DJ, Piantadosi CA, Stamler JS. Nitric oxide in the human respiratory cycle. Nat Med. 2002 Jul;8(7):711-7.

References

1. Culotta E, Koshland DE Jr. NO news is good news. (1992) Science. 258, 1862-1865.

2. Stamler JS, Singel DJ, Loscalzo J. Biochemistry of nitric oxide and its redox-activated forms. (1992) Science. 258, 1898-1902.

3. Wink DA, Hanbauer I, Grisham MB, Laval F, Nims RW, Laval J, Cook J, Pacelli R, Liebmann J, Krishna M, Ford PC, Mitchell JB. Chemical biology of nitric oxide: regulation and protective and toxic mechanisms. (1996) Curr Top Cell Regul. 34, 159-87.

4. Wink DA, Miranda KM, Katori T, Mancardi D, Thomas DD, Ridnour L, Espey MG, Feelisch M, Colton CA, Fukuto JM, Pagliaro P, Kass DA, Paolocci N. Orthogonal properties of the redox siblings nitroxyl and nitric oxide in the cardiovascular system: a novel redox paradigm. (2003) Am J Physiol Heart Circ Physiol. 285, H2264-H2276.

5. Jacintho JD, Kovacic P. Neurotransmission and neurotoxicity by nitric oxide, catecholamines, and glutamate: unifying themes of reactive oxygen species and electron transfer. (2003) Curr Med Chem. 10(24), 2693-2703.

6. Ignarro, LJ, Buga GM, Wood KS, Byrns RE, Chaudhuri G. Endothelium-derived relaxing factor produced and released from artery and vein is nitric oxide. (1987) Proc Natl Acad Sci U S A. 84, 9265-9269.

7. Murad F, Mittal CK, Arnold WP, Katsuki S, Kimura H. Guanylate cyclase: activation by azide, nitro compounds, nitric oxide, and hydroxyl radical and inhibition by hemoglobin and myoglobin. (1978) Adv Cyclic Nucleotide Res. 9, 145-158.

8. Stuehr DJ. Structure-function aspects in the nitric oxide synthases. (1997) Annu Rev Pharmacol Toxicol. 37, 339-359.

9. Antonini E, Brunori M. (1971) in Hemoglobin and Myoglobin in Their Reactions with Ligands, eds. Neuberger A & Tatum EL. (North-Holland, Amsterdam)

10. Palmer RM, Ferrige AG, Moncada S. Nitric oxide release accounts for the biological activity of endothelium-derived relaxing factor. (1987) Nature. 327, 524-526.

11. Saran M, Bors W. Pulse radiolysis for investigation of nitric oxide-related reactions. (1994) Meth Enzymol. 223, 21-35.

12. Beckman JS, Beckman TW, Chen J, Marshall PA, Freeman BA. Apparent hydroxyl radical production by peroxynitrite: implications for endothelial injury from nitric oxide and superoxide. (1990) Proc Natl Acad Sci U S A. 87, 1620-1624.

13. Crow JP, Beckman JS. The role of peroxynitrite in nitric oxide-mediated toxicity. (1995) Curr Top Microbiol Immunol. 196, 57-73.

14. Gaston B. Nitric oxide and thiol groups. (1999) Biochim Biophys Acta. 1411, 323-333.

15. Beckman JS, Carson M, Smith CD, Koppenol WH. ALS, SOD and peroxynitrite [letter]. (1993) Nature. 364, 584.

16. Liao JC, Hein TW, Vaughn MW, Huang KT, Kuo L. Intravascular flow decreases erythrocyte consumption of nitric oxide. (1999) Proc Natl Acad Sci U S A. 96, 8757-8761.

17. Liu X, Samouilov A, Lancaster JR Jr, Zweier JL. Nitric oxide uptake by erythrocytes is primarily limited by extracellular diffusion not membrane resistance. (2002) J Biol Chem. 277, 26194-26199.

18. Liao JC, Hein TW, Vaughn MW, Huang KT, Kuo L. Intravascular flow decreases erythrocyte consumption of nitric oxide. (1999) Proc Natl Acad Sci U S A. 96, 8757-8761.

19. Foster MW, McMahon TJ, Stamler JS. S-nitrosylation in health and disease. (2003) Trends Mol Med. **9**, 160-168.

20. Jia L, Bonaventura C, Bonaventura J, Stamler JS. S-nitrosohaemoglobin: dynamic activity of blood involved in vascular control. (1996) Nature. 380, 221-226.

21. Ferranti P, Malorni A, Mamone G, Sannolo N, Marino G. Characterisation of S-nitrosohaemoglobin by mass spectrometry. (1997) FEBS Lett. 400, 19-24.

22. Chan NL, Rogers PH, Arnone A. Crystal structure of the S-nitroso form of liganded human hemoglobin. (1998) Biochemistry. 37, 16459-16464.

23. McMahon TJ, Stamler JS. Concerted nitric oxide/oxygen delivery by hemoglobin. (1999) Meth Enzymol. 301, 99-114.

24. Stamler JS, Simon SI, Osborn JA, Mullins ME, Omar J, Thomas M, Singel DJ, Localzo J. (1992) Proc Natl Acad Sci U S A. 89, 444-448.

25. Guyton AC, Ross JM, Carrier O, Walker JR. Evidence for tissue oxygen demand as the major factor causing autoregulation. (1964) Circ Res. 14-15, Suppl. 1: 60-60 (1964).

26. Duling BR, Berne RM Longitudinal gradients in periarteriolar oxygen tension. (1970) Circ Res. 37, 325-322.

27. Gorczynski RJ, Duling BR. Role of oxygen in arteriolar functional vasodilation in hamster striated muscle. (1978) Am J Physiol. 235, H505-H515.

28. González-Alonso J, Richardson RS, Saltin B. Exercising skeletal muscle blood flow in humans responds to reduction in arterial oxyhaemoglobin, but not to altered free oxygen. (2001) J Physiol. 530, 331-341.

29. Yonetani T, Tsuneshige A, Zhou Y, Chen X. Electron paramagnetic resonance and oxygen binding studies of α-nitrosyl hemoglobin. (1998) J Biol Chem. 273, 20323-20333.

30. Doyle MP, Hoekstra JW. Oxidation of nitrogen oxides by bound dioxygen in hemoproteins. (1981) J Inorg Biochem. 14, 351-358.

31. Eich RF, Li T, Lemon DD, Doherty DH, Curry SR, Aitken JF, Mathews AJ, Johnson KA, Smith RD, Phillips GN Jr, Olson JS. Mechanism of NO-induced oxidation of myoglobin and hemoglobin. (1996) Biochemistry. 35, 6976-6983.

32. Liu X, Miller MJ, Joshi MS, Sadowska-Krowicka H, Clark DA, Lancaster JR Jr. Diffusion-limited reaction of free nitric oxide with erythrocytes. (1998) J Biol Chem. 273, 18709-18713; Joshi MS, Ferguson TB Jr, Han TH, Hyduke DR, Liao JC, Rassaf T, Bryan N, Feelisch M, Lancaster JR Jr. Nitric oxide is consumed, rather than conserved, by reaction with oxyhemoglobin under physiological conditions. (2002) Proc Natl Acad Sci U S A. 99, 10341-10346.

33. Herold S, Rock G. Reactions of deoxy-, oxy-, and methemoglobin with nitrogen monoxide. Mechanistic studies of the S-nitrosothiol formation under different mixing conditions. (2003) J Biol Chem. 278, 6623-6634.

34. Palmerini CA, Saccardi C, Arienti G, Palombari R. Formation of nitrosothiols from gaseous nitric oxide at pH 7.4. (2002) J Biochem Mol Toxicol. 16, 135-139.

35. Bunn HF, Forget BG. (1986) in Hemoglobin: Molecular, Genetic and Clinical Aspects, 1st ed., ed. Dyson J. (W. B. Saunders Company, Philadelphia, PA)

THE OXYHEMOGLOBIN REACTION OF NITRIC OXIDE

Abstract

The oxidation of nitric oxide (NO) to nitrate by oxyhemoglobin is a fundamental reaction that shapes our understanding of NO biology. This reaction is considered to be the major pathway for NO elimination from the body; it is the basis for a prevalent NO assay; it is a critical feature in the modeling of NO diffusion in the circulatory system; and it informs a variety of therapeutic applications, including NO inhalation therapy and blood substitute design. Here we show that, under physiological conditions, this reaction is of little significance. Instead, NO preferentially binds to the minor population of the hemoglobin's vacant hemes in a cooperative manner, nitrosylates hemoglobin thiols, or reacts with liberated superoxide in solution. In the red blood cell, superoxide dismutase eliminates superoxide, increasing the yield of S-nitrosohemoglobin and nitrosylated hemes. Hemoglobin thus serves to regulate the chemistry of NO and maintain it in a bioactive state. These results represent a reversal of the conventional view of hemoglobin in NO biology and motivate a reconsideration of fundamental issues in NO biochemistry and therapy.

Introduction

The chemistry of nitric oxide (NO) interactions with hemoglobin has served as a ubiquitous model within the field of NO biochemistry. For example, the oxidative interaction of NO with oxyhemoglobin (oxyHb) to produce nitrate is considered to be the major route of NO catabolism (1–3) as well as a reliable method for assaying NO (4);

likewise the unique ability of NO to induce displacement of a trans-imidazole heme ligand has been proposed as key to its activation of guanylyl cyclase (5). In the specific realm of the cardiovascular system, these reactions: are fundamental elements of models for NO diffusion (6, 7); played a crucial role in the identification of endothelium derived relaxing factor (6–9); and inform a variety of therapeutic applications, including NO-inhalation therapy (10, 11) and blood substitute design (12, 13).

Measurements of the rates of these reactions show that the NO-mediated oxidation of oxyHb to methemoglobin (metHb) is kinetically competitive with the binding of NO to unoccupied hemes in Hb—with specific rate constants of 3.7×10^7 M^{-1} sec^{-1} and 2.6×10^7 M^{-1} sec^{-1} respectively (14–16). The rates of NO oxidation of oxymyoglobin and NO binding to ferrous myoglobin are also very similar (3.4×10^7 M^{-1} sec^{-1} vs. 2.5×10^7 M^{-1} sec^{-1}) (16). Such a rapid route of NO metabolism is, however, difficult to reconcile with mammalian NO production rates (17), which are orders of magnitude too low to sustain physiological NO levels (10 nM – 1 μM) (7, 18–20), were NO to be freely consumed in these reactions.[1]

Previous studies of the NO oxyHb reaction, however, had been performed with NO concentrations 10-fold greater than protein (16). Under physiological conditions, the concentration ratio is starkly different, with NO concentrations 1,000-fold lower than Hb (20). Moreover, there is always a population of heme sites that are unoccupied. In highly oxygenated Hb, as found in arterial blood, this population is small (≈1%) but is

[1] The measured NO synthesis rate is 1.3 millimol per day for the average person (17). To maintain a basal NO concentration of 10 nm - 1 μM in vivo (6, 7, 18–20), 130 to 13,000 mol of NO would be consumed per day in reaction with Hb (assuming $k_{ox} = 3.7 \times 10^7$ M^{-1} sec^{-1} (14), 5 L vascular volume). The hypothetical NO consumption rate, therefore, is 10^5- to 10^7-fold greater than the actual production rate.

nevertheless in excess of NO. The influence of these vacant hemes, in the physiological situation, cannot be ignored; they might successfully compete for NO with the much larger fraction (≈99%) of oxygen-ligated hemes, if NO binding to hemes in oxyHb were cooperative, that is, if NO addition rates were to increase with increasing oxygen saturation. This possibility has not been raised in previous discussions of NO and Hb chemistry (1–7, 16, 21–24). On the contrary, the demonstrated lack of cooperativity in the binding of NO to deoxyhemoglobin (deoxyHb) (14)—which indicates that the intrinsic NO addition rate constants do not change with NO saturation—implicitly shapes the current perspective. It is important to recognize, however, that these results do not imply that the NO addition rates to oxygenated Hb are similarly independent of the oxygen saturation, and thus cannot be assumed to apply to the physiological situation. In addition to these oxidation and addition reactions, recent studies (20, 25, 26) make it clear that additional reactions, in particular S-nitrosylation, should be considered in any assessment of the chemical interplay of NO and human Hb. The S-nitrosylation reaction assumes particular importance inasmuch as it conserves, rather than consumes, NO bioactivity.

In this article, we discuss the reactions that occur on exposure of Hb to NO at relative concentrations that reflect the physiological situation. We show that the addition of NO to oxyHb takes advantage of the cooperative effects of oxygen binding and thus effectively competes with the oxidation reaction. We further find that at high oxygen saturations, reactions that S-nitrosylate the protein occur to a significant extent. Taken as a whole, these data indicate that the interaction of NO with oxyHb, rather than destroying NO bioactivity as widely misapprehended, acts to preserve it—that Hb very cleverly

introduces new chemistry, when oxygen saturation is high, that limits oxidation and channels the NO groups into products that preserve their bioactivity. This picture represents a substantial reversal of the conventional thinking on the chemistry of Hb as it pertains to NO biology and has fundamental implications for the general chemistry of heme containing proteins.

Methods

Reaction Product Analysis.

To investigate the reaction of NO with oxyHb, we begin by adopting the conventional viewpoint that: NO consumption involves a competition between the oxidation reaction (Eq. 1) and the adduct-forming addition reaction (Eq. 2); and that the specific rate constants for these reactions, namely k_{ox} and k_{add}, are independent of the degree of oxygen saturation (Y) of the hemes.

$$Fe(II)O_2 + NO \rightarrow Fe(III) + NO_3^- \quad [1]$$

$$Fe(II) + NO \rightarrow Fe(II)NO \quad [2]$$

These two assumptions define a perspective of the NO reaction that we refer to as the ‘‘simple competition model.’’ Our analysis of the reaction products, as described in this section, enables us to test the adequacy of this model for describing the chemistry and to recognize and interpret deviations from the behavior implied by it.

In our experiments, NO is introduced as a limiting reagent in an amount substantially smaller than the total amount of oxy- and deoxyhemes. On completion of the reaction, the following relation can be shown to exist among the products:

$$[Fe(II)NO]/[Fe(III)] = (k_{add}/k_{ox})([Fe(II)]_o/[Fe(II)O_2]_o) \quad [3]$$

in which $[Fe(II)]_o$ and $[Fe(II)O_2]_o$ are respectively the initial concentrations of deoxy- and oxyheme. The simple form of Eq. 3 takes advantage of the fact that, independent of Y, at least one of the reactions proceeds under pseudo-first order conditions, and that $k_{ox} \approx k_{add}$. The mass balance constraint $[Fe(II)NO] + [Fe(III)] = [NO]_o$ enables us to express the product concentrations relative to the initial concentration of NO, namely $[NO]_o$, as:

$$[Fe(II)NO]/[NO]_o = [1 - Y]/[1 - Y + \kappa Y] \quad [4]$$

in which κ is k_{ox}/k_{add}, and

$$[Fe(III)]/[NO]_o = 1 - [Fe(II)NO]/[NO]_o \quad [5]$$

Eqs. 4 and 5 provide the key relationships by which we test the simple competition model—specifically, Eq. 4 indicates that the fractional yield of nitrosylhemoglobin (nitrosylHb) as a function of Y assumes the form of an arc, ranging from 100% yield at Y = 0 to 0% yield at Y = 100%. The degree of curvature of the arc is determined by κ; it is a straight line for $\kappa = 1$, but is bowed to one or the other side of this diagonal line as κ is alternatively increased or decreased. For no value of κ does the curve cross the diagonal. It is also worth noting that the derivative of the curve is given by:

$$d([Fe(II)NO]/[NO]_o)/dY = -\kappa/[1 - Y + \kappa Y]^2 \quad [6]$$

hence as $Y \rightarrow 0$, the tangential slope is $-k_{ox}/k_{add}$, and as $Y \rightarrow 1$, it is $-k_{add}/k_{ox}$. These properties are useful for recognizing possible Y dependences of κ that are inconsistent with the simple model. Similarly, Eq. 5 provides a test for the presence of additional reactions, beyond oxidation (Eq. 1) and addition (Eq. 2): if additional reactions are significant, then [Fe(III)] and [Fe(II)NO] will not account for the total NO ($[NO]_o$) consumed in the reaction, whence $[Fe(III)]/[NO]_o + [Fe(II)NO]/[NO]_o < 1$.

NO Treatment of Hb.

HbA_0 was obtained from Apex Bioscience (Research Triangle Park, NC). Buffer exchange was achieved by dialysis. Deoxygenation was performed by gas exchange with argon in a tonometer. NO was added from a stock solution prepared under ultrapure helium and purified across alkali and cold traps. Stock solutions of NO were prepared in phosphate buffered saline containing 100 μM diethylene triamine pentaacetic acid (DTPA), pH 7.4. NO injections were made via a gas-tight Hamilton syringe with Teflon seal. The concentration of NO in stock solutions was assayed by electrode and by a Sievers 280 NO analyzer (Boulder, CO).

Titration of Normoxic Hb with NO.

Air-oxygenated Hb was titrated with 0.22 μM NO. Samples were analyzed immediately after NO addition by UV-visible spectrophotometry; time between additions varied from 3 to 5 min.

Measurements of S-Nitroso-, Iron Nitrosyl-, and Met-Hb.

Nitroso/nitrosyl derivatives of Hb were measured by using a photolysis-chemiluminescence technique [6-fold excess $HgCl_2$ over protein was added to displace S-nitrosothiol (SNO) (26)]. Samples were kept on ice for a period of 5 min to 2 hr before analyses. MetHb was monitored by UV-visible spectroscopy as the difference absorption above the linear baseline (600–700 nm), and by EPR (below).

EPR Analysis.

EPR spectroscopy was carried out with samples in 4-mm i.d. fused silica tubes, at 76° K, on a Varian E-9 spectrometer. UV-visible spectra were taken after NO addition. The sample was then placed in a deoxygenated EPR tube and plunged into liquid N_2. EPR spectra of nitrosylHb or dinitrosyl iron complexes (DNICs) were recorded in a single 4-min scan over 400 G on a Varian E-9 spectrometer operating at 9.274 GHz, with 10-mW microwave power, 10–20 G amplitude of field modulation at 100 kHz, and time constant of 0.250 sec. Spectra of high-spin metHb were recorded with a scan of 1,000 G, 20 G modulation amplitude, time constant of 0.128 sec, under otherwise identical conditions. NitrosylHb was measured by double integration of EPR spectra and by comparison to EPR spectra of $Hb(NO)_4$ standardized with UV-visible spectroscopy. The reproducibility of nitrosylHb measurements was estimated to be ±6% by repeated trials.

Measurement of Oxygen Saturation.

Oxygen saturation of Hb was verified by UV-visible spectroscopy by using a 1-mm anaerobic cuvette.

Extinction Coefficients.

The extinction coefficient spectra of metHb, deoxyHb, iron nitrosylHb, and oxyHb were generated from pure solutions of each species. HbA was diluted into PBS (pH 7.4) to a known final heme concentration [as calculated by the pyridine-hemochromagen method (23)]. MetHb was synthesized by adding excess $K_3Fe(CN)_6$. DeoxyHb was measured after the addition of dithionite, and nitrosyl- and oxyHb were measured after saturation with each ligand.

Modeling of UV-Visible Difference Spectra.

Difference spectra were obtained by subtracting the UV-visible spectrum of a given sample before the addition of NO from those after. The simple competition model discussed above predicts that such difference spectra could be approximated by a linear combination of two standard difference spectra: an oxyHb minus metHb spectrum, which gauges the progress of the NO oxidation reaction, and a deoxyHb minus iron nitrosylHb, which gauges the NO addition reaction; the sum of the combining coefficients is fixed by the mass balance ($[NO]_o$). Standard difference spectra were obtained from UV-visible spectra of authentic samples of metHb, oxyHb, nitrosylHb, and deoxyHb. We determined combining coefficients by a least squares fitting procedure. Inasmuch as the deoxy- and/ or oxyheme concentrations can decline during the competition, an additional component (deoxyHb minus oxyHb) could be expected.

Results and Discussion

EPR spectroscopy was used to assess the formation of nitrosyl heme on addition of NO to Hb preparations with oxygen saturations (Y) in the range 0–80% (typical EPR spectra are shown in Fig. 2.1A and B). EPR signal intensities were used to quantify the proportion of nitrosylated hemes relative to the NO initially added; the results of this quantification are plotted vs. Y in Fig. 2.1C (10 mM phosphate) and D (100 mM phosphate). The data obtained at high phosphate levels follow the behavior described by Eq. 4, the solid curves through the data points are graphs of Eq. 4 with κ values for the two depicted curves averaging 1.40 ± 0.06. The data obtained at the lower phosphate level, however, exhibit a notable deviation from the simple model: they cross the diagonal, thus showing a progressive overproduction of nitrosyl heme. Furthermore, the limiting tangential slopes indicate that κ is decreasing with increasing Y. By empirical curve fitting, we found that the data in Fig. 2.1 C are well described by a function of the form $(1 + Y)/(1 + cY)$ (c, a constant). (The solid lines in Fig. 2.1 C are graphs of this function with least-squares best values of the parameter c). This functional form can be assimilated to that of Eq. 4, provided κ is allowed to vary with Y [specifically, $\kappa = (c - 1)(1 - Y)/(1 + Y)$]. This result indicates that over the 0 to 80% range of oxygen saturation, κ decreases 7-fold and suggests, by extrapolation, a 100-fold decrease at 90% saturation. We attribute this variation in κ primarily to an increase in k_{add},, as k_{ox} does not vary by more than a factor of 2, as judged from the limiting slopes and the literature values for k_{ox} (Y = 100%) and k_{add} (Y = 0%).

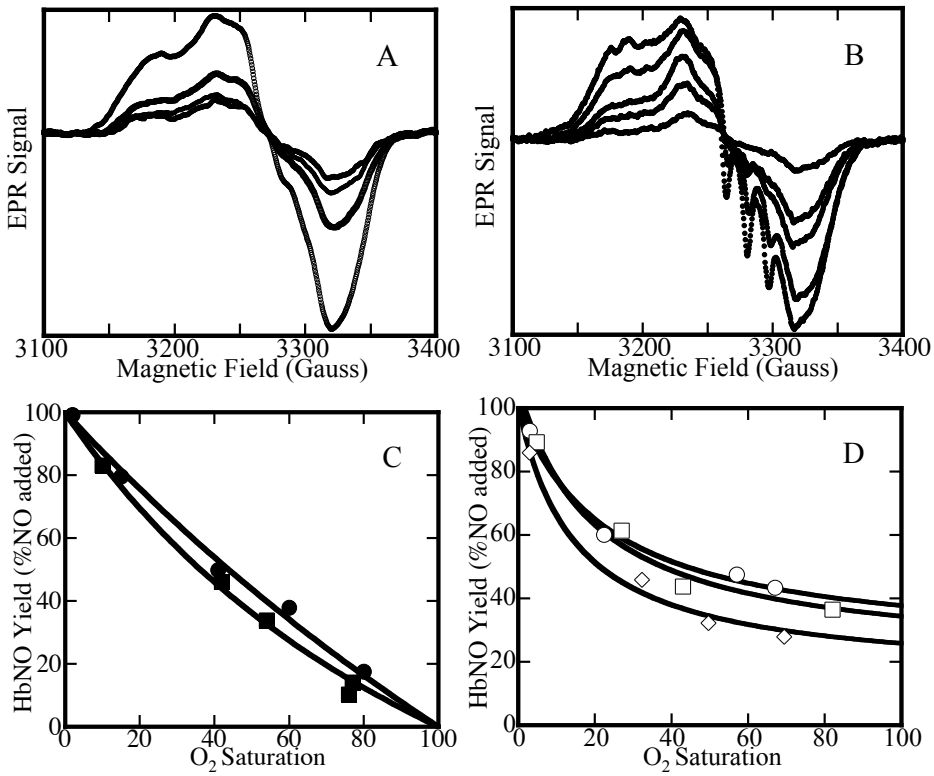


Figure 2.1 Production of iron nitrosylHb by addition of NO to variously oxygenated Hb. (A) EPR spectra of iron-nitrosyl Hb derivatives formed by incubation of 19 μM NO with 393 μM Hb at various degrees of oxygen saturation in 10 mM phosphate buffer, pH 7.4. The oxygen saturations for the largest through smallest EPR signals are 5.5, 32, 50, and 69%, respectively. Spectra show predominantly six coordinate α and β nitrosyl hemes, as typically observed for Hb in R state. (B) EPR spectra of iron-nitrosyl Hb derivatives formed by incubation of 55 μM NO with 380 μM Hb at various degrees of oxygen saturation in 100 mM phosphate, pH 7.4. The oxygen saturations for the largest through smallest EPR signals are 1, 15, 41, 60, and 80%, respectively. Spectra show a significant component of five coordinate a nitrosyl hemes (triplet structure) associated with Hb in T state. (C) Trials conducted with Hb in 10 mM phosphate, pH 7.4. The symbols are experimental results and the solid lines represent a best fit to the functional form for cooperative NO binding. Open diamonds, 393 μM Hb incubated with 19 μM NO; open circles, 350 μM Hb incubated with 15 μM NO plus 0.05% borate (added to bring the buffer concentration to 100 mM as in D); open squares, 365 μM Hb incubated with 15 μM NO and 1,190 units/ml SOD. (D) Trials conducted with Hb in 100 mM phosphate, pH 7.4. The symbols are experimental results, and the lines represent a best fit to the functional form for simple competition between oxidation and NO addition reactions (Eq. 4). Filled circles, 380 μM Hb incubated with 55 μM NO; filled squares, 375 μM Hb incubated with 7 μM NO. Application of the simple competition function to data of C or the cooperativity function to data of D gives an order of magnitude increase in x^2.

We also assessed the formation of oxidized ferric hemes with EPR (data not shown) and UV-visible difference spectroscopy (Fig. 2.2). The results obtained from samples in

100 mM phosphate conform to the simple competition model: the dashed lines in the figure, which are calculated from the curves depicted in Fig. 2.1D following Eq. 5, agree extremely well with the experimental measurements. Experiments conducted in 10 mM phosphate, however, show a stark deviation from the simple model behavior. Qualitatively, the results show that heme oxidation never grossly exceeds heme nitrosylation. Moreover, there is a progressive shortfall in the Fe(III) and Fe(II)NO products. This shortfall is indicated by the departure of the experimental points (10 mM phosphate) in Fig. 2.2, from the curves calculated from the curves depicted in Fig. 2.1D following Eq. 5, and amounts to as much as ~20% of added $[NO]_o$. This behavior strongly suggests the presence of additional NO reaction pathways.

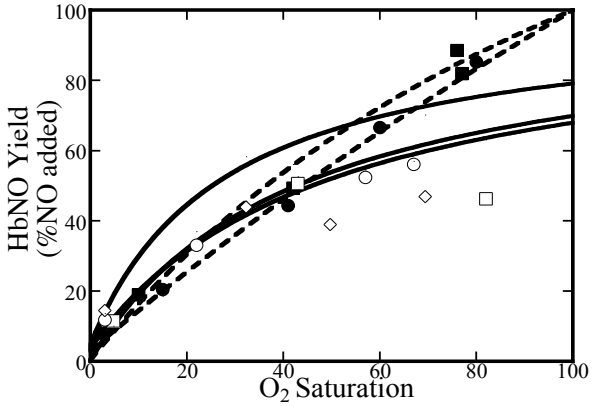


Figure 2.2 Production of metHb by reaction of NO is disfavored with increasing oxygen saturation. The samples used in Fig. 2.1 were assayed for metHb production by UV-visible difference spectroscopy. The data are normalized to added [NO]. As in Fig. 2.1, open diamonds, 10 mM phosphate; open circles, 10 mM phosphate plus borate; open squares, 10 mM phosphate plus SOD; filled circles and filled squares, 100 mM phosphate. The dotted (10 mM phosphate) and dashed (100 mM phosphate) lines are calculated by using Eq. 5 and Fe(II)NO yields in Fig. 2.1 C and D, respectively. Data show metHb to be disfavored in low phosphate, particularly at high oxygen saturation. Deviations of the data points below the curves suggest the presence of additional reactions for NO. Systematic deviations are most pronounced in low phosphate at high oxygen saturation-i.e., under physiological conditions.

In summary, we find that NO binding to oxyHb is cooperative; that oxidation to ferric heme (metHb) is limited under physiological conditions; and that additional chemistry is occurring in the more oxygenated Hb species that are prevalent *in vivo*. Our findings might seem at odds with previous literature suggesting that NO binding to Hb is noncooperative (14). The proper conclusion to draw from these prior studies, however, is that NO (ligand) binding to nitrosylHb shows little cooperativity with varying NO-saturation—a scenario of little physiological relevance, because NO is never the dominant ligand *in vivo*. Our results reflect the physiological situation in which the ligand, NO, binds to Hb with some degree of oxygen saturation. The functional behavior in this situation is, not surprisingly, cooperative. In this regard, experiments of particular interest are those conducted in the presence of high phosphate concentrations (100 mM), which perturb the allosteric modulation of ligand affinity by disfavoring the relaxed [R (oxy)] structure among the partially ligated hemoglobins, as evidenced by the hyperfine structure in the EPR (Fig. 2.2) (27). Thus, normal T (deoxy)/R (oxy) interconversion in Hb appears to be essential for ‘‘normal’’ NO function (Fig. 2.1 and 2.3). Taken together, the EPR results demonstrate that when the oxygen-induced allosteric transition is unhindered, NO binding to oxygenated Hb is cooperative—a situation that leads to enhanced iron nitrosyl- and limited metHb formation.

To extend these results to arterial oxygen saturation (of ≈99%) and physiological NO concentrations (≈1 μM), we used photolysis–chemiluminescence to measure nitrosyl derivatives of Hb (Fig. 2.3 A). In these experiments, normoxic Hb is in excess of NO, but NO is in excess of the vacant hemes, a scenario disfavoring NO addition. Our results show that even at high oxygen saturation, a substantial fraction of the NO— rather than

forming nitrate by the oxidation reaction—forms chemiluminescence-detectable nitrosyl derivatives. Of further interest, the yield of nitrosyl species increases with increasing [Hb] up to a maximum of approximately 50% of NO added (relative to the [Hb] the nitrosyl yield varies from 3 to 0.6%) (Fig. 2.3 A). In the simple competition model, the fraction of nitrosylation products would be independent of protein concentration. These results thus clearly demonstrate that additional reactions, beyond NO binding to vacant hemes to form the nitrosyl-heme derivative, are occurring under these conditions.

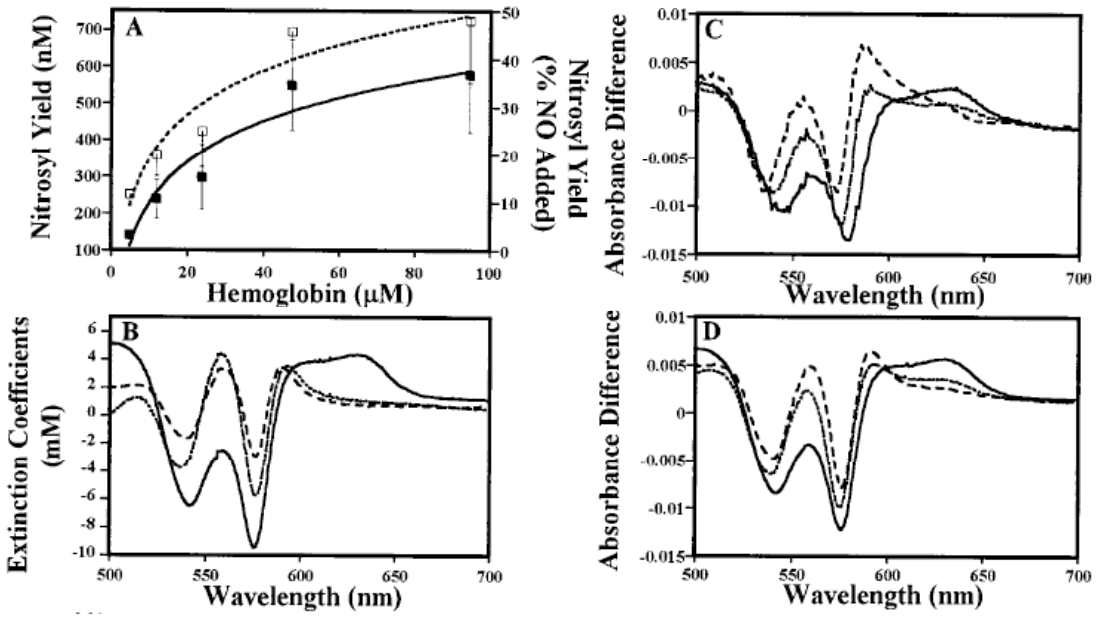


Figure 2.3. NO addition under normoxic conditions (≈99% O_2 saturation) produces nitrosylated Hb. (A) Nitrosyl content of oxyHb (10 mM phosphate/100 μM DTPA, pH 7.4) after exposure to 1.2 μM NO, as measured by photolysis-chemiluminescence (26). Nitrosyl yield increases as a function of Hb concentration (P , 0.05). Solid symbols, absolute yield of NO bound to Hb (FeNO plus SNO); open symbols, percentage of NO added. Data shown are the average of 7 to 19 experiments 6SE. (B) Standard difference spectra of metHb (solid line), deoxyHb (dotted line), and iron nitrosylHb (dashed line) vs. oxyHb (see Materials and Methods for conditions). (C) Difference spectra generated from the exposure of NO to normoxic (≈99% oxygen sat.) Hb. NO was added (in 10 aliquots totaling 2.2 μM) to 33 μM Hb in 100 mM phosphate (solid line) or 10 mM phosphate (dotted line) or 10 mM phosphate plus 0.05% borate (dashed line). Notably, the spectrum in 100 mM phosphate shows the formation of metHb (e.g., peak at 630 nm; see B for comparison); the spectrum in 10 mM phosphate shows formation of iron nitrosyl Hb and some metHb [e.g., peak at 595 nm (nitrosyl) and small peak at 630 nm

(met); see B for comparison]; and the spectrum in 10 mM phosphate plus borate shows predominantly iron nitrosylHb (e.g., peak at 595 nm; see B for comparison). (D) Calculated fits for difference spectra shown in C, demonstrating simple (noncooperative) competition between NO binding and oxidation reactions in high phosphate (solid line, 95% metHb) and cooperative binding in low phosphate (dotted line, 54% iron nitrosylHb; only 50% of the added NO accounted for) and low phosphate plus borate (dashed line; 85% iron nitrosylHb). Specifically, spectra in C were fitted, by a least-squares process, to either the simple competition model or the cooperativity model without a mass balance constraint.

To gain further insight into this chemistry, we used the discriminating power of difference absorption spectroscopy. Difference spectra obtained by titration of submicromolar concentrations of NO against 33 μM Hb in room air (99% O_2 saturation) are shown in Fig. 2.3 C; standard difference spectra of authentic met-, deoxy-, and nitrosylHb relative to oxyHb are shown in Fig. 2.3 B. If the chemistry were to proceed according to the simple model, then at Y = 99% the oxidation reaction would predominate and the observed difference spectra would closely resemble the metHb minus oxyHb standard difference spectrum. This behavior was observed only at high phosphate concentrations (Fig. 2.3 C and D), consistent with the EPR results above. At low phosphate concentrations, we found that the difference spectra point largely toward the formation of nitrosylated heme: much of the difference spectrum can be accounted for by the deoxyHb minus nitrosylHb standard spectrum (Fig. 2.3 C). To produce adequate difference-spectrum simulations, it was necessary to include a deoxyHb minus oxyHb component (presumably reflecting compensation for the nitrosylative loss of vacant hemes), and, most significantly, to relax the mass-balance constraint: a measurable fraction of $[NO]_o$ was not accounted in the Hb spectra (Fig. 2.3 C and D); the spectra account for only 50% in low phosphate and 80% in low phosphate plus borate. Taken as a whole, these data extend to normoxic conditions the conclusions made above, namely:

direct oxidation by NO is not the predominant reaction at low NO to heme ratios; addition of NO to vacant hemes remains competitive; and further reaction pathways, beyond oxidation and addition, must be occurring.

One additional species that could compete for NO is superoxide —liberated by the autooxidation of oxygenated Hb (28). To examine this possibility, we repeated the experiments detailed in Fig. 2.3 A in the presence of superoxide dismutase (SOD) (Fig. 2.4 A). At all concentrations of Hb used, the presence of SOD increased the yield of Hb nitrosyl derivatives (i.e., total NO bound) to approximately 100% of $[NO]_o$ (Fig. 2.4 A). Similarly, SOD led to increases in the yield of nitrosylated hemes detected in the EPR experiments (Fig. 2.1 C). Evidently, under these conditions, superoxide is a significant competitor for NO, or perhaps SOD alters the reactivity (oxidation and/or ligand binding) of Hb. Interestingly, when these experiments were performed with stroma-free Hb, a RBC preparation that contains normal levels of SOD, similar results were observed (Fig. 2.4 A). It is further notable that analogous effects on the nitrosyl yield—assessed by EPR, chemiluminescence, and difference spectroscopy—were obtained when borate was included in the buffer medium (Figs. 2.1 A, 2.2, and 2.3 C). Borate most likely exerts this effect by altering the ligand on-rate for NO or the reactivity of the oxygen ligand with NO, or perhaps the intrinsic autooxidation rate of Hb. Phosphate levels may also influence these parameters.

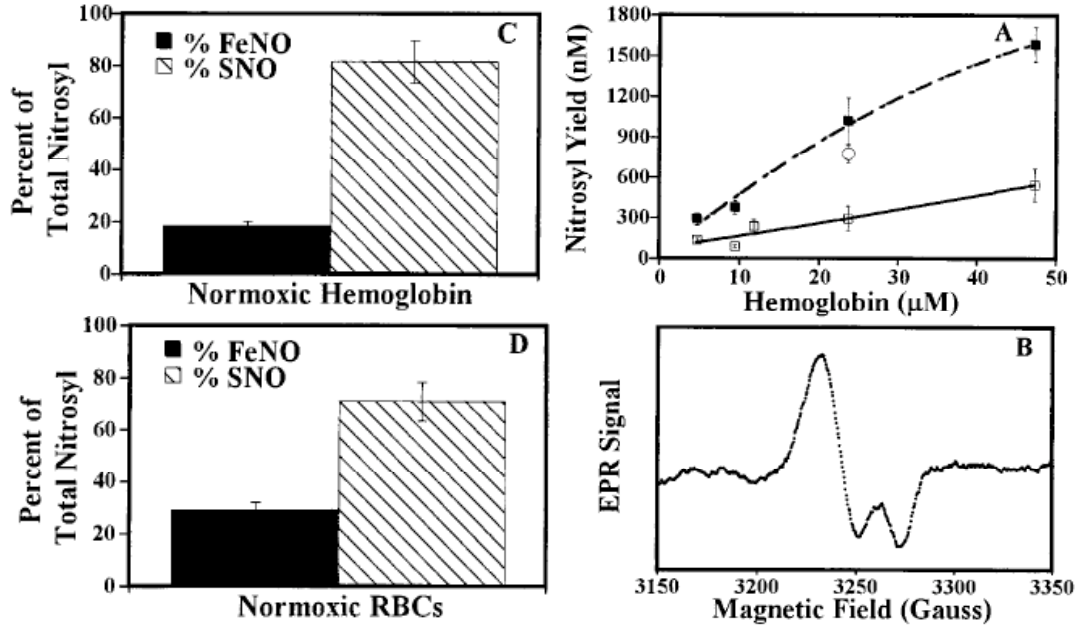


Figure 2.4. S-nitrosoHb and iron nitrosylHb formed under various physiological air-oxygenated conditions. (A) SOD increases the yield of NO bound to Hb. The experiments in Fig. 2.3 A were repeated in the absence (solid line; 1.2 μM NO) or presence (dashed line; 1.5 μM NO) of 1,190 units/ml of SOD, which enhances the yield of nitrosyl species to approximately 100% of the NO added. Similar nitrosyl yields were obtained by using stroma-free Hb (25 μM), which is enriched in endogenous SOD (open circle). Data shown are the average of five to nine experiments 6SE. (B) EPR spectrum of a DNIC formed by exposure of oxyHb (≈99% sat; 3.93 μM) to NO (36 μM). (C) S-nitrosoHb and iron nitrosylHb formed by exposure of oxyHb (≈99% sat., 48 μM) to NO (1.2 μM). SNO (hatched bar) and FeNO (solid bar) were measured by photolysis-chemiluminesence (26). Data shown are the average of 12 experiments 6SE. (D) Measurement of intraerythrocytic S-nitrosoHb and iron nitrosylHb formed by exposure of oxygenated RBCs (mean [Hb], 25 μM) to 1 μM NO. Isolation of Hb and measurements were as previously described (26). Data are the mean of 12 experiments 6SE.

An important clue to additional reaction pathways comes from our analyses under normoxic conditions: nitrosyl yields as high as 6% of Hb were observed by photolysis-chemiluminesence, notwithstanding the fact that the proportion of heme vacancies is only ≈1%. These nitrosyl species, moreover, did not affect the UV-visible spectra. EPR of samples under these conditions exhibit spectra similar to the DNICs exhaustively studied by Vanin (29), albeit they account for a small percentage of NO added (Fig. 2.4 B).

DNICs are known to form from SNOs with which they exist in equilibrium (29). Indeed, chemiluminesence analysis of the products formed on addition of 1.2 μM NO to 48 μM oxyHb, which produces nitrosyl yields of approximately 500 nM (Figs. 2.1 A and 2.3 A), show that ≈80% of this nitrosyl yield is SNO (Fig. 2.4 C). Moreover, treatment of aerated RBCs with physiological concentrations of NO (1 μM) resulted in relatively high yields of intracellular S-nitroso-oxyHb (Fig. 2.4 D). Specifically, analyses revealed (after inherent time delays of ≈30 min) yields of intracellular S-nitrosoHb, iron-nitrosylHb, and metHb of 103 ± 38 nM, 42 ± 15 nM, and 0 nM (i.e., none detectable), respectively (n = 12), and the further appearance of nitrosyl heme adducts on lowering of the oxygen tension, in general agreement with studies on isolated Hb (Figs. 2.1, 2.3 A, and 2.4 A and C).

Although the oxidation reaction (Eq. 1) has been given great significance in NO biology, our data demonstrate that it is likely to be of little significance under normal physiological conditions. Because of the low concentration of NO relative to Hb, vacant hemes are in excess over NO. This excess, together with the cooperativity of ligand binding in oxyHb, enables the addition of NO to heme to compete with the oxidation reaction even at high oxygen saturation. Moreover, in oxygenated Hb, additional reactive pathways that preserve NO bioactivity are available, including the production of SNO and DNIC. These results are in keeping with *in vivo* observations of Hb nitrosyl derivatives, the levels of which are generally unrelated to metHb concentration (27), directly responsive to NO administration (27), and dynamically controlled by allosteric state of Hb (26, 30) but otherwise unrelated to Hb oxygen saturation (26, 27, 30). These findings also help reconcile NO biochemistry with NO production rates in mammals

(17)—which are orders of magnitude too low to sustain physiological NO levels, were the oxyHb reaction dominant. In addition, they rationalize the ability of inhaled NO, which is purportedly inactivated by Hb in the lungs (10, 11, 31), to lower systemic blood pressure (11), increase aortic tissue cGMP levels (32), avert sickling of RBCs (33), improve blood flow to ischemic tissues (34), and increase glomerular filtration rate (35).

These discoveries have a strong bearing both on the way NO–heme interactions are modeled and on our understanding of NO biology. The current view of the NO interaction with Hb *in vivo* is derived from a model in which the elimination as NO_3^- is dominant and NO release from Hb is inconsequential (1, 3, 4, 6, 7, 15, 16, 36). In reality, Hb musters additional reaction pathways to keep the balance in favor of maintaining the NO group in a bioactive state. These chemical reactions with thiols, metals, and superoxide are the essential elements of the extended paradigm of NO biochemistry presented some years ago (37).

Our results have important implications for rational design of blood substitutes, NO scavengers, and therapeutic NO donors. Additionally, they predict that measurements of NO with the oxyHb assay will tend to underestimate NO production, unless appropriate precautions are taken, and more generally point to limitations of Hb-based approaches for identification of NO bioactivity. Finally, these findings raise fundamental questions. For example, nitrate remains the major metabolic product of NO *in vivo*, but the question now arises as to its source. It is tempting to suggest the involvement of a heme protein that can neither enforce the cooperativity of ligand binding, nor recruit the thiol reaction pathway. These properties are exemplified in the bacterial flavohemoglobin whose recently identified enzymatic function involves the oxidation of NO to nitrate (38, 39).

Whereas the primordial bacterial Hb is designed to metabolize NO (39), mammalian Hb is designed to secure and deliver it (20, 25, 26). These observations suggest that the molecular evolution of Hb was impacted by its NO-related functions.

References

1. Kelm, M. & Yoshida, K. (1996) in Metabolic Fate of Nitric Oxide and Related N-Oxides, eds. Feelisch, M. & Stamler, J. S. (Wiley, London) 1st Ed., pp. 47–58.

2. Pietraforte, D., Mallozzi, C., Scorza, G. & Minetti, M. (1995) Biochemistry 34, 7177–7185.

3. Wennmalm, A., Benthin, G. & Petersson, A. S. (1992) Br. J. Pharmacol. 106, 507–508.

4. Feelisch, M., Kubitzek, D. & Werringloer, J. (1996) in The Oxyhemoglobin Assay, eds. Feelisch, M. & Stamler, J. S. (Wiley, London) 1st Ed., pp. 455–478.

5. Traylor, T. G. & Sharma, V. S. (1992) Biochemistry 31, 2847–2849.

6. Liu, X., Miller, M. J., Joshi, M. S., Sadowska-Krowicka, H., Clark, D. A. & Lancaster, J. R., Jr. (1998) J. Biol. Chem. 273, 18709–18713.

7. Lancaster, J. R., Jr. (1994) Proc. Natl. Acad. Sci. USA 91, 8137–8141.

8. Palmer, R. M., Ferrige, A. G. & Moncada, S. (1987) Nature (London) 327, 524–526.

9. Ignarro, L. J., Buga, G. M., Wood, K. S., Byrns, R. E. & Chaudhuri, G. (1987) Proc. Natl. Acad. Sci. USA 84, 9265–9269.

10. Roissant, R., Falke, F. J., Lopez, F., Slama, K., Pison, U.&Zapol, W. M. (1993) New Engl. J. Med. 328, 399–405.

11. Wessel, D. L., Adatia, I., Giglia, T. M., Thompson, J. E. & Kulik, T. J. (1993) Circulation 88, 2128–2138.

12. Alayash, A. I. & Cashon, R. E. (1995) Mol. Med. Today 1, 122–127.

13. Doherty, D. H., Doyle, M. P., Curry, S. R., Vali, R. J., Fattor, T. J., Olson, J. S. & Lemon, D. D. (1998) Nat. Biotechnol. 16, 672–676.

14. Cassoly, R. & Gibson, Q. H. (1975) J. Mol. Biol. 91, 301–313.

15. Doyle, M. P. & Hoekstra, J. W. (1981) J. Inorg. Chem. 14, 351–358.

16. Eich, R. F., Li, T., Lemon, D. D., Doherty, D. H., Curry, S. R., Aitken, J. F., Mathews, A. J. X. J. K., Smith, R. D., Phillips, G. N., Jr. & Olson, J. S. (1996) Biochemistry 35, 6976–6983.

17. Castillo, L., Beaumier, L., Ajami, A. M. & Young, V. R. (1996) Proc. Natl. Acad. Sci. USA 93, 11460–11465.

18. Pinsky, D. J., Patton, S., Mesaros, S., Brovkovych, V., Kubaszewski, E., Grunfeld, S. & Malinski, T. (1997) Circ. Res. 81, 372–379.

19. Vallance, P., Patton, S., Bhagat, K., MacAllister, R., Radomski, Moncada, S. & Malinski, T. (1995) Lancet 346, 153–154.

20. Jia, L., Bonaventura, C., Bonaventura, J. & Stamler, J. S. (1996) Nature (London) 380, 221–226.

21. Marletta, M. A., Tayeh, M. A. & Hevel, J. M. (1990) Biofactors 2, 219–225.

22. Moore, E. G. & Gibson, Q. H. (1976) J. Biol. Chem. 251, 2788–2794.

23. Antonini, E. & Brunori, M. (1971) Frontiers in Biology, eds. Neuberger, A. & Tatum, E. L. (North-Holland, Amsterdam) 21, p. 13.

24. Sharma, V. S., Traylor, T. G., Gardiner, R. & Mizukami, H. (1987) Biochemistry 26, 3837–3843.

25. Gow, A. J. & Stamler, J. S. (1998) Nature (London) 391, 169–173.

26. Stamler, J. S., Jia, L., Eu, J. P., McMahon, T. J., Demchenko, I. T., Bonaventura, J., Gernert, K. & Piantadosi, C. A. (1997) Science 276, 2034–2037.

27. Takahashi, Y., Kobayashi, H., Tanaka, N., Sato, T., Takizawa, N. & Tomita, T. (1998) Am. J. Physiol. 274, H349–H357.

28. Misra, H. P.&Fridovich, I. (1972) J. Biol. Chem. 247, 6960–6962.

29. Vanin, A. F., Malenkova, I. V.&Serezhenkov, V. A. (1997) Nitric Oxide 1, 191–203.

30. Hall, D. M., Buettner, G. R., Mathes, R. D. & Gisolfi, C. V. (1994) J. Appl. Physiol. 77, 548–553.

31. Westfelt, U. N., Benthin, G., Lundin, S., Stenqvist, O. & Wennmalm, A. (1995) Br. J. Pharmacol. 114, 1621–1624.

32. Kermarrec, N., Zunic, P., Beloucif, S., Benessiano, J., Drouet, L. & Payen, D. (1998) Am. J. Respir. Crit. Care Med. 158, 833–839.

33. Head, C. A., Brugnara, C., Martinez-Ruiz, R., Kacmarek, R. M., Bridges, K. R., Kuter, D., Bloch, K. D. & Zapol, W. M. (1997) J. Clin. Invest. 100, 1193–1198.

34. Fox-Robichaud, A., Payne, D., Hasan, S. U., Ostrovsky, L., Fairhead, T., Reinhrdt, P. & Kubes, P. (1998) J. Clin. Invest. 101, 2497–2505.

35. Troncy, E., Francoeur, M., Salazkin, I., Yang, F., Charbonneau, Leclerc, G., Vinay, P. & Blaise, G. (1997) Br. J. Anaesth. 79, 631–640.

36. Sharma, V. S. & Ranney, H. M. (1978) J. Biol. Chem. 253, 6467–6472.

37. Stamler, J. S., Singel, D. J. & Loscalzo, J. (1992) Science 258, 1898–1902.

38. Gardner, P. R., Gardner, A. M., Martin, L. A. & Salzman, A. L. (1998) Proc. Natl. Acad. Sci. USA 95, 10378–10383.

39. Hausladen, A., Gow, A. J. & Stamler, J. S. (1998) Proc. Natl. Acad. Sci. USA 95, 14100–14105.

ROUTES TO S-NITROSO-HEMOGLOBIN FORMATION WITH HEME REDOX AND PREFERENTIAL REACTIVITY IN THE β-SUBUNITS

Abstract

Previous studies of the interactions of NO with human hemoglobin have implicated the predominance of reaction channels that alternatively eliminate NO by converting it to nitrate, or tightly complex it on the α-subunit ferrous hemes. Both channels could effectively quench NO bioactivity. More recent work has raised the idea that NO groups can efficiently transfer from the hemes to cysteine thiols within the β-subunit cys(β-93) to form bioactive nitrosothiols. The regulation of NO function, through its chemical position in the hemoglobin, is supported by response to oxygen and to redox agents that modulate the molecular and electronic structure of the protein. In this article, we focus on reactions in which Fe(III) hemes could provide the oxidative requirements of this NO-group transfer chemistry. We report a detailed investigation of the reductive nitrosylation of human met-Hb, in which we demonstrate the production of SNO-Hb through a heme-Fe(III)NO intermediate. The production of SNO-Hb is strongly favored (over nitrite) when NO is gradually introduced in limited total quantities; in this situation, moreover, heme nitrosylation, occurs primarily within the β-subunits of the hemoglobin tetramer. SNO-Hb can similarly be produced when Fe(II)NO hemes are subjected to mild oxidation. The reaction of deoxygenated hemoglobin with limited quantities of nitrite, leads to the production of β-subunit Fe(II)NO hemes, with SNO-Hb produced upon subsequent oxygenation. The common theme of these reactions is the effective coupling of heme-iron and NO redox chemistries. Collectively they establish a connectivity

between hemes and thiols in Hb, through which NO is readily dislodged from storage on the heme to form bioactive SNO-Hb.

Introduction

The transfer of NO-groups within human hemoglobin from hemes to cys(β-93) thiols to form a bioactive nitrosothiol represents a novel, intramolecular biochemistry that is both of fundamental interest, and has considerable implications for understanding the physiological effects of NO in the regulation of vascular tension and blood flow. A requirement of this transfer, common to biological S-nitrosylation (1), is the redox activation of the NO group (2). In this article, we report the results of experiments that probe the idea that heme-iron valence change can support the oxidative requirements of NO-group transfer, and thus efficiently lead to the production of SNO-Hb. As a model of the reaction between ferric hemes and NO, the reductive nitrosylation of human methemoglobin, is examined in detail. Product distribution assays reveal that SNO-Hb is formed as a nitrosation product, which, moreover, is substantially favored over NO_2^- when NO is gradually introduced as a limiting reagent; furthermore, in this situation, heme nitrosylation, occurs primarily within the β-subunits of the Hb tetramer. A kinetic analysis unambiguously reveals the intermediacy of heme-Fe(III)NO in this reaction. To extend our observations to reactions that could mimic this chemistry, but do not require an accumulation of the methemoglobin reactant, we additionally examined oxidation of Fe(II)NO in Hb as well as Hb reactions with nitrite. We report that SNO-Hb can similarly be produced when Fe(II)NO species are subjected to mild oxidation. Further we show that upon exposure to limited quantities of nitrite, oxy-Hb is unreactive, but deoxy-

Hb leads to the production of β-subunit Fe(II)NO hemes, with SNO-Hb produced upon subsequent oxygenation. These reactions, which have common characteristic of coupling of heme-iron valence change with NO chemistry, establish a connectivity between hemes and thiols in Hb, through which NO is readily dislodged from storage on the heme to form SNO-Hb, with selective processing in the β-subunits.

Materials and Methods

Solutions of human hemoglobin A_0 (Apex Bioscience, NC) were prepared in either 100 mM HEPES or PBS, pH 7.4, as described previously, (3). Reductive nitrosylation reactions were conducted by slowly delivering aliquots, via gas-tight Hamilton syringes, to the methemoglobin solution at $[NO]_o$/[heme] ratios varying nominally from 0.05 to 0.75 (where $[NO]_o$ is the initial concentration of the added NO). Solutions were mixed by vortexing immediately upon the addition. In some experiments a succession of additions was made, in the manner of a titration. The protein concentration was kept in excess of 75 μM in all experiments, to avoid substantial dissociation of Hb into dimers, and below 250 μM to maintain solution ideality. Reaction progress after each addition was monitored by UV/VIS spectroscopy. The spectra were analyzed by decomposition of the contributions from met-, Fe(II)NO-, and Fe(III)NO-Hb, by methods similar to those described by us previously (3), and elaborated below. At selected time points, samples of the reacting mixture were taken for further product analysis: samples were either frozen by immersion in liquid nitrogen for characterization by EPR spectroscopy (4-7) or directly analyzed for nitrite and for nitrosothiols by Greiss and Saville assays, following previously described methods (3). EPR spectra were recorded with a Varian E-109 X-

band spectrometer that has been modified by the addition of a field-control unit obtained through the University of Denver (8). Samples were immersed in liquid nitrogen during the EPR measurements. The reactant/product analyses made prior to the completion of the reaction were employed in the determination of the reaction kinetics. Gepasi (9) and Dynafit (10) software was used in the kinetic analysis.

Other reactions and product analyses were carried out by analogous methods. Reactions with nitrite were conducted by mixing oxyhemoglobin solutions (~ 4 mM in heme), with sodium nitrite at ~100:1 heme:nitrite ratios. The solutions were allowed to stand for minutes to hours, then deoxygenated by sparging with argon. Samples were withdrawn just before or just after deoxygenation for product characterization. $Hb(NO)_4$ oxidation was conducted in ~ 2 mM solutions with an excess of potassium ferricyanide; the formation of products was followed by UV/VIS spectroscopy. Samples were cleansed of low molecular weight species by centrifugation through a G-25 column, then analyzed for products.

The procedure for decomposition of UV/VIS spectra, described previously (3), was modified in the present study. We introduced, among the standards, the spectrum of authentic heme-Fe(III)NO Hb. To obtain this standard spectrum the kinetic data obtained in reductive nitrosylation experiments were subject to principal component analysis (11), as described in detail elsewhere (12). The reference Fe(III)NO spectrum obtained by this procedure is similar to the spectrum reported by Alayash *et al.* (13) that is largely $Hb[Fe(III)NO]_4$ (at pH 8) with apparent traces of unreacted met-hemes. The reference spectra utilized are exhibited in Fig. 3.1.

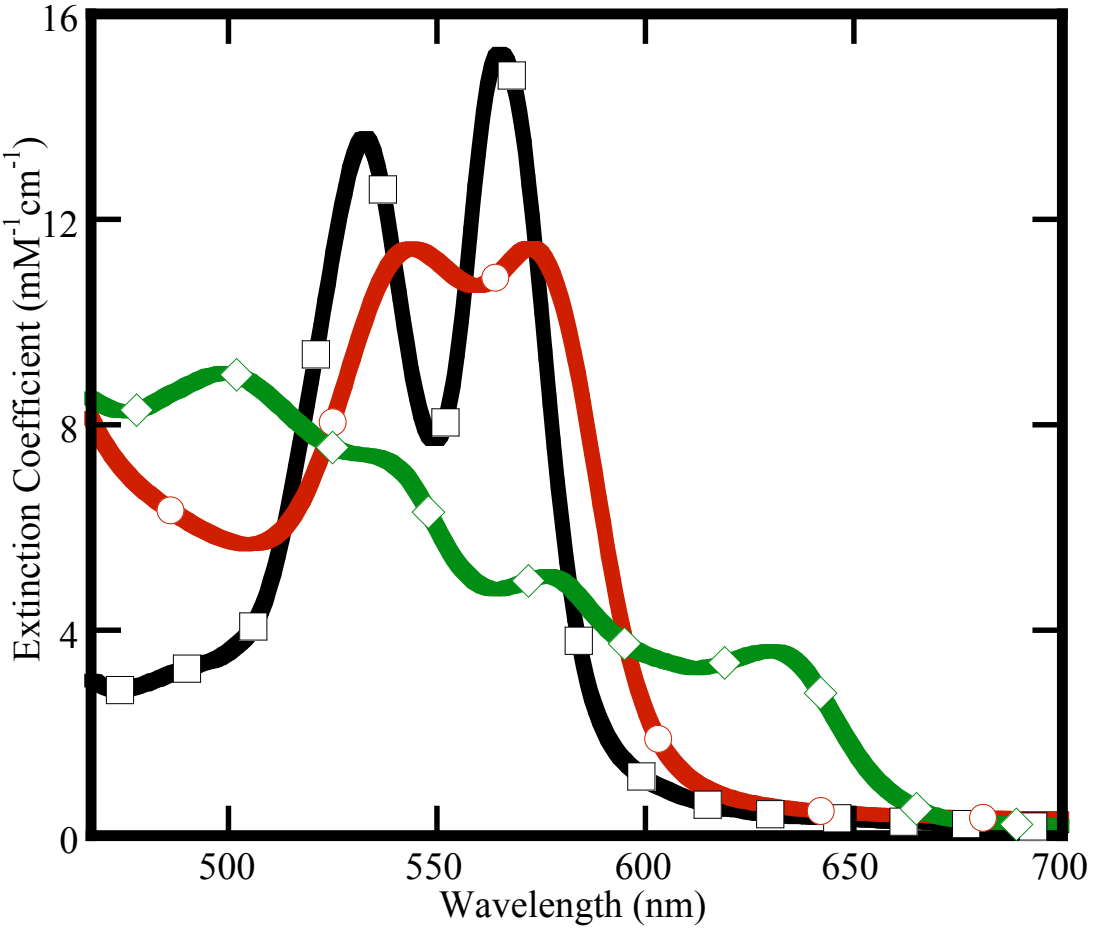


Figure 3.1 Visible absorption spectra of species involved in the reductive nitrosylation reaction. Standard spectra, pH 7.4, of met-Hb (◇), Fe(II)NO-Hb (○), and Fe(III)NO-Hb (□). The methemoglobin and Fe(II) nitrosyl hemoglobin spectra are from authentic standards; the Fe(III) nitrosyl hemoglobin spectrum was determined by using factor analysis techniques and scaled as described in the text.

To improve the performance of the least-squares fitting routine used in the spectral analysis, all reference and experimental spectra were numerically differentiated; the least-squares fitting was done using these derivative spectra. We also augmented the experimental and reference spectra to introduce constraints on the component concentrations. Application of constraints proved useful, for example, in proscribing non-physical, negative values for trace species.

EPR spectra of the samples generally included high and low spin methemoglobin components (14), as well as a feature assignable to Fe(II)NO. In conventional first-derivative EPR displays, the met-Hb signals have an effectively flat response in the region of the Fe(II)NO feature. The latter spectra were analyzed, using a decomposition procedure (analogous to that employed in the UV/VIS spectroscopy), involving two components - corresponding to NO occupying alternatively β-subunits or α-subunits (with six-fold coordination) (15-17). Hyperfine structure suggestive of penta-coordination of the α-subunit Fe(II)NO hemes (15) was not observed in any EPR spectra.

Results

Reductive Nitrosylation Product Analysis. Although the reductive nitrosylation of oxidized heme-proteins has been studied for over sixty years (18-24), the reaction of NO with methemoglobin remains only partially understood. In the case of simple monomeric heme-proteins, reductive nitrosylation has been most simply summarized by the equation:

a) heme-Fe(III) + NO(aq) ↔ heme-Fe(III)NO ↔ heme-Fe(II)NO^+;

b) heme-Fe(II)NO^+ + OH^-(aq) → heme-Fe(II) + H^+(aq) + NO_2^-(aq);

c) heme-Fe(II) + NO(aq) → heme-Fe(II)NO;

net) heme-Fe(III) + 2NO(aq) + OH^-(aq) → heme-Fe(II)NO + NO_2^-(aq) +H^+(aq); [1]

it has been appreciated, however, that the situation with tetrameric hemoglobins, composed of distinct α- and β-subunits, is more complex (24, 25). While subunit-inequivalence has been reported in the uptake of NO (13, 24, 25) such effects in the latter

steps of the reaction, and their impact on the nature of distribution of the final reaction products has not been previously investigated. Moreover this reaction has not been previously studied in situations where the NO is limiting, as in the biological situation.

By means of the Saville assays we determined that, in addition to the heme-Fe(II)NO and nitrite products of (Eq. 1), a nitrosothiol derivative of Hb is among the species produced upon exposure of methemoglobin to NO. Recent studies have clearly demonstrated that human Hb sustains S-nitrosylation at cys(β-93) of the β-subunit (26-29). Collectively, these results implicate the formation of SNO-hemoglobin in the reductive nitrosylation of met-Hb. To verify that these three products account for all of the introduced and reacted NO, we compared the sum of their detected concentrations versus $[NO]_o$, (with all concentrations considered on a per heme basis). These data are plotted in Fig. 3.2 (top). The linear variation with unit slope exhibited by the data demonstrate the material balance between the introduced NO and the Fe(II)NO, nitrite, plus nitrosothiol products.

The presence of a nitrosothiol product could be rationalized as reflecting a competition between the pathways involving formal NO^+ transfer to, alternatively, hydroxide (reaction b) or protein thiol(ate) species:

$$\text{heme-Fe(II)}NO^+ + RS^-(aq) \rightarrow \text{heme-Fe(II)} + RSNO; \qquad [2]$$

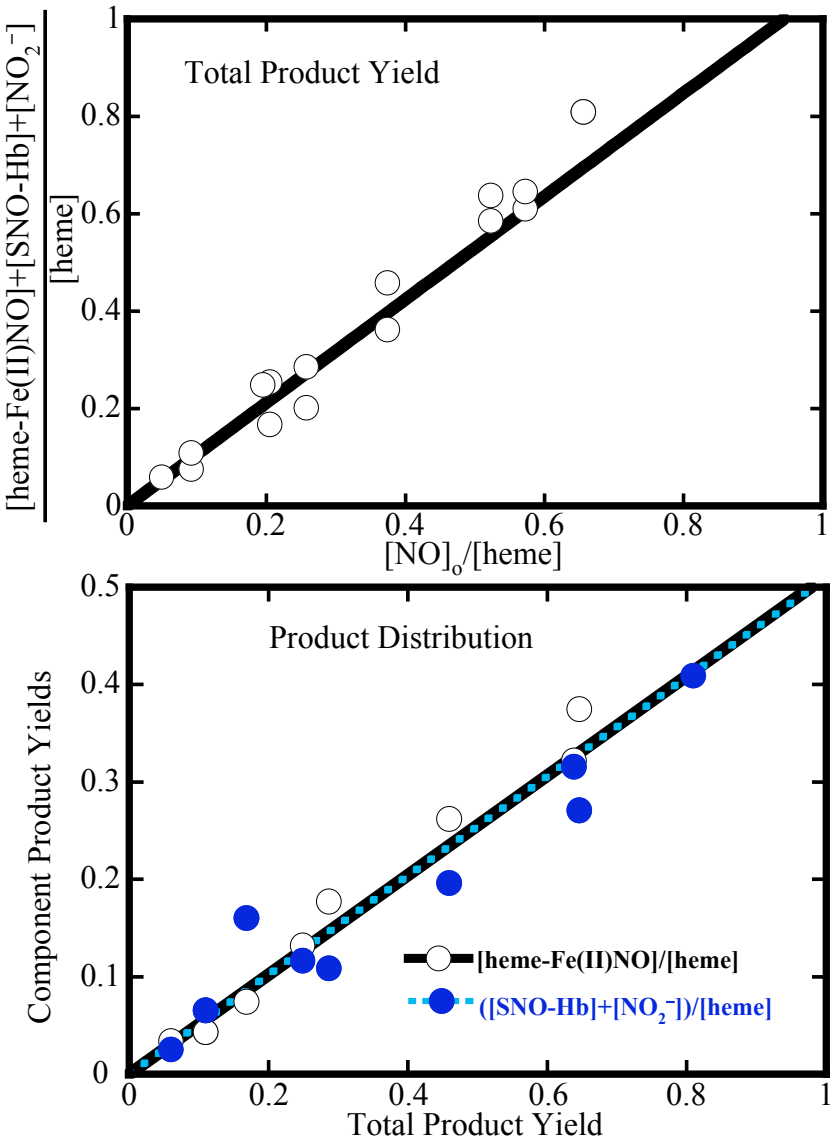


Figure 3.2 NO-group mass balance in the reductive nitrosylation of human met-Hb with NO. (top panel) The total amount of the reaction products – heme-Fe(II)NO, nitrite, and S-nitrosothiol is presented as a function of the amount of NO introduced. The symbols ○ correspond to experimental determinations; the solid line represents the best, linear fit to the experimental points (slope 1.06 ± 0.03; R=0.990). (bottom panel) Relative yields of ferrous heme nitrosyl products and the S-nitrosothiol plus nitrite products versus the total product yield. The symbols ○ correspond to experimental determinations of ferrous heme nitrosyl; the solid line represents the best, linear fit to these experimental points (slope 0.51±0.01; R=0.996). The symbols ● correspond to experimental determinations of S-nitrosothiol plus nitrite; the dashed line represents the best, linear fit to these experimental points (slope 0.51±0.02; R=0.992). Amounts are tabulated relative to the amount of heme present in the reaction medium. Product analysis was carried out as described in the text.

Either pathway would presumably lead to the concomitant production of an equivalent of heme-Fe(II), which is immediately converted to Fe(II)NO. To test this idea, we compared the total concentration of the products to: a) the heme-Fe(II)NO concentration; and b) the sum of the nitrite and nitrosothiol concentrations, as shown in Fig. 3.2 (bottom). The correlations are essentially identical, and demonstrate that protein nitrosothiol and nitrite are produced, in toto, on an equimolar basis with the nitrosyl ferrous-heme: Fe(II)NO and nitrite plus nitrosothiol each account for half of the reacted NO.

The factors that determine the distribution of products between nitrite versus protein nitrosothiol remain to be more fully elucidated. We have observed that at low $[NO]_o$/[heme] ratios (less than ~0.1), protein nitrosothiol and ferrous nitrosyl heme account for essentially all of the products. The preference for nitrosothiol is to be a sharply decreasing function of the $[NO]_o$/[heme] ratios: at ratios as small as 2, nitrite and protein nitrosothiol are produced in essentially equal amounts. Further analysis of the Fe(II)NO products by EPR spectroscopy reveal a striking and previously unrecognized preference for nitrosylation of β-subunit hemes, as evidenced in the spectra shown in Fig. 3.3. We observed β- vs. α-subunit preferences ranging from ~7:1 to ~3:1 at $[NO]_o$/[heme] ratios varying from 0.05 to 0.75; while at $[NO]_o$/[heme] ratios ≥ 2, the $(\text{heme-Fe(II)NO})_4$ protein is obtained. The spectrum of this product, which of course exhibits no subunit preference, is also shown in Fig. 3.3. The fundamental trends in nitrite vs. protein nitrosothiol and β- vs. α-subunit preference are similar: strong

preferences are exhibited only at low $[NO]_o$/[heme] ratios; at ratios > ~0.75 the relevant product ratios approach unity.

As a check on the possibility that the product distributions are influenced by "bolus" effects (30) associated with the addition of NO solutions, we conducted a series of experiments in which NO was derived from the decomposition of limited amounts of the nonoate DEA/NO (31), which was pre-mixed into the Hb solution. In these experiments, reported in detail elsewhere (32), we also find a highly consistent preference for S-nitrosylation over nitrite formation, and a β-subunit preference of the Fe(II)NO product.

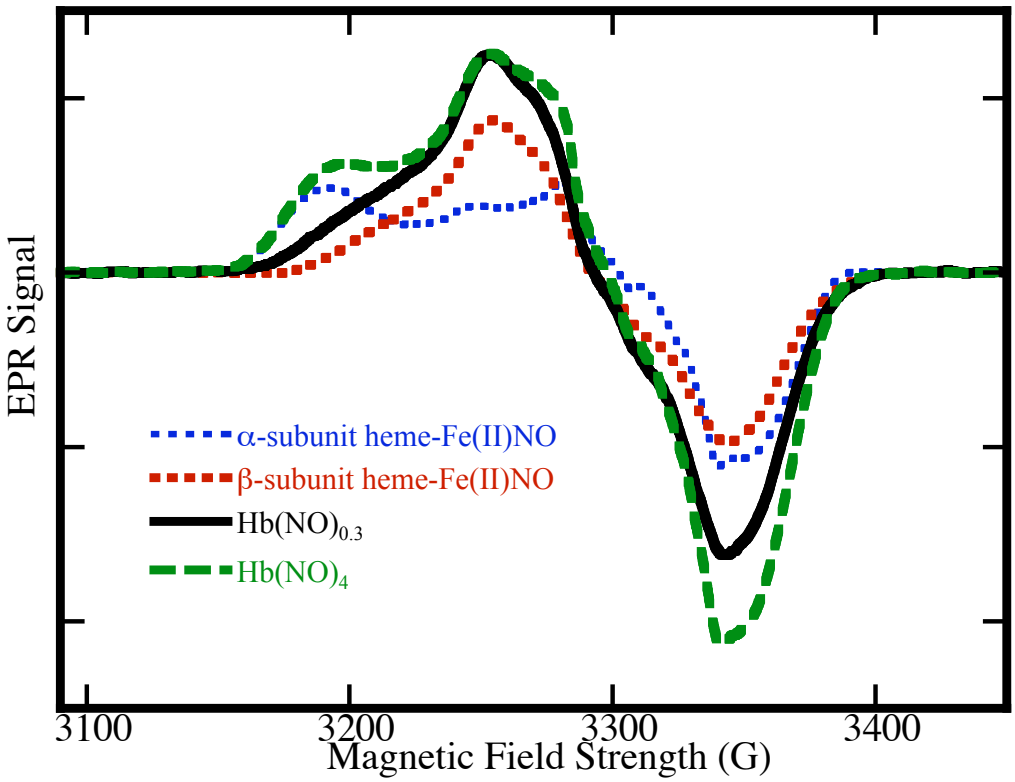


Figure 3.3 EPR spectra of Fe(II)NO obtained by reductive nitrosylation of met-Hb with NO. EPR spectra were obtained at 9.29 GHz, with 10 mW incident power, and with field modulation of 10 G at 100 kHz. The external field was scanned over a range of 400 G in 2 min with a detection time constant of 0.128 seconds. The experimental spectra shown were obtained with samples reacted with $[NO]_o$/[heme] ratios of: 0.2 (solid line), 2 (dashed line). Reconstructions made as weighted combinations of α- and β-subunit spectra (dotted lines) are indistinguishable from the experimental spectra. The spectrum

obtained with a $[NO]_o$/[heme] ratio of 0.2 reflects a β- vs. α-subunit preference of 88 ± 8 % (variance between methods adapted from Refs. 18-22). The spectrum obtained with a $[NO]_o$/[heme] ratio of 2 reflects equal a- and b-subunit populations in the $(Fe(II)NO)_4$ protein. EPR signals from residual met-Hb lie outside the field range included in the spectra presented here.

Collectively, our results suggest that the reductive nitrosylation of human Hb, with limiting amounts of NO, may most simply be considered to occur as a weighted sum of independent subunit reactions. We assume that the α-subunits only generate nitrite, but that β-subunits produce either nitrite or SNO. At progressively lower $[NO]_o$/[heme] ratios, β-subunit processing and SNO production is increasingly favored. At the very low $[NO]_o$/[heme] ratios characteristic of the physiological situation; the chemistry would tend toward:

$$\beta\text{-heme-Fe(III)} + 2\ NO(aq) \rightarrow \beta\text{-heme-Fe(II)NO} + \text{cys}(\beta\text{-93})\text{-NO} \qquad [3],$$

with nitrosothiol and β-subunit ferrous heme nitrosyl as the exclusive products of this novel, sub-unit selective reaction.

The dominance of reaction (3) at low NO levels implies a substantial subunit inequivalence in the binding of NO to form the ferric nitrosyl heme intermediate and/or the subsequent reaction of that intermediate to form the products. Previous studies of the NO binding to met-Hb (13, 24, 25) show that equilibrium favors the β-subunit only by a factor of ~1.5. While the subunit dependence of Fe(III)NO reaction rates have not been examined in detail, it has been noted that the reductive nitrosylation occurs "considerably faster" with isolated β-chains (β-subunit tetrameric protein) than with α-chains (25). In these previous studies, with NO present in excess, the reaction would presumably involve

Hb $(Fe(III)NO)_4$ intermediates. At very low $[NO]_o$/[heme] ratios, however, hybrids such as α_2(met)β(met)β(Fe(III)NO), would be the predominant initial reactive intermediates. It is tempting to suggest that the differential reactivity of the various intermediates mustered under different experimental conditions may play an important role in governing the substantial product/subunit selectivity and its dependence on $[NO]_o$/[heme] ratios.

The observed chemistry rationalizes a number of observations made in previous studies of this reaction. A fundamental issue is the lack of mass balance. Hoshino *et al.* (24), recently reported that the reductive nitrosylation of methemoglobin, in excess NO, yielded ~0.9 heme-Fe(II)NO (detected as nitrate after oxidation in air) but only about ~0.4 NO_2^- per heme, even though hydroxide and water were considered as the only nucleophiles. (For whale myoglobin (24), the product yields closely followed (Eq. 1)). These observations likely reflect S-nitrosylation of Hb in competition with (and independent of) hydroxide or other putative nitrosation targets. The product distribution reported by Hoshino *et al.* (24), in fact very closely follow the stoichiometry expected for a process that completes both α- and β-subunit reactions. The observation of Wade and Castro (23) that met-Hb is extremely ineffective, as compared to, for example, horse metmyoglobin, in promoting the apparent nitrosation of exogenous nucleophiles may, in part, reflect interference from the nitrosothiol-forming reaction. Our results also clarify certain observations of Addison and Stephanos (22), which were interpreted as indicating that the protein product obtained by complete reductive nitrosylation of methemoglobin is modified in the course of the reaction: Addison and Stephanos, however, suggested that this modification entails nitrosation of a histidine or lysine rather than the thiol.

Finally, the variation of the levels of heme-Fe(II)NO hemoglobin complexes that have been detected in blood by EPR methods (33-40), may be influenced by the levels of heme-Fe(III)NO and other EPR undetectable species that can interchange with the heme Fe(II)NO species under different methods of sample treatment.

Reductive Nitrosylation Kinetic Analysis.

As a check on the overall soundness of the decomposition analysis and on the role of Fe(III)NO as an intermediate, we analyzed the UV/VIS spectra recorded before steady state was reached, to obtain concentration versus time profiles, exhibited in Fig. 3.4 (top). The data are analyzed with a *de minimis* model composed of: i) equilibrium uptake of NO by met-Hb (Eq. 1, reaction a); ii) reduction of Fe(III)NO and formal loss of NO^+ (Eq. 1 reaction b or Eq. 2); iii) uptake of NO by the reduced heme (Eq. 1 reaction c).

The solid lines in Fig. 3.4 (bottom) show traces calculated on the basis of the kinetic model above, with parameter values obtained by least-squares adjustment. The quality of the fit is similar in all of the measurements. We followed the kinetic behavior from shortly after mixing to stationary phase in five samples at various buffer compositions (PBS, HEPES, and 100 mM phosphate) and initial heme:NO ratios (3:1 to 1:1). As detailed below we obtain a precise determination of the rate constant for the reduction step (ii), but only a rough estimate of the equilibrium constant for step (i). The transfer of NO to reduced hemes (step iii) is likewise only found to be extremely fast relative to step (ii).

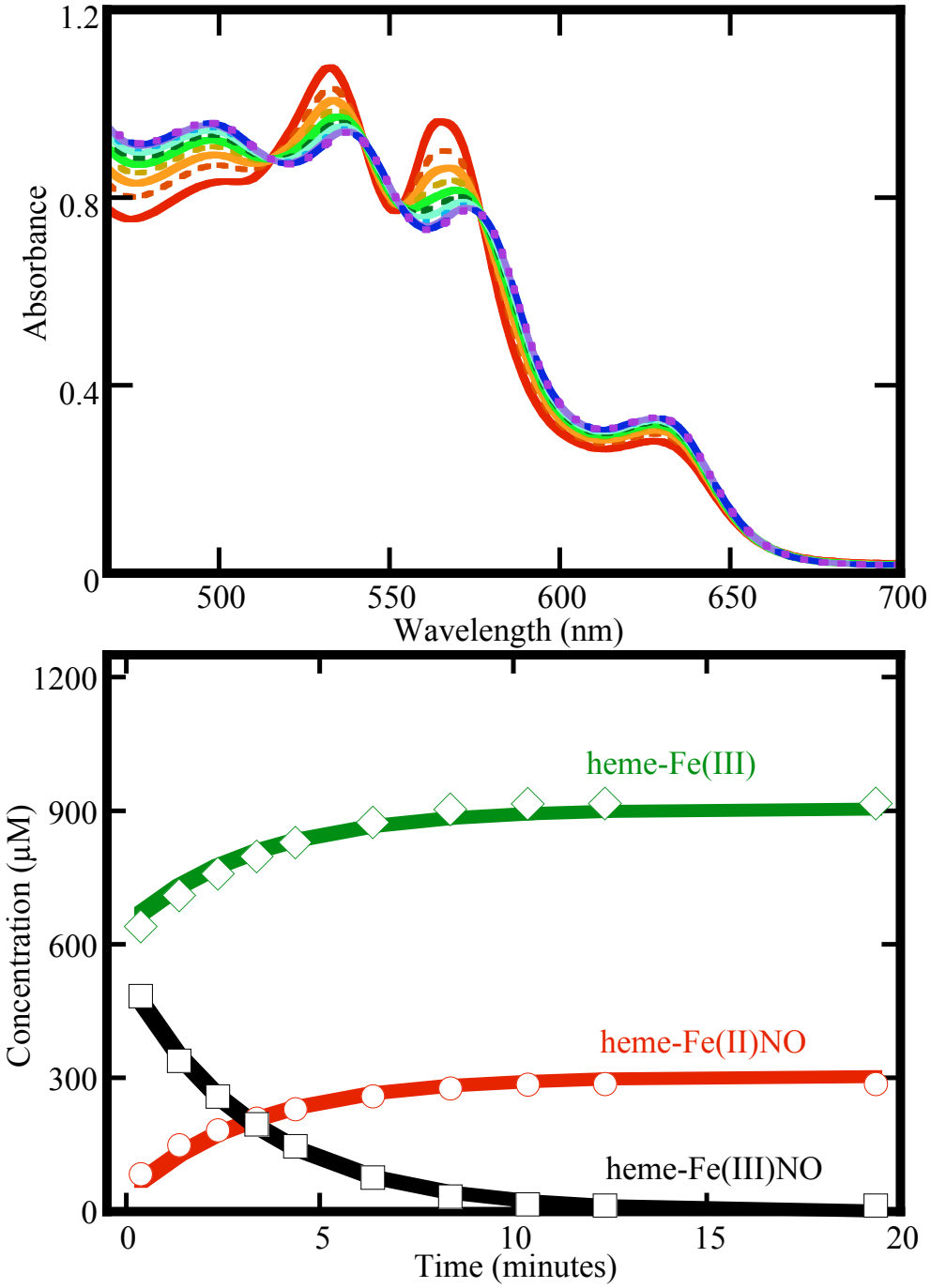


Figure 3.4 Kinetics of reductive nitrosylation in a deoxygenated aqueous solution prepared with met-Hb 1.2 mM in heme, 0.7 mM NO, 100 mM phosphate buffer, pH 7.4, and 150 mM NaCl. (Top panel) Time series of visible spectra of the reacting solution. Successive spectra were initiated at time intervals of 1 minute. The first spectrum was recorded 22 seconds after mixing the reagents. (Bottom panel) Concentration versus time.

In previous studies of met-heme interactions with NO in human Hb, Sharma *et al.* (25) and Alayash *et al.* (13) used stopped-flow methods to elucidate the detailed behavior of the initial binding step. Both groups reported equilibrium constants of ~$3x10^3$ M^{-1}, and a subunit inequivalence in the reaction, with the β-subunit hemes exhibiting roughly five-fold greater on- and off-rates than the α-subunit hemes. Ford and co-workers (24) obtained an equilibrium constant of similar magnitude $13x10^3$ M^{-1} by analyzing the effect of [NO] on the reduction rate. Within this range, our kinetic analysis was insensitive to the value of this equilibrium constant, and we opted to fix this parameter at 1.0 $x10^4$ M^{-1} in the analysis. For the reduction step, the effective rate constant, first order in Fe(III)NO, was reported as 0.0018 sec^{-1} (pH 7, 25 ºC), by Addison and Stephanos (22), and 0.00063 sec^{-1} (pH 7, 20 ºC) by Alayash *et al.* (13) Ford and co-workers (24) measured the rate as a function of pH from which a value of 0.0019 sec^{-1} obtains at pH 7.4. The values that we determine , range from 0.0012 ± 0.0001 sec^{-1} (PBS) to 0.0027 ± 0.0001 sec^{-1}(HEPES, 100 mM phosphate), in good agreement with the previously determined values. The overall quality of the analysis and its consistency with prior observations, provides strong support for the procedure used, and thus identifies the central role of the Fe(III)NO intermediate in this reaction.

Additional SNO-Hb Producing Reactions.

The salient feature of the reductive nitrosylation reaction is the coupling of met-heme reduction with formal NO oxidation to trigger nitrosation. The signature of this reaction in Hb, when the NO is limiting, is the SNO formation in the nitrosation reaction and the β-subunit preference in the heme nitrosylation. This interplay of met-hemes with

NO could be approached by a number of different starting conditions, which might nevertheless lead to the same set of products. In a physiological context, reactions which do not require the presence of a pre-existing reservoir of met-Hb for reaction with incident NO are of particular interest.

The activity of NO as an oxidant of hemoglobin, in both oxy- and deoxy-forms is well-documented (3), (41). Accordingly, a sequence composed of an oxidative reaction that forms met-Hb, followed by a reductive nitrosylation leading to SNO-Hb and restoration of a reduced-heme, is in principle possible. In this scheme, heme-redox acts in a cyclic fashion, with no met-Hb reservoir required. In a reaction with oxygenated Hb, this sequence could lead to: a) SNO-production; b) the formation of a Fe(II)NO in an amount that exceeds the number of originally available vacant Fe(II) centers – thus, an apparent cooperativity in NO addition (3), (42), which stems from changes in vacant heme concentrations during NO uptake, rather than favorable changes in rate or equilibrium constants. This process could assume special significance for hemoglobins repeatedly exposed to NO - for example, membrane-bound hemoglobins (43) exposed to a slow flux of NO passing into a cell. The loss (to nitrate or nitroxyl) of one equivalent of NO, in this scheme, would be circumvented if other oxidants were involved. Accumulation of met-Hb would still not be required provided that the oxidation could follow NO addition - that is, if the reaction entails the oxidation of Fe(II)NO.

To explore the feasibility of the latter process, we have initiated studies to assay the production of SNO-Hb accompanying the oxidation of heme-Fe(II)NO species. In Fig. 3.5, we present results of experiments that show that $Hb(NO)_4$ reacts in the presence of excess ferricyanide to convert Fe(II)NO hemes to met-hemes, with approximately one

SNO-Hb produced for every two Fe(II)NO lost. Overall, this product distribution suggests the formal oxidation of Fe(II)NO to a Fe(III)NO species that then reacts to form S-nitrosothiol (or nitrite products), liberating a vacant heme-Fe(II), which, being more easily oxidized than heme-Fe(II)NO (as the association equilibrium constant for NO and heme-Fe(II) is much greater than for heme-Fe(III) and NO), readily accedes to oxidation under these conditions.

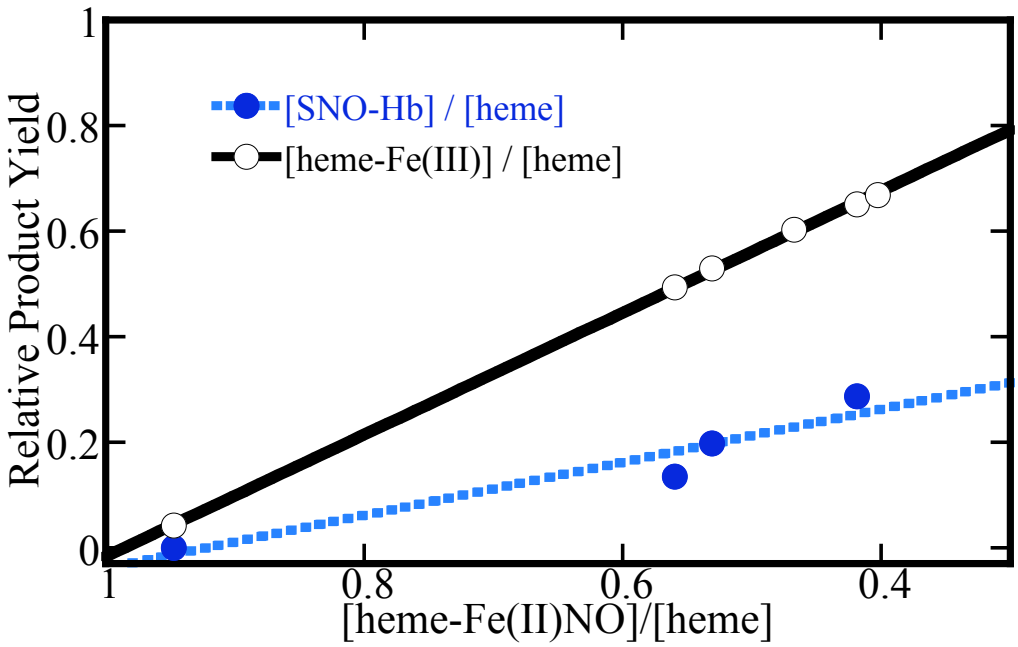


Figure 3.5 Conversion of heme-Fe(II)NO centers to heme-Fe(III) and SNO-Hb upon exposure of Hb(NO)4 to ferricyanide. Samples of the reaction medium are withdrawn at various points in the course of the reaction for analysis of the amounts of heme-Fe(II)NO, heme-Fe(III), and nitrosothiol – relative to the total heme in the medium. The symbols ○ (left scale) compare heme-Fe(III) production to heme-Fe(II)NO depletion; the solid line represents the best, linear fit to these experimental points (slope –1.15 ±0.01; intercept = 1.14 ±0.01 ; R=0.9998) indicative of a one-to-one conversion of heme-Fe(II)NO to heme-Fe(III). The symbols ● compare experimental S-nitrosothiol production to heme-Fe(II)NO depletion; the dashed line represents the best, linear fit to these experimental points (slope -0.50±0.11; intercept 0.46±0.07; R=0.96). Product analysis was carried out as described in the text.

The reaction of nitrite with hemoglobin provides a further route to the simultaneous presentation of heme Fe(III) and NO (41, 44-46). The possible significance in the context

of nitric oxide biology has been thoughtfully considered by Reutov and Sorokina (47), who posited that owing to the well-known nitrite reductase activity of hemoglobin, nitrite could be considered an integral component of NO biochemistry, rather than a metabolic dead-end. To examine this idea, and determine whether SNO-Hb is produced in this interaction, we first incubated oxyhemoglobin with ~0.01 equivalents (on a per-heme basis) of nitrite. No discernible changes were present in the EPR spectrum over a time span of as much as 15 minutes. The only feature in the spectrum derived from the small fraction (~1%) of met-heme in the oxy-Hb solution, which was not discernibly changed by the nitrite addition. Deoxygenation of these mixtures after various incubation times led to an immediate change in the EPR spectrum with roughly equal increases in met-heme and heme-Fe(II)NO signals, as illustrated in Fig. 3.6 (top and bottom, respectively). These results are consistent with the simple understanding of the nitrite reaction with deoxy-Hb according to the following scheme (41, 44):

$$\text{heme-Fe(II)} + NO_2^-(aq) + H^+(aq) \rightarrow \text{heme-Fe(III)} + NO + OH^-(aq), \qquad [4]$$

NO will ultimately lodge at available heme vacancies to form Fe(II)NO. Interestingly, as we have reported elsewhere (43), oxygenation leads to elimination of the Fe(II)NO and the formation of SNO-Hb – in effect the reverse of reaction (4), with nitrosothiol formation (Eq. 2), rather than nitrite regeneration. Overall, this chemistry reveals a catalytic role for Hb – in conjunction with its oxygenation/deoxygenation cycle – in converting nitrite to the SNO-Hb.

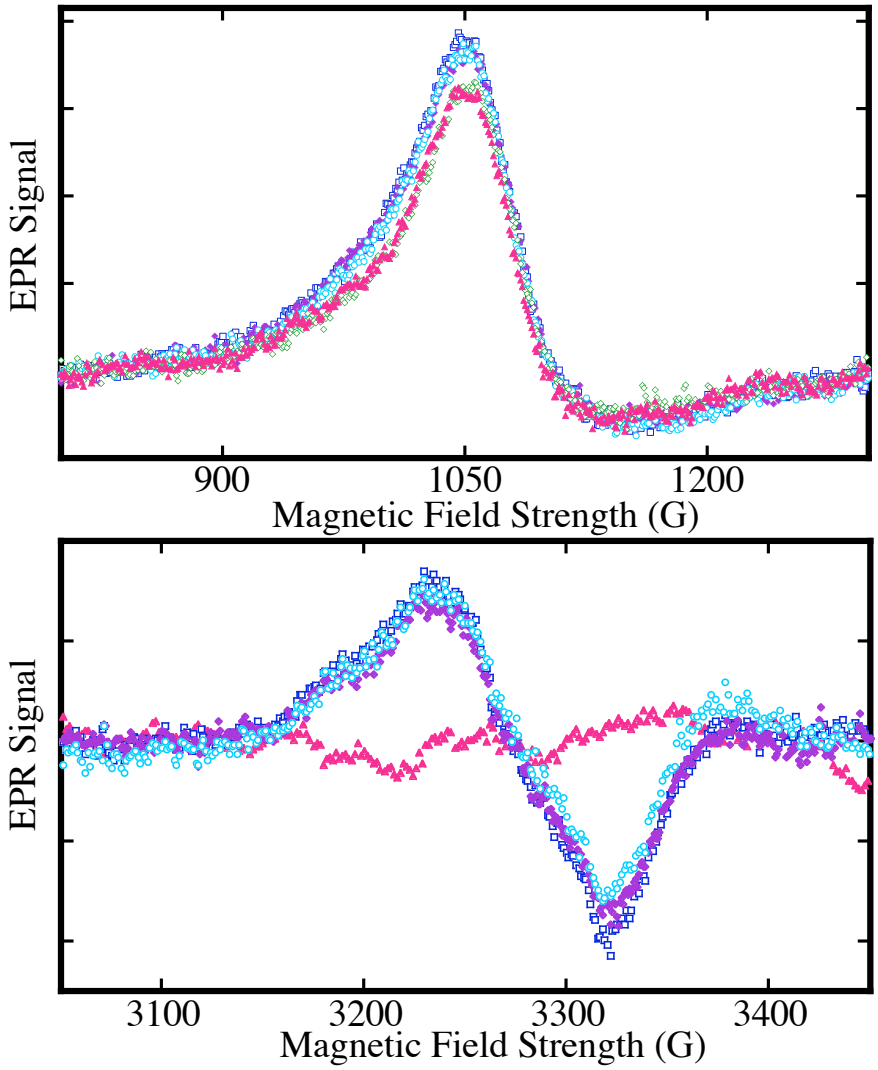


Figure 3.6 EPR spectra from Fe(II)NO and Fe(III) hemes obtained by exposure of hemoglobin to nitrite. EPR spectra were obtained at 9.28 GHz, with 10 mW incident power, and with field modulation of 20 G at 100 kHz. The external field was scanned for 4 min with a detection time constant of 0.128 seconds over to range: 800 – 1300 G to detect high-spin heme-Fe(III) (upper panel) or 3050 – 3450 G to detect heme-Fe(II)NO (lower panel). A spectrum of a sample of a neat, 3.8 mM oxyhemoglobin solution, frozen in liquid nitrogen is displayed (▲) in both panels; the trace in the lower panel was used as a base-line for subtraction from subsequent scans. Spectra were subsequently obtained from samples withdrawn from the solution after incubation with 37 μM nitrite for periods of 5 (□), 12 (◆), and 24 (○) min, followed by deoxygenation and freezing in liquid nitrogen (both panels). SNO-Hb is observed upon re-oxygenation of such samples. A spectrum obtained without deoxygenation after an incubation time of 10 min (◇) is also shown (upper panel).

Discussion

We have shown that NO can be transported from the heme binding site (distal pocket) to the thiol of cys(β-93), which lies on the opposite face of the heme (next to the proximal histidine residue). The production of SNO-Hb in this transfer can be supported by heme-iron redox chemistry. When NO is limiting, SNO-Hb is the major product formed in the reductive nitrosylation reaction, with preference for the β-subunits of hemoglobin. We have also shown that SNO-Hb production rather generally accompanies the formal interaction of NO and heme-Fe(III), regardless of the sequence of NO addition and heme-oxidation – sequences including NO reaction with heme-Fe(III), oxidation of heme-Fe(II)NO, or reaction of nitrite with deoxy-Hb in an oxygenation/deoxygenation cycle.

The chemistry reported here has several implications of potential importance to NO hemoglobin interactions in blood. Inasmuch as the NO-group is present in limited concentrations, any reductive nitrosylation reaction would tend to process the NO-group exclusively within the β-subunit. This subunit selective processing could provide a means by which NO can avoid being trapped by the α-hemes to yield the five-coordinate α-heme-Fe(II)NO complexes which could quench NO bioactivity (48). Moreover, the results reveal a means by which the NO-group can be dislodged from heme-Fe(II)NO complexes to make the nitrosothiol hemoglobin derivative: the perceived unfavorability of NO dissociation from nitrosylated ferrous hemes (49), can be circumvented by oxidation to the ferric heme-nitrosyl species, thus facilitating NO-group transfer to

protein thiol. In conjunction with this oxidation, reaction (4) depicts NO-group transfer from a β-subunit heme species that holsters NO bioactivity (heme-Fe(II)NO) to one that arms it (protein-SNO) for potential release via, for example, transfer to other thiols (50, 51). Inasmuch as NO is a potent oxidant of both oxy- and deoxy-Hb, the methemoglobin requirement may be potentiated through NO itself, in a cycle of heme-oxidation/reductive-nitrosylation, that does not require or involve any met-Hb accumulation. The oxidative and NO-group requirements can also be supported by interaction of heme vacancies with nitrite, as part of a greater NO-group biological chemistry.

The results presented here clarify some issues relevant to SNO-Hb function raised in several recent publications. Apparent cooperativity in the formation of heme-Fe(II)NO by exposure of oxygenated hemoglobin to NO has been observed under certain conditions *in vivo* by us, and in red blood cell preparations by Huang *et al.* (52) and Han *et al.* (53) Moreover, while Huang *et al.* (52) suggest that their *in vivo* experiments do not show this apparent cooperativity, the systematic differences between the experimental data and the theoretical predictions indicate that while such effects are attenuated under their conditions, an excess of heme-Fe(II)NO is produced, at higher oxygen saturations. Preference for the β-subunits is evident in the Fe(II)NO EPR spectra presented in the work of Huang *et al.* (52). The latter authors also measure SNO-production and obtain nearly equivalent yields of Fe(II)NO and SNO-Hb under a variety of conditions. In related experiments, Joshi *et al.* (30) fail to detect Fe(II)NO at very high oxygenation and non-physiological NO levels. Notably, they do observe the production of SNO-Hb in yields that are similar to those reported by Gow *et al.*, (3) and are independent of the

manner of NO addition. The observations reported in all of these studies share features that are common to the reductive nitrosylation chemistry reported here.

Han *et al.* (53) suggest, on the basis of the cyanide blocking experiments, that reductive nitrosylation is not significant to the production of SNO-Hb. Their results, however, only compel the conclusion that in the presence of high cyanide levels some met-heme independent SNO-Hb production occurs. Our mechanistic conclusions are supported by direct observations of all of the relevant chemical species, detailed material balance, and global kinetic analysis – there is no ambiguity regarding the centrality of the heme-Fe(III)NO intermediate.

Finally, it is worth pointing out that in the experiments of Han *et al.* (53) and Huang *et al.* (52), very high protein concentrations are used. While this choice reflects the concentrations within red blood cells, it can obscure the fundamental chemistry of hemoglobin at the molecular level. Analysis of the chemical behavior of concentrated protein solutions that is significantly depleted in the activity of water may require more elaborate models for bolus and diffusion effects, and attention to chemical activities. Ultimately, with a clearer picture of the relevant, molecule scale behavior of hemoglobins, an integrated model of cardiovascular NO function, encompassing molecular, cellular, and system wide variables may be developed.

Addendum

We determine the distribution of α and β heme nitrosylation products through factor analysis of EPR spectra. EPR spectroscopy is selective for heme-Fe(II)NO (as well as high- and low-spin methemoglobins), present as a minority among an EPR-silent

majority of oxy- or deoxyhemes. In addition to indicating the presence and quantity of heme-Fe(II)NO species, EPR spectra of human Hemoglobin exhibit subunit-inequivalences that make it possible to determine proportions of NO on the α- vs. β-subunits by decomposition of the spectra according to their subunit contributions.

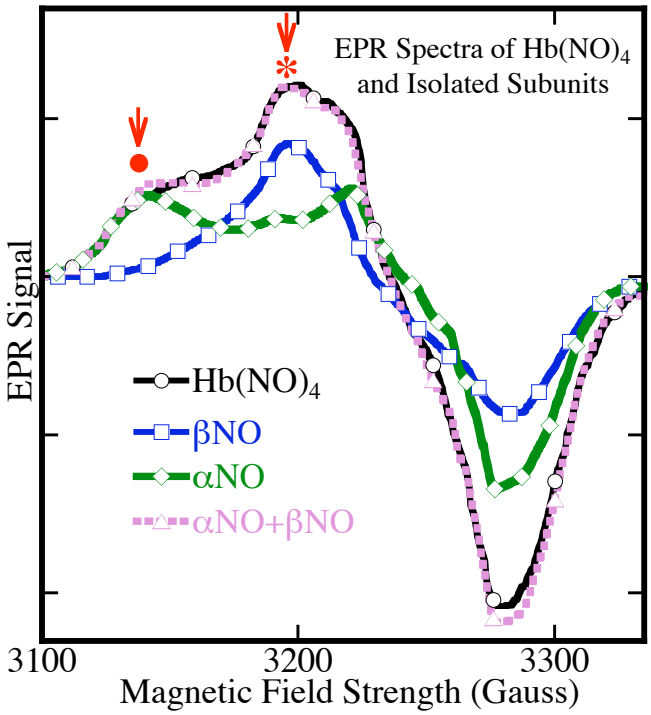


Figure 3.7 X-band EPR spectrum of nitrosylhemoglobin spectral components termed βNO (□) and αNO (◇), from isolated subunits (6). The sum (△) of these spectral components is seen to be identical to the EPR spectrum of $Hb(NO)_4$. (○). Asterisk (*), and bullet (•)mark spectral positions that feature the βNO or αNO species respectively. C) Ratio of * and • used for decomposition of SNO-oxyhemoglobin EPR spectra.

The subunit spectra (Fig. 3.7, αNO and βNO) clearly show distinctions, but the composite spectrum formed simply by addition of the subunit spectra (Fig. 3.7, αNO+βNO) is essentially identical to that of the tetrameric $\alpha_2(NO)/\beta_2(NO)$ hemoglobin (Fig. 3.7, $Hb(NO)_4$). (Asterisks mark the positions at which either the αNO (left) or βNO (middle) species predominate). The "hybrids" $\alpha_2(NO)/\beta_2(deoxy)$ and $\alpha_2(deoxy)/\beta_2(NO)$ were shown to exhibit spectra equivalent to those of the isolated αNO or βNO subunits,

respectively (14). Taken together, these results establish the current approach for analyzing nitrosylhemoglobin EPR spectra which is directly applicable to Fe(II)NO complexes in SNO-hemoglobin as S-nitrosylation affects neither the heme EPR or UV/Vis spectra.

References

1. Stamler, J. S. (1994) Cell 78, 931-6.

2. Stamler, J. S., Singel, D. J. & Loscalzo, J. (1992) Science 258, 1898-902.

3. Gow, A. J., Luchsinger, B. P., Pawloski, J. R., Singel, D. J. & Stamler, J. S. (1999) Proc. Natl. Acad. Sci. USA 96, 9027-32.

4. Hille, R., Olson, J. S. & Palmer, G. (1979) J. Biol. Chem. 254, 12110-20.

5. Hille, R., Palmer, G. & Olson, J. S. (1977) J. Biol. Chem. 252, 403-405.

6. Reisberg, P., Olson, J. S. & Palmer, G. (1976) J. Biol. Chem. 251, 4379-83.

7. Taketa, F., Antholine, W. E. & Chen, J. Y. (1978) J. Biol. Chem. 253, 5448-51.

8. Quine, R. W., Eaton, G. R., Eaton, S. S., Koska, A. & Bowman, M. K. (1986) J. Magn. Reson. 69, 371–374.

9. Mendes, P. (1997) Trends Biochem. Sci. 22, 361-363.

10. Kuzmic, P. (1996) Anal. Biochem. 237, 260-273.

11. Malinowski, E. R. (1991) Factor Analysis in Chemistry (Wiley, New York).

12. We determined that, in all spectra, the deoxy- and oxy-Hb species were of negligible concentration. Singular value decomposition further indicated that the kinetic variation of the spectra involves two predominant components. This result is consistent with a chemical process like (Eq. 1), in which - against a background of excess met-hemes - Fe(III)-nitrosyl hemes are effectively converted to Fe(II)-nitrosyl and met-hemes. The presence of a third component that is relatively weak, but above noise, indicates that this framework is an approximation to the overall chemistry. Within this framework, we used target factor analysis to identify the authentic Fe(III)nitrosyl-Hb spectrum. A test factor (11) composed of the difference between the first kinetic trace (rich in Fe(III)nitrosyl-Hb) and an arbitrary linear combination of Fe(II)nitrosyl- and met-Hb spectra was used to predict the hypothetical Fe(III)nitrosyl-Hb, consistent with each linear combination. To select the best Fe(III)nitrosyl-Hb spectrum from among these hypothetical spectra we employed three criteria: the least-squares difference between the test and predicted vector is below a selected threshold; the predicted spectrum is non-negative at all wavelengths; the predicted spectrum is a monotonically decreasing function of wavelength beyond 565 nm. In scaling the resultant spectrum, we took advantage of the quasi-isosbestic points at 516, 543, 554, 577 nm that are evidenced in the UV/VIS spectra during the kinetic runs. Within the chemical framework noted

above, the Fe(III)nitrosyl-Hb absorbance at these points must be approximately equal to the average of Fe(II)nitrosyl- and met-Hb spectra.

13. Alayash, A. I., Fratantoni, J. C., Bonaventura, C., Bonaventura, J. & Cashon, R. E. (1993) Arch. Biochem. Biophys. 303, 332-8.

14. Henry, Y. & Banerjee, R. (1970) J. Mol. Biol. 50, 99-110.

15. Kon, H. (1968) J. Biol. Chem. 243, 4350-7.

16. Shiga, T., Hwang, K. J. & Tyuma, I. (1969) Biochemistry 8, 378-83.

17. Henry, Y. & Banerjee, R. (1973) J. Mol. Biol. 73, 469-82.

18. Hartree, E. F. & Keilin, D. (1937) Nature 139, 548.

19. Chien, J. C. W. (1969) J. Am. Chem. Soc. 91, 2166-2168.

20. Ehrenberg, A. & Szczepkowski, T. W. (1960) Acta. Chemica. Scandinavica 14, 1684-1692.

21. Wayland, B. B. & Olson, L. W. (1974) J. Am. Chem. Soc. 96, 6037-41.

22. Addison, A. W. & Stephanos, J. J. (1986) Biochemistry 25, 4104-13.

23. Wade, R. S. & Castro, C. E. (1990) Chem. Res. Toxicol. 3, 289-91.

24. Hoshino, M., Maeda, M., Konishi, R., Seki, H. & Ford, P. C. (1996) J. Am. Chem. Soc 118, 5702 -5707.

25. Sharma, V. S., Traylor, T. G., Gardiner, R. & Mizukami, H. (1987) Biochemistry 26, 3837-43.

26. Jia, L., Bonaventura, C., Bonaventura, J. & Stamler, J. S. (1996) Nature 380, 221-6.

27. Stamler, J. S., Jia, L., Eu, J. P., McMahon, T. J., Demchenko, I. T., Bonaventura, J., Gernert, K. & Piantadosi, C. A. (1997) Science 276, 2034-7.

28. Chan, N. L., Rogers, P. H. & Arnone, A. (1998) Biochemistry 37, 16459-64.

29. Ferranti, P., Malorni, A., Mamone, G., Sannolo, N. & Marino, G. (1997) FEBS Lett 400, 19-24.

30. Joshi, M. S., Ferguson, T. B., Jr., Han, T. H., Hyduke, D. R., Liao, J. C., Rassaf, T., Bryan, N., Feelisch, M. & Lancaster, J. R., Jr. (2002) Proc. Natl. Acad. Sci. USA 99, 10341-6.

31. Keefer, L. K., Nims, R. W., Davies, K. M. & Wink, D. A. (1996) Methods Enzymol. 268, 281-93.

32. Williams, E. M. (2001) (Middlebury College, Middlebury, VT).

33. Kosaka, H., Watanabe, M., Yoshihara, H., Harada, N. & Shiga, T. (1992) Biochem. Biophys. Res. Commun. 184, 1119-24.

34. Kosaka, H., Tanaka, S., Yoshii, T., Kumura, E., Seiyama, A. & Shiga, T. (1994) Biochem. Biophys. Res. Commun. 204, 1055-60.

35. Jacob, T. D., Nakayama, D. K., Seki, I., Exler, R., Lancaster, J. R., Jr., Sweetland, M. A., Yousem, S., Simmons, R. L., Billiar, T. R., Peitzman, A. B. & *et al.* (1994) J. Appl. Physiol. 76, 1794-801.

36. Romand, J. A., Pinsky, M. R., Firestone, L., Zar, H. A. & Lancaster, J. R., Jr. (1994) J. Appl. Physiol. 76, 1356-62.

37. Roccatello, D., Mengozzi, G., Alfieri, V., Pignone, E., Menegatti, E., Cavalli, G., Cesano, G., Rossi, D., Formica, M., Inconis, T., Martina, G., Paradisi, L., Sena, L. M. & Piccoli, G. (1997) Nephrol. Dial. Transplant. 12, 292-7.

38. Weinberg, J. B., Gilkeson, G. S., Mason, R. P. & Chamulitrat, W. (1998) Free Radic. Biol. Med. 24, 191-6.

39. Takahashi, Y., Kobayashi, H., Tanaka, N., Sato, T., Takizawa, N. & Tomita, T. (1998) Am. J. Physiol. 274, H349-57.

40. Gladwin, M. T., Ognibene, F. P., Pannell, L. K., Nichols, J. S., Pease-Fye, M. E., Shelhamer, J. H. & Schechter, A. N. (2000) Proc. Natl. Acad. Sci. USA 97, 9943-8.

41. Doyle, M. P., Pickering, R. A., DeWeert, T. M., Hoekstra, J. W. & Pater, D. (1981) J. Biol. Chem. 256, 12393-8.

42. Gow, A. J. & Stamler, J. S. (1998) Nature 391, 169-73.

43. McMahon, T. J., Moon, R. E., Luchsinger, B. P., Carraway, M. S., Stone, A. E., Stolp, B. W., Gow, A. J., Pawloski, J. R., Watke, P., Singel, D. J., Piantadosi, C. A. & Stamler, J. S. (2002) Nat. Med. 8, 711-7.

44. Stepuro, I. I., Chaikovskaya, N. A., Solodunov, A. A. & Artsukevich, A. N. (1997) Biochemistry (Mosc) 62, 960-6.

45. Kosaka, H., Tyuma, I. & Imaizumi, K. (1983) Biomed. Biochim. Acta 42, S144-8.

46. Tomoda, A., Tsuji, A. & Yoneyama, Y. (1981) Biochem. J. 193, 169-79.

47. Reutov, V. P. & Sorokina, E. G. (1998) Biochemistry (Mosc) 63, 874-84.

48. Yonetani, T., Tsuneshige, A., Zhou, Y. & Chen, X. (1998) J. Biol. Chem. 273, 20323-33.

49. Gibson, Q. H. & Roughton, F. J. W. (1957) Journ. Physiol. 136, 507-511.

50. McMahon, T. J., Exton Stone, A., Bonaventura, J., Singel, D. J. & Stamler, J. S. (2000) J. Biol. Chem. 275, 16738-45.

51. Pawloski, J. R., Hess, D. T. & Stamler, J. S. (2001) Nature 409, 622-6.

52. Huang, Z., Louderback, J. G., Goyal, M., Azizi, F., King, S. B. & Kim-Shapiro, D. B. (2001) Biochim. Biophys. Acta 1568, 252-60.

53. Han, T. H., Hyduke, D. R., Vaughn, M. W., Fukuto, J. M. & Liao, J. C. (2002) Proc. Natl. Acad. Sci. USA 99, 7763-8.

NITRIC OXIDE MIGRATION FROM CYS(β-93) TO β-HEME-IRON(II)NO

Introduction

The chemical interactions of nitric oxide and hemoglobin in the human respiratory system were discussed in a recent publication with our collaborators at Duke University Medical Center. This publication is included as Appendix A in this thesis. The major part of the article describes studies of NO/hemoglobin chemistry in human subjects and red blood cells at various oxygen conditions conducted at Duke University Medical Center. It also gives a brief account of some *in vitro* experiments carried out by the author at Montana State University that provides a basis for rationalizing some of the *in vivo* findings. In particular, the experiments demonstrate apparent heme-to-thiol and thiol-to-heme transfers of the NO group. In this Chapter, a more detailed account of these experiments is provided. First, the results of several experiments which demonstrate the slow, but spontaneous transfer of the NO moiety from the nitrosothiol on SNO-hemoglobin to form heme-Fe(II)NO are reported. A noteworthy finding in these experiments is the substantial preference for formation of the heme-Fe(II)NO on the β-subunit of the hemoglobin. Secondly, the results of experiments carried out with oxygen cycling are reported. In fresh samples of heme-Fe(II)NO formed by incubation of deoxy-hemoglobin with nitrite the EPR spectrum of the heme-Fe(II)NO species disappears upon oxygenation of the system, with concurrent formation of an unidentified free-radical. At low NO levels, SNO-hemoglobin is also formed with the oxygenation. Upon re-

deoxygenation the radical signal disappears and remaining nitrite reacts to form heme-Fe(II)NO. This cycle can be repeated until the nitrite is exhausted.

Materials and Methods

Materials and methods used for experiments in this chapter mainly follow the procedures described in Chapters 2 and 3. SNO-hemoglobin A_o samples were prepared by the method of Jia *et al*. (1), including separation of low-molecular weight reagents by gel chromatography. Samples were characterized by UV/Vis and EPR spectroscopies in a manner described in detail in Chapter 2. The spectra are simulated as linear combinations of standard UV/Vis basis spectra. The coefficients of the linear combination, which give the concentrations of each heme species, are found by adjustment to give least-squares best agreement between the simulated and observed spectra. Greiss and Saville assays, also detailed in Chapter 2, were used to detect nitrosothiols (SNO-hemoglobin).

EPR spectroscopy is used to detect methemoglobin, determine the concentration of nitrosyl hemoglobin, and determine the subunit distribution of the heme-Fe(II)NO by the fraction of NO ligands associated with hemes of the α- vs. the β-subunits. Acquisition parameters for the EPR experiments are as described previously (2). Absolute concentrations were determined, with a reproducibility of ~90%, by comparison of the double-integral of the EPR signals against $Hb(NO)_4$ standards, the concentrations of which were established by UV/Vis spectroscopy. Subunit distributions were determined by a modification of the procedures used by Hille, Taketa, (3, 4), and Bemski and co-workers (5). In their procedures, it is assumed that: the heme-Fe(II)NO EPR spectra in

tetrameric-hemoglobin is simply the sum of spectral contributions of complexes on the α and β hemes, and the subunit spectra are identical to the spectra exhibited by nitrosyl derivatives of the isolated subunits, illustrated in the addendum to Chapter 3 (6, 7) (preparations that likely consist of β-tetramers (β-(heme-Fe(II)NO)$_4$) and possibly α-dimers (α-(heme-Fe(II)NO)$_2$).

Experiments and Results

EPR characterization of SNO-hemoglobin

We first show that heme iron-nitrosyl EPR spectra are not perturbed by S-nitrosylation of the globin, by comparing EPR spectra of Hb(NO)$_4$ and (SNO)$_2$-Hb(NO)$_4$ samples, shown in Fig. 4.1. Cleary there is no significant distinction between the two spectra. This correspondence justifies use of previously established methods for determining the distribution of NO over the α- and β-subunit hemes in characterizing SNO-hemoglobins and mixtures that include it (7).

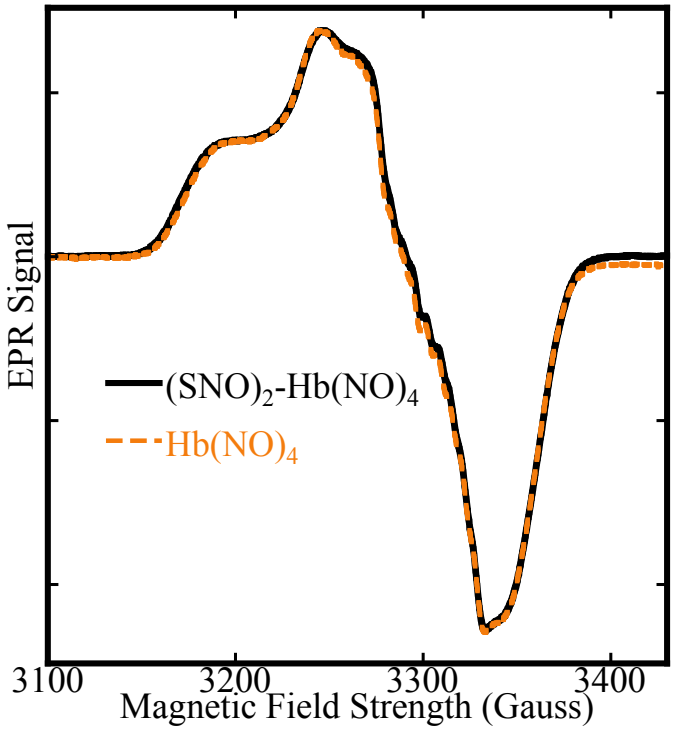


Figure 4.1 X-band EPR spectrum of nitrosylhemoglobin, $(SNO)_2$-$Hb(NO)_4$.

Thiol-to-heme-transfer

Hemoglobins that were nominally fully ligated with dioxygen ligands were S-nitrosylated by exposure to an excess of (Cys-β93)-NO – which had been prepared by reaction of cysteine in acidified nitrite. After incubation for ten minutes, the excess reagent was removed by size-exclusion chromatography. Immediately after the chromatography, and at time intervals extending to several days, the composition of the sample was characterized by UV/Vis and EPR spectroscopy; the nitrosothiol content was assayed by the Greiss and Saville colorimetric methods. The UV/Vis spectrum of a typical SNO-oxyhemoglobin preparation (sample 3, *vide infra*) is shown in Fig. 4.2 A. Least-squares analysis of the spectrum shows it to be a composite of oxy- and methemoglobin spectra with 89% oxyhemoglobin, and 11% oxidized hemoglobin,

respectively, and a total concentration of 1.65 mM in heme. No significant population of deoxyhemoglobin or heme-nitrosylhemoglobin was found in this sample by UV/Vis spectroscopy. EPR spectroscopy of the sample showed only the methemoglobin. After incubation at 4 °C for an interval of 4 days EPR spectrum shown in Fig 4.2 B was obtained. This spectrum clearly shows in addition to methemoglobin signals a strong signal from heme-Fe(II)NO.

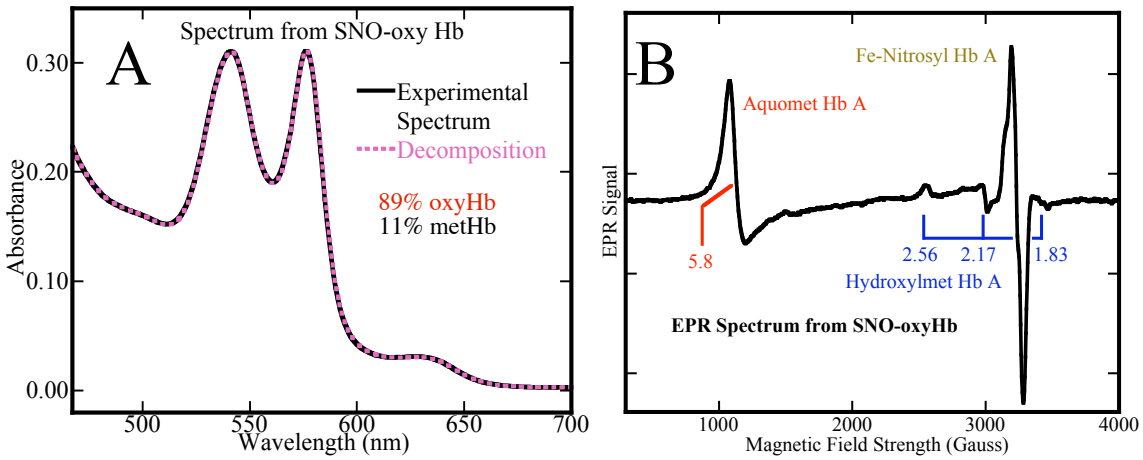


Figure 4.2 UV/Vis and EPR spectra of SNO-oxyhemoglobin (Sample 3 see Fig. 4.3). A) UV/Vis decomposition of Sample 3 at 0 hours. B) X-band 4000 Gauss wide EPR spectrum showing high spin (effective $g_1 = 5.8$, S = 5/2) and low spin ($g_2 = 5.8$, S = 1/2) metHb, and β-heme-Fe(II)NO of sample 3 at 36 hours.

We conducted similar analyses on four different samples. A quantitative summary of the results these experiments is given in the accompanying table. The summary shows a different times after preparation the fraction of nitrosyl-, oxy- and of met-hemoglobin; the fraction of the on the heme-Fe(II)NO on the β-subunit; and the fraction of thiols nitrosylated.

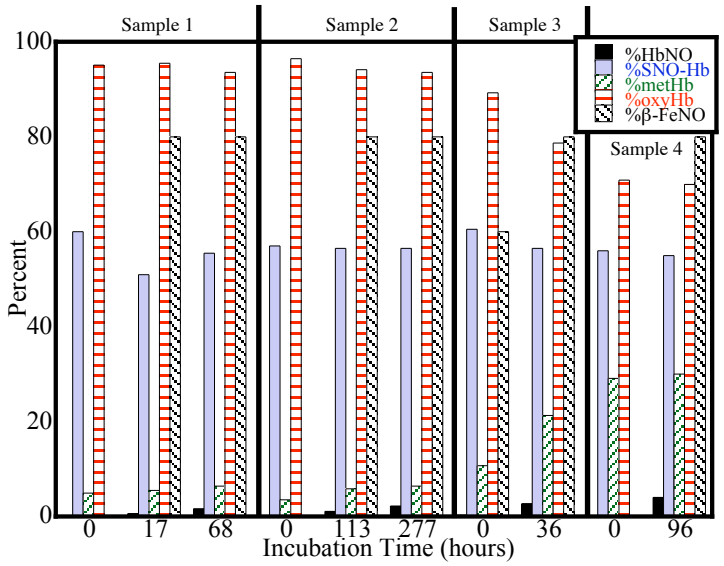


Figure 4.3 Hemoglobin species percents tallied for incubation experiments. This figure tabulates the percent for a given species. The time in hours for each sample, as well as, percentage of total possible for a given species. For example, Sample 1 at time 0 has 60% of the possible, 2 per hemoglobin, Cys-β93s S-nitrosylated. Given an EPR spectrum of heme-Fe(II)NO the percentage of β is graphed. Sample 1, at 68 hours has ≈80% of its EPR line shape coming from an heme-(β-Fe(II)NO) species, however, the total percentage of HbNO is less then 3%.

In every case, there is a gradual loss of S-nitrosothiol and compensating increase in heme-Fe(II)NO. While the overall, process is slow, there is nevertheless a spontaneous transfer of the NO moiety to the heme. Since this process requires reduction of the formal nitrosonium species, it is noteworthy that that oxidation of the heme continues during NO transfer, at levels at least as great as that of the NO transferred. This observation suggests that the overall chemistry might couple heme oxidation with formal NO^+ reduction. Further information regarding the overall chemistry comes from EPR spectra of the heme-Fe(II)NO products.

In Fig. 4.3 we show a series of EPR spectra obtained for samples at various times after preparation. By analysis of the spectral lineshapes in terms of α-6 and β-6

component spectra illustrated in the addendum to Chapter 3, we determine that the heme-Fe(II)NO has a greater that >80% β character, that is at least two thirds of the heme-Fe(II)NO in the sample occupy heme in the protein β-subunit.

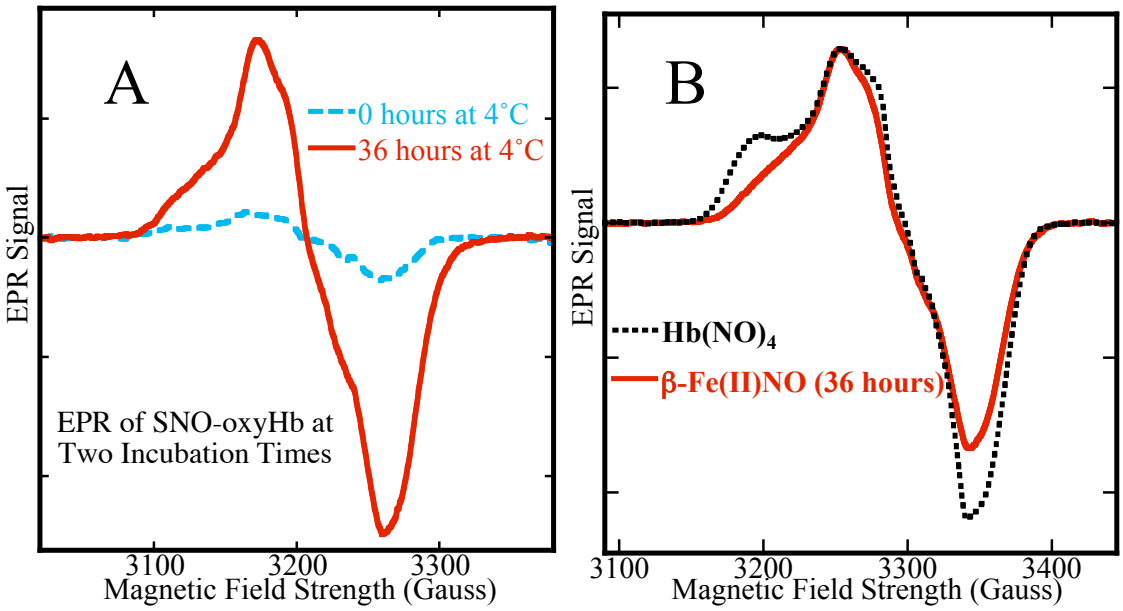


Figure 4.4 NO migrating on hemoglobin. A) Comparison of EPR spectra of sample 3 at incubation times of 0 and 36hours. B) Comparison of 36 hour spectrum with $Hb(NO)_4$.

If the release of NO from SNO-hemoglobin occurred by limited homolysis, then the generated NO would probably occupy α- and β-hemes equally. Such chemistry, apart from leaving open the question of reduction of the implicated thiyl radical, cannot explain the observed subunit specificity. We suggest that the reaction must involve a formal transfer between (Cys-β93)-NO and an adjacent vacant β-subunit heme, with the reducing equivalent supplied by electron transfer from another heme in the tetramer. The process is likely potentiated by the known drive to form symmetric methemoglobin hybrids: gradual oxidation of hemoglobin produce mainly fully oxidized methemoglobins

and half-oxidized hybrids (8). Half-oxidized hybrids of hemoglobins with NO ligands have also been reported as especially stable (9).

Overall, then we envision this reaction as occurring on hemoglobin tetramers with a single oxidized heme, and three ligand-occupied hemes. On dynamical loss of the O_2 ligand on an S-nitrosylated β-subunit, a coordinated electron-NO transfer leads to formation of a β-subunit outfitted with thiolate and heme-Fe(III)NO; the latter species is then deactivated by reduction coupled with oxidation of a neighboring heme. The overall chemistry is given in equation [4.1].

$$(SNO)_2\text{-Hb}\ (O_2)_3[\text{Fe(III)}] \rightarrow (SNO)\text{-Hb}(O_2)\ [\beta\text{-Fe(II)NO}]\ [\text{Fe(III)}]_2 \qquad [4.1]$$

Transfer of both S-nitrosyl groups would lead to formation of hemoglobin a hybrid:

$$(SNO)_2\text{-Hb}(O_2)_3[\text{Fe(III)}] \rightarrow \text{Hb}\ [\beta\text{-Fe(II)NO}]_2\ [\text{Fe(III)}]_2\ , \qquad [4.2]$$

that is reminiscent of "hemoglobin X" that has been found *in vivo* (9). In this process β-subunit selectivity emerges principally from the proximity of the (Cys-β93)-NO and theme on the β-subunit and secondarily form the redox properties of the β-subunit heme.

Heme-to-thiol transfer

The primary motivation for these experiments was to probe for effects that nitrite, which can form from NO in aqueous oxygenated media (10), might exhibit, and which, if not understood, could be confused with the behavior of authentic NO. A very large literature exists on nitrite reactions with both oxy- and deoxy-hemoglobin (11-14). These studies were undertaken primarily from the perspective of toxic effects of high levels of

nitrite. They revealed a rapid oxidation of oxyhemoglobin to methemoglobin, with complex kinetics involving a lag phase followed by a fast autocatalytic reaction, and a slower reaction with deoxyhemoglobin that yields heme-Fe(II)NO, via protonation of heme-Fe(II)NO_2^-, loss of hydroxide to furnish heme-Fe(III)NO, and NO (or electron) migration to form heme-Fe(II)NO. As shown in Chapter 3, at modest nitrite levels the latter reaction is predominant, as the lag phase becomes so long that that reaction channel is effectively quenched. In the physiological situation, therefore, the nitrite reductase activity of deoxyhemoglobin is predominant and provides an NO-synthase activity, that is distinct from the arginine converting NOS (nitric oxide synthase) enzyme: its does not require oxygen. In 1998, Reutov (15) published the idea that heme proteins might represent the anaerobic segment of a broader NO cycle in biology. The insight of Reutov lacked critical details. It made no connection to any physiological function. More importantly, it gave no indication of how NO bound to hemoglobin might be processed to exert biological activity. These problems are answered in the context of red blood cell vasodilation. NO-synthesis in RBC from nitrite is an attractive component of the molecular basis of hypoxic vasodilation. It circumvents all problems regarding the competition between fast reactions that scavenge NO activity by storing that activity in a relatively inert from, namely nitrite. We further noted in Chapter 3 that the heme-Fe(II)NO formed by reaction of deoxyhemoglobin with nitrite, can lead to SNO-hemoglobin formation upon oxygenation of the reacting system.

Here we elaborate on the experiments published in Appendix A, and show the spectroscopic characterization of a nitrite hemoglobin samples with repeated cycles of oxygenation and deoxygenation. Characteristic results are illustrated in Fig. 4.5 The

spectra provide a vivid demonstration of the nitrite reductase activity of hemoglobin through the appearance of heme-Fe(II)NO upon initial reaction ("1 min deoxy") of deoxyhemoglobin in the presence of nitrite. More intriguingly, they give a surprising result upon oxygenation ("4 min oxy"): the heme-Fe(II)NO EPR signal disappears and is replaced by an unidentified free-radical – possibly a thiyl radical. This free-radical signal is the EPR signal found by us in blood samples (Appendix A). In parallel studies at Duke University Medical Center, conducted with low nitrite concentrations and probed with high-sensitivity photolytic chemiluminescence assay, it is found that SNO formation upon oxygenation. Re-deoxygenation of the sample ("7 min deoxy") leads to restoration of the heme-Fe(II)NO signal, presumably from unreacted nitrite. This cycle is repeatable until the initial nitrite is exhausted. As the sample ages, the contrast between the spectra obtained under oxygenated and deoxygenated conditions decrease. Eventually, the system cycles only between heme-Fe(II)NO signals characteristic of the deoxy and oxy states of hemoglobin.

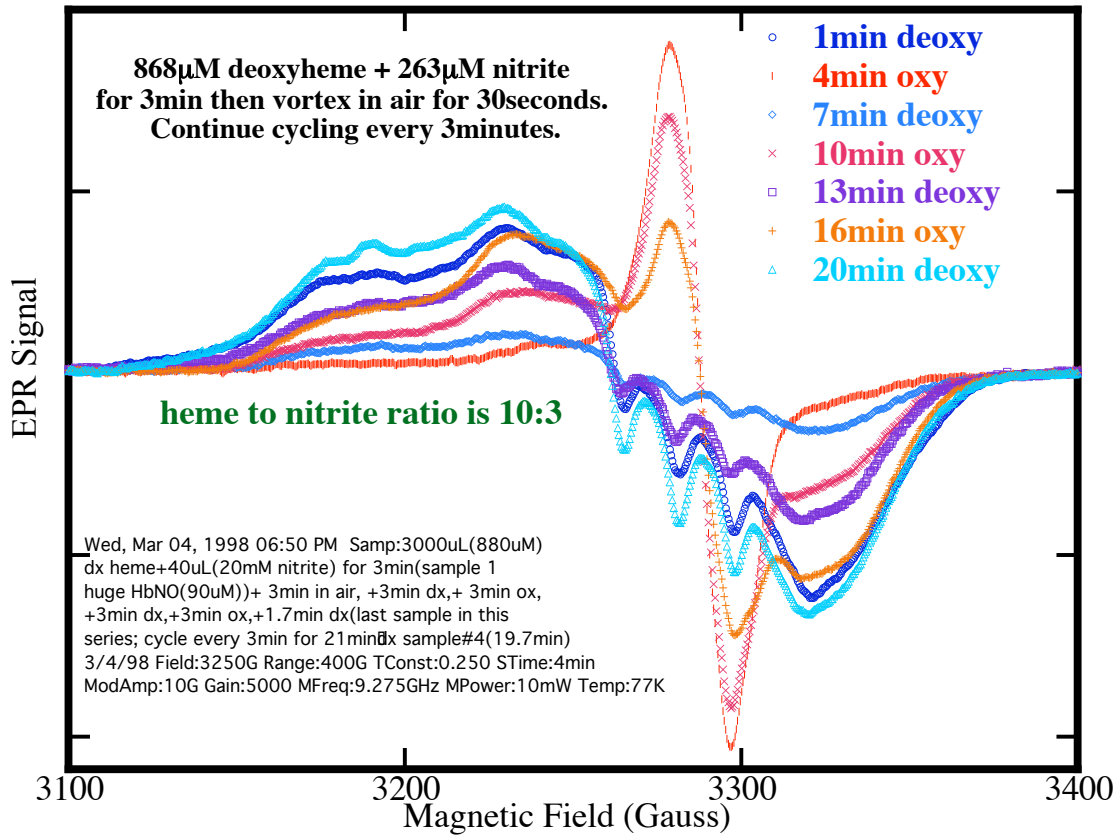


Figure 4.5 Nitrite cycling experiment. 868 µM deoxyhemoglobin + 263 µM nitrite for 1 minute (while the 1st minute elapses the first sample ("1min deoxy") is taken from the main reaction vessel and put into an O_2(g) purged EPR tube and frozen in N_2(liq)). The 1st sample is frozen at 1 minute. However, the rest of the sample reacts for an additional 2 minutes; bringing the total deoxyhemoglobin + nitrite time to 3 minutes. At 3 minutes the reaction vessel is then vortexed in air for 30 seconds and sits while sample 2 ("4min oxy") is taken out and put into an EPR tube and frozen in N_2(liq)); at a total oxygenated time of 1 minute. Total reaction time for the "4min oxy" sample is 4 minutes, 3 minutes as deoxyhemoglobin + nitrite and 1 minute as oxyhemoglobin. After sitting in air for a total of 3 minutes (total reaction time is 6 minutes, 3minutes deoxyHb and 3 minutes as oxyHb) the reaction vessel is again deoxygenated by vortexing for 30 seconds in ultra high purity N_2(g). The "7min deoxy" sample is then removed and added to an O_2(g) purged EPR tube and frozen 1 minute after the just mentioned vortexing began. These steps are repeating until the total reaction time is 20 minutes. It can be understood from this description that the sample freezing times are different from vortexing times. It is important to mention how sensitive the reaction conditions are for this experiment.

Subsequent to publication of these spectra (Appendix A) and our report detailed SNO-hemoglobin formation through nitrite reactions with deoxy hemoglobin (Chapter

3). The idea that nitrite ion has a salutary biochemistry was considered by other researchers. Gladwin and co-workers originally criticized these ideas are representing a "nitrite" artifact(16), but now have changed their view completely and see nitrite as the critical species in RBC induced vasodilation (17, 18). However, Gladwin and co-workers (19) and Rifkind and co-workers (20) suggest that the heme-Fe(III)NO species formed represents the active compound, which exerts its activity through release of NO. Gladwin and co-workers (19) further suggest that since this species is formed only in the reaction with deoxyhemoglobin, then the link between NO availability and tissue oxygen level, required for modeling hypoxic vasodilation is met. The major difficulty with their idea, however, is the abundance of vacant hemes in the deoxyhemoglobin that would scavenge NO on ferrous hemes as quickly as it is released from the ferric hemes. In their experiments sparging with argon is necessary for release of NO. In addition, there is no basis as yet for any suggestion that heme-Fe(III)NO plays that unique role of SNO-hemoglobin (21-23) in exhibiting a graded vasodilatory response as a function of oxygen tension across the physiological oxygen gradient. Notably, both Rifkind (20) and Galdwin (16, 24) report abundant SNO formation in their samples. Thus their observations, taken as a whole, are entirely compatible with all of the ideas presented in this thesis about SNO-hemoglobin in hypoxic vasodilation – in particular, its role in transducing oxygen signals to dispense NO bioactivity, and its formation redox coupling among NO and the heme and thiol groups of hemoglobin.

References

1. Jia, L., Bonaventura, C., Bonaventura, J. & Stamler, J. S. (1996) *Nature* **380,** 221-6.
2. Gow, A. J., Luchsinger, B. P., Pawloski, J. R., Singel, D. J. & Stamler, J. S. (1999) *Proc Natl Acad Sci U S A* **96,** 9027-32.
3. Hille, R., Olson, J. S. & Palmer, G. (1979) *J Biol Chem* **254,** 12110-20.
4. Taketa, F., Antholine, W. E. & Chen, J. Y. (1978) *J Biol Chem* **253,** 5448-51.
5. Louro, S. R., Ribeiro, P. C. & Bemski, G. (1981) *Biochim Biophys Acta* **670,** 56-63.
6. Henry, Y. & Banerjee, R. (1973) *J. Mol. Biol.* **73,** 469-82.
7. Reisberg, P., Olson, J. S. & Palmer, G. (1976) *J. Biol. Chem.* **251,** 4379-83.
8. Mansouri, A. & Winterhalter, K. H. (1974) *Biochemistry* **13,** 3311-4.
9. Kruszyna, R., Kruszyna, H., Smith, R. P., Thron, C. D. & Wilcox, D. E. (1987) *J Pharmacol Exp Ther* **241,** 307-13.
10. Ignarro, L. J., Fukuto, J. M., Griscavage, J. M., Rogers, N. E. & Byrns, R. E. (1993) *Proc Natl Acad Sci U S A* **90,** 8103-7.
11. Spagnuolo, C., Rinelli, P., Coletta, M., Chiancone, E. & Ascoli, F. (1987) *Biochim Biophys Acta* **911,** 59-65.
12. Smith, R. C., Gore, J. Z. & Doyle, M. P. (1991) *Free Radic Biol Med* **11,** 373-7.
13. Lissi, E. (1998) *Free Radic Biol Med* **24,** 1535-6.
14. Doyle, M. P., Pickering, R. A., DeWeert, T. M., Hoekstra, J. W. & Pater, D. (1981) *J Biol Chem* **256,** 12393-8.
15. Reutov, V. P. & Sorokina, E. G. (1998) *Biochemistry (Mosc)* **63,** 874-84.
16. Xu, X., Cho, M., Spencer, N. Y., Patel, N., Huang, Z., Shields, H., King, S. B., Gladwin, M. T., Hogg, N. & Kim-Shapiro, D. B. (2003) *Proc Natl Acad Sci U S A* **100,** 11303-8.
17. Gladwin, M. T. (2004) *J Clin Invest* **113,** 19-21.
18. Gladwin, M. T. & Schechter, A. N. (2004) *Circulation Research***,** 851-55.
19. Cosby, K., Partovi, K. S., Crawford, J. H., Patel, R. P., Reiter, C. D., Martyr, S., Yang, B. K., Waclawiw, M. A., Zalos, G., Xu, X., Huang, K. T., Shields, H., Kim-Shapiro, D. B., Schechter, A. N., Cannon, R. O., 3rd & Gladwin, M. T. (2003) *Nat Med* **9,** 1498-505.
20. Nagababu, E., Ramasamy, S., Abernethy, D. R. & Rifkind, J. M. (2003) *J Biol Chem* **278,** 46349-56.
21. Stamler, J. S., Jia, L., Eu, J. P., McMahon, T. J., Demchenko, I. T., Bonaventura, J., Gernert, K. & Piantadosi, C. A. (1997) *Science* **276,** 2034-7.
22. McMahon, T. J., Pawloski, J. R., Hess, D. T., Piantadosi, C. A., Luchsinger, B. P., Singel, D. J. & Stamler, J. S. (2003) *Blood* **102,** 410-1; author reply 412-3.
23. McMahon, T. J., Exton Stone, A., Bonaventura, J., Singel, D. J. & Stamler, J. S. (2000) *J Biol Chem* **275,** 16738-45.
24. Gladwin, M. T., Lancaster, J. R., Jr., Freeman, B. A. & Schechter, A. N. (2003) *Nat Med* **9,** 496-500.

APPENDICES

APPENDIX A

NITRIC OXIDE IN THE HUMAN RESPIRATORY CYCLE

Nitric oxide in the human respiratory cycle

TIMOTHY J. MCMAHON[1], RICHARD E. MOON[1,2], BEN P. LUCHSINGER[4], MARTHA S. CARRAWAY[1,2], ANNE E. STONE[1,3], BRYANT W. STOLP[2], ANDREW J. GOW[1], JOHN R. PAWLOSKI[1], PAULA WATKE[2], DAVID J. SINGEL[4], CLAUDE A. PIANTADOSI[1,2] & JONATHAN S. STAMLER[1,3]

Departments of [1]Medicine and [2]Anesthesiology, and [3]Howard Hughes Medical Institute, Duke University Medical Center, Durham, North Carolina, USA
[4]Department of Chemistry, Montana State University, Bozeman, Montana, USA
Correspondence should be addressed to J.S.S.; email: staml001@mc.duke.edu

Published online: 3 June 2002, doi:10.1038/nm718

Interactions of nitric oxide (NO) with hemoglobin (Hb) could regulate the uptake and delivery of oxygen (O_2) by subserving the classical physiological responses of hypoxic vasodilation and hyperoxic vasconstriction in the human respiratory cycle. Here we show that in *in vitro* and *ex vivo* systems as well as healthy adults alternately exposed to hypoxia or hyperoxia (to dilate or constrict pulmonary and systemic arteries *in vivo*), binding of NO to hemes (FeNO) and thiols (SNO) of Hb varies as a function of HbO_2 saturation (FeO_2). Moreover, we show that red blood cell (RBC)/SNO-mediated vasodilator activity is inversely proportional to FeO_2 over a wide range, whereas RBC-induced vasoconstriction correlates directly with FeO_2. Thus, native RBCs respond to changes in oxygen tension (pO2) with graded vasodilator and vasoconstrictor activity, which emulates the human physiological response subserving O_2 uptake and delivery. The ability to monitor and manipulate blood levels of NO, in conjunction with O_2 and carbon dioxide, may therefore prove useful in the diagnosis and treatment of many human conditions and in the development of new therapies. Our results also help elucidate the link between RBC dyscrasias and cardiovascular morbidity.

Red blood cells (RBCs) have important but poorly understood roles in regulation of blood-vessel tone and platelet function[1,2]. Their contribution to vascular homeostasis is demonstrated by the causal relationship between RBC dyscrasias and cardiovascular morbidity. Examples include sickle-cell crisis[3], thalassemias[2,4] and polycythemia[5]. RBC counts also affect pulmonary[6] and systemic[7] blood pressure, and elevated hematocrit has been linked to the incidence of stroke[2], stillbirth[8] and ischemic coronary events[9]. In addition, blood transfusions[10], erythropoietin-induced increases in hematocrit[9] and hemoglobin-based blood substitutes[11] are all associated with increased mortality. One explanation that has been offered is that hemoglobin (Hb) regulates nitric oxide (NO) bioavailability, and that an imbalance in the NO:Hb ratio may exist in these disorders. In support of this notion, endogenous NO production protected against cardiovascular morbidity and mortality in transgenic mice overexpressing normal hemoglobin[5] as well as in sickle mice[12].

The interactions of NO with Hb have been considered from two perspectives, one in which NO has served mainly as an analytical surrogate for O_2 (and was thus used at micromolar to millimolar concentrations and/or NO:Hb ≥ 1), and a second in which NO reactions with both hemes and thiols serve as a paradigm for NO function in biology[13–18]. The latter situation is distinguished by low nanomolar amounts of NO at low NO:Hb ratios. Under these conditions, reactions of NO with target sites in the protein are linked to the allosteric properties of Hb (refs. 16,17,19–21), which are identified with an equilibrium between oxygenated (R) and deoxygenated (T) structures[17]. Specifically, the binding of NO groups to reactive thiols (Cysβ93) of Hb is disfavored (and alternatively the binding to hemes is favored) in the T structure, whereas the equilibrium is shifted toward SNO–Hb in oxygenated (R) molecules (equations 1 and 2; Table 1). Accordingly, the ratio of SNO:FeNO is thought to follow oxygen tension (pO_2) *in vivo*[13,16].

The reactions of NO with heme irons and cysteine thiols of Hb have considerable importance from the standpoint of NO bioactivity. Kinetic measurements and bioassay data indicate that heme iron functions to capture NO bioactivity, whereas cysteine thiols function in NO delivery[13,16,20]. NO group release from Cysβ93 in Hb takes place more readily in the deoxygenated (or high spin/T) structure[13,19,22,23]. Accordingly, it has been proposed that dispensing of NO groups is coupled to the deoxygenation- or oxidation-induced allosteric transition in Hb, during which NO groups are transferred to acceptor thiols (RSH) such as glutathione[16,24], or those in the RBC membranes that transduce NO bioactivity[24,25], thereby dilating blood vessels[13,16,19,25] (equations 3 and 4; Table 1); NO within the RBC membrane may also improve RBC rheology[26]. In this model, the generation of RSNO bioactivity through the O_2 dependence of NO–Hb reactions inevitably entails some production of Hb[FeNO] (refs. 19,22) (equations 1 and 2; Table 1).

The potential importance of the vasodilator (and rheological) properties of RBCs can be understood by appreciating that the principal function of RBCs is O_2 delivery, which is primarily determined by blood flow[13,19]. It may therefore be predicted that RBCs possess an intrinsic capacity for regulating their principal

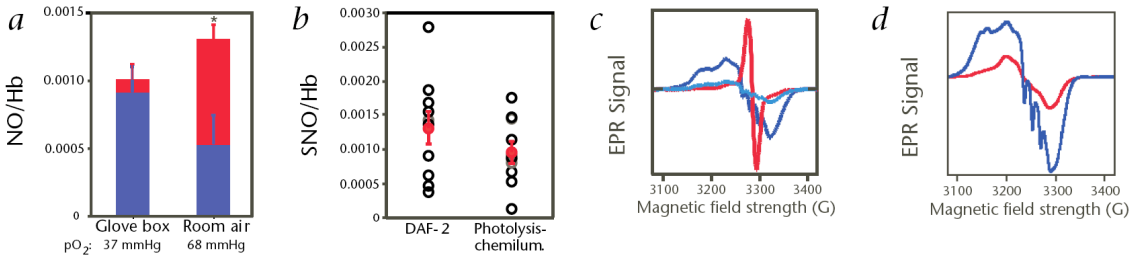


Fig. 1 Oxygenation/deoxygenation-dependent NO reactions in human blood and hemoglobin. ***a***, Levels of SNO–Hb (■) and Hb[FeNO] (■) in paired samples of venous blood processed either in room air or in a glove box set to maintain the native pO_2 (mmHg). Units are moles NO per mole Hb tetramer. Total Hb-bound NO equals the sum of the two bars for each condition. *, $P < 0.05$, paired *t*-test; difference in SNO–Hb levels between the two groups. Data are the mean ± s.e.m. of 6 experiments. ***b***, Levels of SNO–Hb in paired samples of venous blood measured in room air by either the DAF-2 or photolysis-chemiluminescence methods. The actual and mean data ± s.e.m. from 10 normal individuals are shown; the values did not differ significantly ($P = 0.43$, paired *t*-test). ***c***, Oxygenation/deoxygenation-dependent NO reactions in hemoglobin. The Fe(II)NO EPR spectrum (dark blue) in a deoxy-hemoglobin preparation disappears upon oxygenation, and a free-radical signal (red) appears. Re-deoxygenation removes the globin radical signal and restores the Fe(II)NO signal (light blue). ***d***, EPR signals of Fe(II)NO predominantly located on the β-subunit hemes (red) develop spontaneously in SNO-oxyHb preparations. Deoxygenation yields immediate increases in the Fe(II)NO EPR signal (blue).

physiological function. Studies in the rat brain showing that extracellular SNO–Hb can couple local blood flow to tissue oxygen tension by constricting or dilating blood vessels are supportive of this notion[13] and have led to the proposition that Hb/SNO–Hb in RBCs participates in adaptive physiological responses such as hypoxic vasodilation and hyperoxic vasoconstriction, whose mechanistic basis has been a longstanding mystery. To probe the broader applicability of these ideas, in normal humans, we measured arterial and venous blood levels of Hb–NO, determined the disposition of NO bound in Hb (that is, its site of binding) as a function of pO_2, and correlated these findings with studies of model systems and of RBC bioactivity. These data have been interpreted in the context of simultaneous measurements of systemic and pulmonary hemodynamics (including the first report in humans of hyperoxic pulmonary vasodilation).

Initial studies

Exploratory experiments in which blood was exposed to room air at the time of NO measurement showed a predominance of SNO–Hb relative to Hb[FeNO] not only in arterial blood but also in venous samples obtained under normoxic conditions (Fig. 1*a*). To determine whether the exposure to air in the course of sample handling can affect NO disposition within Hb, triggering the formation of SNO–Hb, we measured levels of SNO–Hb and Hb[FeNO] in human venous blood processed either in room air or in a glove box (O_2 controlled chamber) set to a pO_2 approximating that measured in the venous blood. Under the latter condition (pO_2, 37 ± 4 mmHg), Hb[FeNO] predominated, whereas in the same venous blood handled in room air (pO_2, 68 ± 10 mmHg), SNO–Hb increased significantly ($P < 0.05$ by paired *t*-test) (Fig. 1*a*). These measurements of SNO–Hb obtained by photolysis-chemiluminescence were confirmed using DAF-2 methodology in 10 paired samples (2.62 ± 0.468 μM versus 1.93 ± 0.281 μM, n.s.) (Fig. 1*b*).

Altering sample pH induced similar changes in SNO:FeNO ratio (data not shown). These data suggested that (both homo- and heterotropic) allosteric effectors influence the disposition of NO bound to human Hb, and they underscore the importance of controlling independent variables that affect Hb allostery[15]. In subsequent experiments (unless otherwise stated), blood was processed in an O_2-controlled glove box at fixed pCO_2 and pH.

Given that total NO bound to Hb is essentially constant irrespective of pO_2 (Fig. 1*a*), whereas the disposition of the NO bound to hemes and thiols changes, the data are consistent with reports that NO is exchanged between hemes and thiols as a function of pO_2 (refs. 20,22). Although the details of this exchange *in vivo* may involve a system-wide, integrative cardiovascular process, we show that even *in vitro*, minor amounts of Hb[Fe(II)NO] disappear upon oxygenation, as assayed by electron paramagnetic resonance spectroscopy (EPR) (Fig. 1*c*). A free-radical species (variously attributed to a globin-based thiyl or tyrosyl radical[27]), which we find in human blood (data not shown), concomitantly appears (Fig. 1*c*). This interchange of paramagnetic species is reversed by re-deoxygenation (Fig. 1*c*). We also show the spontaneous, albeit slow, evolution of Fe(II)NO species located predominantly on β-subunit hemes (as indicated by the lineshape) in preparations of SNO-oxyHb (Fig. 1*d*). Deoxygenation then leads to a surge in Fe(II)NO signal, with a diminished subunit selectivity (Fig. 1*d*). Overall, these *in vitro* experiments demonstrate the feasibility, at the molecular level, of the chemical transformations implicated by the *ex vivo* measurements in RBCs.

Table 1 Reactions between NO and Hb governed by allosteric principles

CYS-Hb(**[Fe(II)NO]**[Fe(II)]$_3$) + 4 O_2 ↔ CY**SNO**–Hb([Fe(II)O_2]$_4$) + e^- T R	Eq. 1
CYS-Hb(**[Fe(III)NO]**[Fe(II)]$_3$) + 4 O_2 ↔ CY**SNO**–Hb([Fe(II)O_2]$_4$) T R	Eq. 2
SNO–Hb[Fe(II)]O_2 + RSH ↔ R**SNO** + HS-Hb[Fe(II)] + O_2 R T	Eq. 3
SNO–Hb[Fe(II)]O_2 + RSH ↔ R**SNO** + HS-Hb[Fe(III)] + O_2^- R T	Eq. 4

Effect of hypobaric hypoxia on O_2, CO_2 and NO levels

During exposure of human subjects to hypobaric hypoxia (0.56 absolute atmospheres (ATA)), arterial Hb O_2 saturation fell from 95.7 ± 2.5% (baseline mean ± s.d.) to 73.4 ± 7.6% and mixed venous O_2 saturation fell from 75.5 ± 3.4% to 57.1 ± 7.1%. Thus,

Table 2 Effects of hypobaric hypoxia and hyperbaric hyperoxia on blood gases (O_2, CO_2, NO) and hemodynamics

Condition	Normoxia	Hypoxia	Normoxia	Hyperoxia
ATA (FiO_2)	1 ATA (0.21)	0.56 ATA (0.21)	1 ATA (0.21)	3 ATA (1.0)
a.				
Mixed Venous:				
PvO_2 (mmHg)	43 ± 1.9	30 ± 3.2	42 ± 3.0	399 ± 181.3
SvO_2 (%)	75.5 ± 3.4	57.1 ± 7.1	75 ± 4.7	97.7 ± 2.5
pH	7.39 ± 0.02	7.44 ± 0.02	7.39 ± 0.02	7.37 ± 0.02
HbNO *	1.53 ± 0.43	1.45 ± 0.34	1.95 ± 0.98	1.41 ± 0.34
Arterial:				
PaO_2 (mmHg)	94 ± 8.1	38 ± 4.9	91 ± 8.0	1542 ± 234.3
SaO_2 (%)	95.7 ± 2.5	73.4 ± 7.6	95.8 ± 2.6	99.1 ± 0.7
pH	7.40 ± 0.02	7.46 ± 0.02	7.41 ± 0.02	7.42 ± 0.03
$PaCO_2$ (mmHg)	37 ± 3.0	32 ± 2.5	37 ± 2.9	36 ± 2.6
HbNO *	2.13 ± 0.59	1.19 ± 0.31	2.22 ± 0.93	1.66 ± 0.77
b.				
MAP (mmHg)	86 ± 27	87 ± 28	86 ± 26	95 ± 9
SVR (dynes sec cm^{-5})	1061 ± 375	762 ± 284	918 ± 378	1286 ± 309
PAP (mmHg)	13.0 ± 5	18.1 ± 6	13.4 ± 5	12.4 ± 2
PVR (dynes sec cm^{-5})	64 ± 31	83 ± 33	57.5 ± 24	41 ± 11
CO (l/min)	6.5 ± 1.1	9.1 ± 1.9	7.5 ± 1.5	5.85 ± 1.0

a, Blood gases. Hb O_2 saturation (SO_2), total Hb–NO (HbNO) and other blood gas parameters in normal humans under conditions of normoxia (1 ATA), hypobaric hypoxia (0.56 ATA) and hyperbaric hyperoxia (100% O_2 + 3 ATA). *, HbNO is expressed as moles NO/10^3 moles Hb, and did not differ between any two conditions. ***b***, Hemodynamics under conditions in *a* above. Data are the mean ± s.d. of 11–12 normal humans.

the O_2 saturation of arterial blood in hypobaric hypoxia approximated that of mixed venous blood in normoxia (baseline) (Table 2*a*). Mild respiratory alkalosis, reflecting hyperventilation, was also observed (Table 2*a*).

At baseline, venous blood contained mainly Hb[FeNO], whereas SNO–Hb and Hb[FeNO] were present in approximately equal amounts in arterial blood (Fig. 2*a*). The total levels of Hb–NO (SNO+ FeNO) did not differ significantly from artery to vein. In contrast, in hypobaric hypoxia Hb[FeNO] predominated in both artery and vein (Fig. 2*b*). Thus, under low pO_2 conditions that promote the T state in both artery and vein, Hb[FeNO] levels rose relative to and at the expense of SNO–Hb.

Effect of hypobaric hypoxia on hemodynamics

Exposure of human subjects to hypobaric hypoxia resulted in significant increases in pulmonary arterial pressure (PAP) and pulmonary vascular resistance (PVR) (Table 2*b*), consistent with hypoxic pulmonary vasoconstriction (HPV). Cardiac output rose from 6.5 ± 1.1 l/min to 9.1 ± 1.9 l/min. However, mean systemic arterial pressure (MAP) remained unchanged because systemic vascular resistance (SVR) decreased, consistent with hypoxic vasodilation of systemic vessels (Table 2*b*).

Effect of hyperbaric hyperoxia on O_2, CO_2 and NO levels

Blood gases and hemodynamic parameters measured during a second baseline period at sea level (following hypobaric hypoxia) showed a return to initial baseline values (Table 2*a* and *b*). SNO–Hb and Hb[FeNO] levels in both arterial and mixed venous blood also recovered and did not differ significantly from those obtained during the first baseline period (Fig. 2*c*). Moreover, total Hb–NO levels in arterial blood did not differ significantly from those in mixed venous blood. When the Hb O_2 saturation gradient from artery to vein was eliminated by exposure to 3 ATA + 100% O_2 (that is, $SvO_2 \approx SaO_2$), arterial-venous differences in levels of SNO–Hb and Hb[FeNO] were no longer seen; instead, SNO–Hb was abundant in both arterial and mixed venous blood (Fig. 2*d*).

Effect of hyperbaric hyperoxia on hemodynamics

Human subjects exposed to hyperbaric hyperoxia experienced significant decreases in PAP and PVR (Table 2*b*), consistent with hyperoxic pulmonary vasodilation. Cardiac output fell from 7.5 ± 1.5 l/min to 5.85 ± 1.0 l/min while MAP and SVR increased, a response consistent with hyperoxic vasoconstriction in the systemic circulation (Table 2*b*).

Correlation between SNO–Hb levels and Hb O_2 saturation

In an analysis of arterial and mixed venous samples drawn under all conditions (normoxia, hypoxia and hyperoxia), both the absolute concentration of SNO–Hb and the fraction of total Hb–NO present as SNO–Hb were found to correlate significantly ($P = 0.043$ and $P = 0.0034$, respectively; ANOVA) with Hb O_2 saturation (Fig. 2*e*), but not with pO_2 (Fig. 2*f*). However, SNO–Hb correlated with pO_2 between 0 and 150 mmHg ($P = 0.005$), that is, when hyperoxic samples (> 99% saturation) were excluded from the analysis. This pattern of correlation is consistent with the notion that *S*-nitrosylation is dependent on the allosteric state of Hb rather than on O_2 concentration (and related chemistry via N_2O_3).

O_2-dependent bioactivity of native human RBCs

We have previously suggested that NO-dependent, Hb-regulated blood vessel dilation, involving NO group transfer from SNO–Hb to the RBC membrane (band 3 protein)[25], is controlled by pO_2. Because the arterial system is exposed to an O_2 gradient and tissue pO_2 is in the range of 4–20 mmHg (refs. 28,29), we assessed in detail the relationship between pO_2 and the bioactivity of native human RBCs in both pulmonary artery and thoracic aorta. At 20% O_2 (to simulate alveolar and central arterial pO_2), RBCs elicited marked vasoconstriction in both pulmonary arterial and aortic rings (Fig. 3*a*), whereas the addition of RBCs at pO_2 found in respiring tissues (~1% O_2)[28,29] produced a prompt vasorelaxation (followed by a delayed vasoconstriction once the endogenous NO bioactivity had been spent) (Fig. 3*a* and *b*). Moreover, at 0.5–10% O_2 (pO_2 ~3–65 mmHg), conditions which mimic the

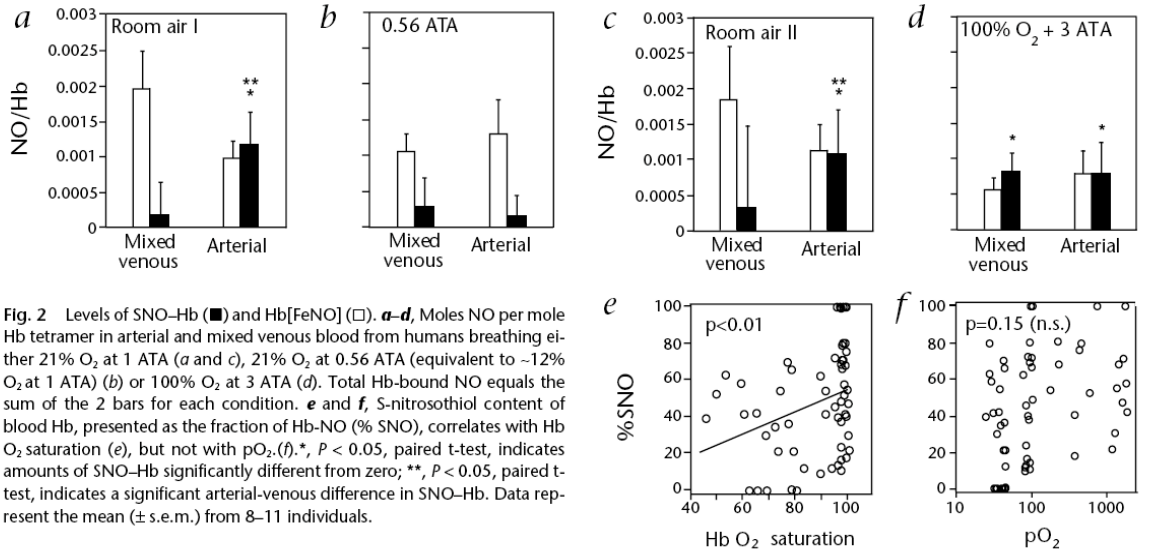


Fig. 2 Levels of SNO–Hb (■) and Hb[FeNO] (□). ***a–d***, Moles NO per mole Hb tetramer in arterial and mixed venous blood from humans breathing either 21% O_2 at 1 ATA (*a* and *c*), 21% O_2 at 0.56 ATA (equivalent to ~12% O_2 at 1 ATA) (*b*) or 100% O_2 at 3 ATA (*d*). Total Hb-bound NO equals the sum of the 2 bars for each condition. ***e*** and ***f***, S-nitrosothiol content of blood Hb, presented as the fraction of Hb-NO (% SNO), correlates with Hb O_2 saturation (*e*), but not with pO_2.(*f*).*, $P < 0.05$, paired t-test, indicates amounts of SNO–Hb significantly different from zero; **, $P < 0.05$, paired t-test, indicates a significant arterial-venous difference in SNO–Hb. Data represent the mean (± s.e.m.) from 8–11 individuals.

physiological O_2 gradient in arterioles, human RBCs produced graded vasorelaxant activity that was inversely related to pO_2 (Fig. 3*b*). Further loading of RBCs with physiological amounts of NO (NO:heme ratios, 1:1,000–1:100) increased the O_2-dependent vasodilator activity in a dose-dependent manner[25] (data not shown). By comparison, cell-free Hb devoid of NO produced contractions that tended to be somewhat greater at lower pO_2 (ref. 13), whereas *S*-nitrosoglutathione (~1-5 nM) produced comparable relaxations that were largely independent of pO_2 (Fig. 3*c*). RBC-mediated relaxation was also seen when endothelial NO synthase (eNOS) was inhibited (data not shown). Our data implicate a role for RBCs in the classical phenomena of hyperoxic vasoconstriction and hypoxic vasodilation and, more generally, in fine-tuning of blood vessel tone in response to pO_2 (Fig. 4).

Discussion

Hemoglobin alternates between two quaternary structures (R and T) that differ in their affinity for NO, O_2 and CO_2. Oxygen saturation governs the equilibrium between R and T structures (when the concentration of all other allosteric modulators is fixed). Under physiological conditions, S-nitrosylation is favored in the R structure whereas the propensity for NO to bind hemes (relative to thiols) is increased in the T state[16,20,21,22]. The cooperative function of Hb in binding O_2 and its disposition toward binding NO groups are thermodynamically linked[19,21] (Fig. 2). Accordingly, NO bioactivity provided by SNO–Hb is inevitably dependent on pO_2, as has been demonstrated pharmacologically both *in vitro* and *in vivo*[13,16,19,22]. These findings suggested a possible molecular basis for the unknown sensor and signal that actuate the rapid, graded responses of blood vessels to pO_2 *in vivo* (distinct from the background responses of isolated blood vessels *in vitro*).

This model has the following requirements: 1) SNO–Hb should be favored in arterial blood; 2) the partitioning between Hb[FeNO] and SNO–Hb (equations 1 and 2) should be regulated by O_2 saturation in the human circulation; 3) RBCs should be capable of constricting as well as dilating blood vessels; and 4) the vasoactivity of RBCs should be critically dependent on pO_2 and

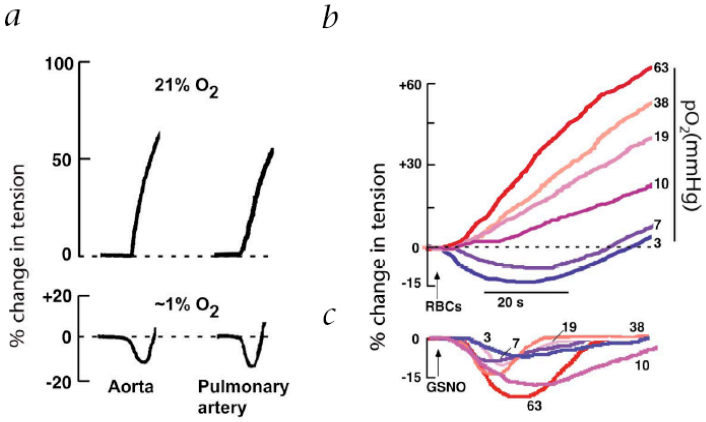


Fig. 3 RBC-mediated hypoxic vasodilation and hyperoxic vasoconstriction. Aortic or pulmonary arterial rings from rabbits were preconstricted to ~2 g isometric tension with phenylephrine in all experiments. ***a***, Representative vascular responses to native human RBCs as a function of initial O_2 tension. RBCs (0.4% final Hct) were added to tissue baths bubbled with 5% CO_2, varying % O_2, and balance N_2. RBCs elicited vasoconstriction at 21% O_2, and biphasic responses, characterized by initial vasorelaxation, at ~1% O_2 (pO_2, 7 mmHg). ***b***, Graded relaxation (and switch from contraction to relaxation) by RBCs as a function of pO_2 ranging from 0.5% O_2 (pO_2 = 3 mmHg) to ~10% O_2 (pO_2 = 63 mmHg). Data are representative of 3–8 experiments for each set of conditions. ***c***, S-nitrosoglutathione (GSNO, 3nM)-induced vasorelaxation over the range of pO_2 from 3 to 63 mmHg.

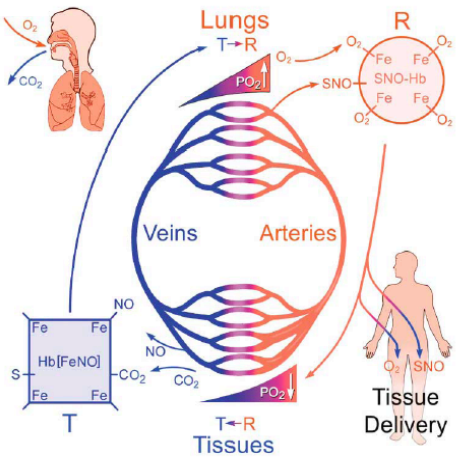


Fig. 4 Simplified 2-state model of the human respiratory cycle: a 3-gas system involving NO, CO_2 and O_2. In this model, allosteric effectors O_2 and CO_2 govern the equilibrium between R and T structures of Hb, which in turn dictates whether NO bioactivity is dispensed to dilate blood vessels or sequestered to constrict them; dynamic and graded changes in arteriolar tone are conjectured to couple blood flow to metabolic demand ('hypoxic vasodilation and hyperoxic vasoconstricion'). NO bioactivity can also be rationalized in terms of equilibrium between SNOs in the blood and tissues, the position of which is regulated by the allosteric state of hemoglobin. Two populations of Hb are present in RBCs: a cytosolic form, which mainly subserves O_2 and CO_2 delivery, and a membrane-bound form, which mainly subserves NO processing (not illustrated).

thus capable of transducing an O_2 gradient into a graded physiological response. Here we verify these predictions in healthy humans. Our findings thus suggest not only that NO is a critical component of the human respiratory cycle—a third gas, which functions to regulate O_2 delivery—but also that RBCs contribute significantly to the classical physiological responses of hypoxic vasodilation and hyperoxic vasoconstriction (Fig. 4); our data thus provide a mechanistic basis for a long-standing mystery.

The amounts of NO bound to Hb that we measure in human blood (~1:1000 NO per Hb tetramer, 1–3 μM) using two different methods are similar to those we have previously measured in rodents (0.3–3 μM)[13,16]. These data are consistent with one mass spectroscopic[30] and two EPR (refs. 31,32) studies on human blood that detected micromolar concentrations of FeNO, and with chemical analyses of blood from 5 rats[23] and 19 human babies[33] in which micromolar levels of SNO–Hb were detected. They are also consistent with EPR measurements in the mouse[34], rat[31,35] and sheep[36] that show basal Hb[Fe(II)NO] concentrations in the range of 1–3 μM. Although the EPR signature from Hb[Fe(II)NO] is unequivocal in these studies, some groups have not been able to confirm these measurements. Factors that may influence Hb–NO detectability include: the inherent sensitivity limit of typically used methods (1–10 μM in blood); variability of the 5 (versus 6) coordinate components of the EPR spectrum[34,36], which further influences both the sensitivity and specificity of the spectroscopy; the formation of species such as Fe[(III)NO] (refs. 22,27) or SNO which are not detected by EPR (Fig. 1*c* and *d*); a large and notable natural variation in the Hb–NO levels (to be contrasted with O_2 and CO_2 levels) (Fig. 1*b*; Table 2*a*), and major differences in the way samples are processed[13,16,30–33,37]. For example, Gladwin *et al.* used a method based on I_3^- (ref. 37) (and other chemicals), which generates thick precipitates in hyperosmolar multicomponent solutions. In addition, those measurements were made long after venipuncture, at pH 10, without controlling for CO_2 and pO_2. In contrast, our measurements are made on blood Hb in buffers whose composition affects Hb allostery in known ways (for example, via PO_4^{3-}, Cl^-, HCO_3^- and O_2) and which is then processed and purified within one minute[14]. Caution is therefore warranted in the use of NO:Hb assays that rely on chemical reagents that affect Hb allostery and chemistry, and whose effects are likely to be different for the partially nitrosylated species present in blood than for the standards used in assays[37]. We suggest that EPR and photolysis-based techniques, which are well-established probes of NO–Hb interactions, are methods of choice.

Our data show that the SNO:FeNO ratio is a function of HbO_2 saturation, and not simply of pO_2 (which might conceivably have had a chemical basis in the formation of nitrosating species, such as N_2O_3), and are thus consistent with both previous mechanistic studies (excluding N_2O_3 involvement under physiological conditions[20,21]) and the linkage between O_2-governed allostery and the SNO to FeNO chemical dynamic. The amount of NO bound to Hb appears essentially constant during arterial-venous cycling (Fig. 2), consistent with the small amounts of SNO needed to regulate blood flow (~0.1% of total Hb–NO), but the relative amounts of SNO and FeNO, that is, the position of the equilibrium between NO bound to hemes and thiols in Hb, varies (equations 1–4; Table 1). Hb O_2 saturation alone is sufficient for regulating this variation (Figs. 1 and 2), although Hb allostery *in vivo*, of course, is regulated by multiple variables that undergo rapid change as RBCs move through the circulation.

The mechanisms by which hypoxia elicits regional and organ-specific changes in vascular tone and blood flow (specifically, vasoconstriction in the lung and vasodilation in peripheral vascular beds) are multifactorial[38–41] and poorly understood. It is important to note that isolated blood vessels are incapable of the rapid responses to small changes in pO_2 that occur *in vivo* to alter blood flow, and thereby match ventilation with perfusion in the lungs and the delivery of O_2 with tissue metabolic requirements. Moreover, eNOS activity (endothelium-derived relaxing factor, EDRF) is directly dependent on O_2 and is thus paradoxically impaired in proportion to hypoxia; eNOS primarily transduces shear, rather than hypoxia-mediated vasodilation. It has even been shown that low pO_2 increases NO production in peripheral organs independently of NOS activity[42], implicating a role for a blood-borne O_2 sensor and NO delivery agent in the phenomenon of hypoxic vasodilation. In the present work we show in humans that a degree of hypoxia sufficient to bring about changes in SNO–Hb levels converts normal RBCs from constrictors to vasodilators, and is associated with a decrease in SVR of over 25%. It should be emphasized that minimal fluxes of SNO, on the order of only 1–10 nM (refs. 19,43) (Fig. 3*c*), are sufficient to bring about this degree of change (as SVR/PVR are functions of vessel radius to the fourth power); such fluxes would be scarcely detectable against a micromolar NO background (Fig. 2). Collectively, the data suggest that RBCs themselves are O_2 sensors that regulate peripheral blood flow for the purpose of O_2 delivery, contributing to the classical physiological responses of hypoxic vasodilation and hyperoxic vasoconstriction, and in fact provide the only cellular mechanism shown to be capable of

transducing a physiological oxygen gradient (~90–3 mmHg) into graded vasodilator activity (Fig. 3).

Our observation that hyperoxia lowers PVR is the first such report in humans, but the involvement of RBCs remains to be determined. In contrast, it has been clearly shown that hypoxic pulmonary vasoconstriction (HPV) is dependent on Hb (ref. 6), and this dependence is well rationalized by the sequestration of endothelial NO by the hemes of T-structured molecules[6,20,21]. However, it is also true that HPV is partially opposed and thereby modulated by endogenous NO bioactivity[44], which is derived at least partly from the endothelium of moderately hypoxic alveolar regions. In contrast, eNOS activity would fall in extremely hypoxic alveolar units where the contribution of SNO–Hb to NO bioactivity would be accentuated. Such coordinated and complementary effects of NO derived from both endothelium and RBCs could serve to optimize ventilation/perfusion matching.

There is a well established clinical disconnect between the O_2 content of blood and the delivery of O_2 to tissues. The major determinant of O_2 delivery is the flow of oxygenated blood in the microcirculation rather than O_2 saturation. The importance of this distinction is brought into focus by the increase in mortality and ischemic events associated with blood transfusions[10,45], erythropoietin-mediated normalization of hematocrit[9], and Hb-based blood substitutes[11]. Blood flow is controlled, in part, by NO/SNO. Our data thus raise the possibility that the NO level in blood may provide an index of microcirculatory flow of importance in clinical decision-making (Fig. 4). Specifically, the ability to monitor and manipulate levels of RBC-NO may prove useful in the assessment of blood gases, in the diagnosis and treatment of diseases of the heart, lung and blood, and in the rational development of therapeutics, including NO donors, erythropoietin therapy and blood substitutes.

Methods

Exploratory measurements in venous blood. Human venous blood was drawn via an antecubital vein. Hb–NO was measured in paired samples processed either in room air or in an O_2-controlled glove box (as described below).

Approval bodies. All human experiments were approved by the Institutional Review Board of Duke University Medical Center, and the animal studies were approved by the Animal Care and Use Committe.

Measurement of Hb–NO. Photolysis-chemiluminescence and DAF-2 are complementary methods: SNO–Hb is measured as the loss or gain in signal produced by $HgCl_2$ (6-fold excess over Hb), respectively.

Photolysis-chemiluminescence. RBCs were processed in fixed concentrations of allosteric effectors as described below. Hemolysate protein (~99% Hb) was partially purified by gel filtration (5,000*g*, 60 s) over a G-25 fine Sephadex chromatography column (Pharmacia, Uppsala, Sweden) (25-fold volume excess) equilibrated with PBS (pH 7.40, with 0.5 mM EDTA). An airtight Hamilton glass syringe was used to transfer 90 μl of sample (final [Hb], 100 μM) for injection as described[14]. The specificity of the method for SNO and FeNO has been recently verified in yeast deficient in enzymes that control levels of FeNO and SNO, respectively, as well as mice deficient in SNO-metabolizing activity (data not shown).

DAF-2 assay. For DAF-2 assays, one half of the hemolysate was adjusted to 100 μM Hb with PBS-containing DAF-2 (final pH 7.4) either with or without $HgCl_2$, and incubated for 10 min. Centricon 10-kD filters (10,600*g*, 20 min) were then used to exclude Hb prior to fluorescence measurement. The filtrates were transferred to microplates (Dynex Technologies, Southhampton, UK) and treated with acid (0.4 N HCl, final concentration) to generate nitrosating equivalents and then with excess NaOH to maximize fluorescence (excitation and emission: 485 nm and 520 nm, respectively). Standard curves were constructed using SNO–Hb[19].

Electron paramagnetic resonance spectroscopy (EPR). Spectroscopy was carried out as described[21]. The Fe(II)NO-spiked hemoglobin samples were prepared in PBS pH 7.4, 300 μM nitrite, with a heme concentration of 1 mM, and an Fe(II)NO concentration of 50 μM. SNO-oxyhemoglobin samples (0.5 mM protein) were prepared as described[16].

Experimental protocol for manipulation of O_2 tension *in vivo*. After signing informed consent, each subject underwent physical examination, electrocardiography, chest radiography, spirometry and blood hemoglobin (Hb) measurement to establish normal health. On the day of study, volunteers underwent right heart catheterization (with placement of a Swan–Ganz catheter) and radial arterial catheter placement under topical anesthesia. Cardiac output (CO, thermodilution method), pulmonary artery pressure (PAP), pulmonary capillary wedge pressure (PCWP) and systemic arterial pressures (MAP) were monitored continuously throughout the study (SVR and PVR were derived). The subjects were then exposed to changes in atmospheric pressure in a temperature-controlled environmental chamber. Each subject was accompanied by at least two inside tenders, including a physician. In addition, a physician outside the chamber continuously monitored the study. Subjects were sequentially exposed to the following: 1) normoxia (baseline I), 21% O_2 (room air) at normobaric pressure of 1 ATA (~760 Torr); 2) hypobaric hypoxia, 21% O_2 at hypobaric pressure of 0.56 ATA (~429 Torr) (simulating altitude); 3) normoxia (baseline II), 21% O_2 at normobaric pressure of 1 ATA; and 4) hyperbaric hyperoxia, 100% O_2 at hyperbaric pressure of 3 ATA (~2280 Torr) (simulating depth).

Changes in atmospheric pressure lasted until blood gases and hemodynamics had equilibrated, and did not exceed 50 min, whereas the normoxic periods lasted 30 min. Steady-state hemodynamics (CO, PCWP, PAP, PVR, MAP and SVR) and arterial and mixed venous blood measurements (pH, blood gases, and Hb–NO) were obtained during each maneuver with the subject in the supine position. Inspired gas was supplied *via* a mouthpiece (with a noseclip in place).

Blood sample acquisition and processing. Blood samples were drawn into gas-tight blood gas syringes containing sodium heparin and placed on ice. Blood-gas analysis for pO_2, pCO_2 and pH was performed within 10 min of obtaining the samples, and processing for Hb–NO content was performed within 60 min. Blood-gas analysis at 3 ATA was performed in the hyperbaric chamber using an Instrumentation Laboratories (Barcelona, Spain) Model 113 blood gas/pH analyzer calibrated at 3 ATA. Samples drawn at 3 ATA and arterial blood at 1 ATA were processed further in room air. Mixed venous samples obtained in room air and both arterial and mixed venous blood samples obtained under hypobaric conditions were processed in an oxygen-controlled glove box (Coy Instruments, Grass Lake, Michigan) (5% CO_2/balance N_2) set to a pO_2 closely approximating the measured pO_2 of the sample(s) (4.9% average), and which in no individual was more than 10% different from the actual pO_2. Buffers and reagents used in the measurement of Hb–NO were prepared the night prior to an experiment and left to equilibrate either in the glove box (set to 4.5% O_2) or on the benchtop (1 ATA) overnight. Compensation for the minimal, evaporative loss of reagents overnight was made at the beginning of an experiment using similarly handled (for example, partially deoxygenated) deionized water.

Bioassay experiments. New Zealand white rabbits were anesthetized with sodium pentobarbital and killed. The thoracic aorta and second- or third-order pulmonary arteries were collected. Rings (3 mm) were mounted in tissue baths filled with Krebs–Henseleit solution (pH 7.4) and bubbled with mixtures of varying percentages of O_2/5% CO_2/bal N_2 (producing pO_2s ranging from 3 to 100 mmHg) as described[19]. Precontraction to ~2 g resting tension was accomplished with phenylephrine (Sigma). PBS-washed RBCs were added to produce a 0.4% final hematocrit in the tissue baths.

Acknowledgments

We thank Y. Yan for technical assistance. This work was supported by grants from the NIH (K08 HL04014 to T.J.M.; HL04424-09 to C.A.P.), and NSF (MCB-0091228 to D.J.S.).

Competing interests statement

The authors declare that they have no competing financial interests.

RECEIVED 5 FEBRUARY; ACCEPTED 30 APRIL 2002

1. Andrews, D.A. & Low, P.S. Role of red blood cells in thrombosis. *Curr. Opin. Hematol.* **6**, 76–82 (1999).
2. Hart, R.G. & Kanter, M.C. Hematologic disorders and ischemic stroke. A selective review. *Stroke* **21**, 1111–1121 (1990).
3. Embury, S.H., Mohandas, N., Paszty, C., Cooper, P. & Cheung, A.T. *In vivo* blood flow abnormalities in the transgenic knockout sickle cell mouse. *J. Clin. Invest.* **103**, 915–920 (1999).
4. Reddy, P.L., Bowie, L.J. & Callistein, S. Binding of nitric oxide to thiols and hemes in hemoglobin H: implications for α-thalassemia and hypertension. *Clin. Chem.* **43**, 1442–1447 (1997).
5. Ruschitzka, F.T. *et al*. Nitric oxide prevents cardiovascular disease and determines survival in polyglobulic mice overexpressing erythropoietin. *Proc. Natl. Acad. Sci. USA* **97**, 11609–11613 (2000).
6. Deem, S., Swenson, E.R., Alberts, M.K., Hedges, R.G. & Bishop, M.J. Red-blood-cell augmentation of hypoxic pulmonary vasoconstriction: hematocrit dependence and the importance of nitric oxide. *Am. J. Respir. Crit. Care Med.* **157**, 1181–1186 (1998).
7. Cirillo, M., Laurenzi, M., Trevisan, M. & Stamler, J. Hematocrit, blood pressure, and hypertension. The Gubbio Population Study. *Hypertension* **20**, 319–326 (1992).
8. Stephansson, O., Dickman, P.W., Johansson, A. & Cnattingius, S. Maternal hemoglobin concentration during pregnancy and risk of stillbirth. *JAMA* **284**, 2611–2617 (2000).
9. Besarab, A. *et al*. The effects of normal as compared with low hematocrit values in patients with cardiac disease who are receiving hemodialysis and epoetin. *N. Engl. J. Med.* **339**, 584–590 (1998).
10. Hebert, P.C. *et al*. A multicenter, randomized, controlled clinical trial of transfusion requirements in critical care. Transfusion Requirements in Critical Care Investigators, Canadian Critical Care Trials Group. *N. Engl. J. Med.* **340**, 409–417 (1999); erratum: **340**, 1056 (1999).
11. Ketcham, E.M. & Cairns, C.B. Hemoglobin-based oxygen carriers: development and clinical potential. *Ann. Emerg. Med.* **33**, 326–337 (1999).
12. French, J.A., 2nd *et al*. Mechanisms of stroke in sickle cell disease: sickle erythrocytes decrease cerebral blood flow in rats after nitric oxide synthase inhibition. *Blood* **89**, 4591–4599 (1997).
13. Stamler, J.S. *et al*. Blood flow regulation by S-nitrosohemoglobin in the physiological oxygen gradient. *Science* **276**, 2034–2037 (1997).
14. McMahon, T.J. & Stamler, J.S. Concerted nitric oxide/oxygen delivery by hemoglobin. *Methods Enzymol.* **301**, 99–114 (1999).
15. Antonini, E. & Brunori, M. Hemoglobin and myoglobin in their reactions with ligands. in *Frontiers in Biology* (ed. Neuberger, A. & Tatum, E.L.) 13 (Elsevier, Amsterdam, 1971).
16. Jia, L., Bonaventura, C., Bonaventura, J. & Stamler, J.S. S-nitrosohaemoglobin: a dynamic activity of blood involved in vascular control. *Nature* **380**, 221–226 (1996).
17. Perutz, M.F., Wilkinson, A.J., Paoli, M. & Dodson, G.G. The stereochemical mechanism of the cooperative effects in hemoglobin revisited. *Annu. Rev. Biophys. Biomol. Struct.* **27**, 1–34 (1998).
18. Stamler, J.S., Lamas, S. & Fang, F.C. Nitrosylation. The prototypic redox-based signaling mechanism. *Cell* **106**, 675–683 (2001).
19. McMahon, T.J., Stone, A.E., Bonaventura, J., Singel, D.J. & Stamler, J.S. Functional coupling of oxygen binding and vasoactivity in S-nitrosohemoglobin. *J. Biol. Chem.* **275**, 16738–16745 (2000).
20. Gow, A.J. & Stamler, J.S. Reactions between nitric oxide and haemoglobin under physiological conditions. *Nature* **391**, 169–173 (1998).
21. Gow, A.J., Luchsinger, B.P., Pawloski, J.R., Singel, D.J. & Stamler, J.S. The oxyhemoglobin reaction of nitric oxide. *Proc. Natl. Acad. Sci. USA* **96**, 9027–9032 (1999).
22. Pezacki, J.P., Ship, N.J. & Kluger, R. Release of nitric oxide from S-nitrosohemoglobin. Electron transfer as a response to deoxygenation. *J. Am. Chem. Soc.* **123**, 4615–4616 (2001).
23. Padron, J., Peiro, C., Cercas, E., Llergo, J.L. & Sanchez-Ferrer, C.F. Enhancement of S-nitrosylation in glycosylated hemoglobin. *Biochem. Biophys. Res. Commun.* **271**, 217–221 (2000).
24. Lipton, A.J. *et al*. S-nitrosothiols signal the ventilatory response to hypoxia. *Nature* **413**, 171–174 (2001).
25. Pawloski, J.R., Hess, D.T. & Stamler, J.S. Export by red blood cells of nitric oxide bioactivity. *Nature* **409**, 622–626 (2001).
26. Tsuda, K., Kimura, K., Nishio, I. & Masuyama, Y. Nitric oxide improves membrane fluidity of erythrocytes in essential hypertension: an electron paramagnetic resonance investigation. *Biochem. Biophys. Res. Commun.* **275**, 946–954 (2000).
27. Balagopalakrishna, C. *et al*. Superoxide produced in the heme pocket of the β-chain of hemoglobin reacts with the β-93 cysteine to produce a thiyl radical. *Biochemistry* **37**, 13194–13202 (1998).
28. Coburn, R.F., Ploegmakers, F., Gondrie, P. & Abboud, R. Myocardial myoglobin oxygen tension. *Am. J. Physiol.* **224**, 870–876 (1973).
29. Gorczynski, R.J. & Duling, B.R. Role of oxygen in arteriolar functional vasodilation in hamster striated muscle. *Am. J. Physiol.* **235**, H505–H515 (1978).
30. Freeman, G., Dyer, R.L., Juhos, L.T., St. John, G.A. & Anbar, M. Identification of nitric oxide (NO) in human blood. *Arch. Environ. Health* **33**, 19–23 (1978).
31. Kosaka, H. *et al*. Direct proof of nitric oxide formation from a nitrovasodilator metabolised by erythrocytes. *Biochem. Biophys. Res. Commun.* **204**, 1055–1060 (1994).
32. Roccatello, D. *et al*. Early increase in blood nitric oxide, detected by electron paramagnetic resonance as nitrosylhaemoglobin, in haemodialysis. *Nephrol. Dial. Transplant* **12**, 292–297 (1997).
33. Funai, E.F., Davidson, A., Seligman, S.P. & Finlay, T.H. S-nitrosohemoglobin in the fetal circulation may represent a cycle for blood pressure regulation. *Biochem. Biophys. Res. Commun.* **239**, 875–877 (1997).
34. Weinberg, J.B., Gilkeson, G.S., Mason, R.P. & Chamulitrat, W. Nitrosylation of blood hemoglobin and renal nonheme proteins in autoimmune MRL-lpr/lpr mice. *Free Radic. Biol. Med.* **24**, 191–196 (1998).
35. Kohno, M., Masumizu, T. & Mori, A. ESR demonstration of nitric oxide production from nitroglycerin and sodium nitrite in the blood of rats. *Free Radic. Biol. Med.* **18**, 451–457 (1995).
36. Takahashi, Y. *et al*. Nitrosyl hemoglobin in blood of normoxic and hypoxic sheep during nitric oxide inhalation. *Am. J. Physiol.* **274**, H349–H357 (1998).
37. Gladwin, M.T. *et al*. Relative role of heme nitrosylation and β-cysteine 93 nitrosation in the transport and metabolism of nitric oxide by hemoglobin in the human circulation. *Proc. Natl. Acad. Sci. USA* **97**, 9943–9948 (2000).
38. Park, K.H., Rubin, L.E., Gross, S.S. & Levi, R. Nitric oxide is a mediator of hypoxic coronary vasodilatation. Relation to adenosine and cyclooxygenase-derived metabolites. *Circ. Res.* **71**, 992–1001 (1992).
39. Daut, J. *et al*. Hypoxic dilation of coronary arteries is mediated by ATP-sensitive potassium channels. *Science* **247**, 1341–1344 (1990).
40. Pinard, E., Puiroud, S. & Seylaz, J. Role of adenosine in cerebral hypoxic hyperemia in the unanesthetized rabbit. *Brain Res.* **481**, 124–130 (1989).
41. Baur, T.S., Brodowicz, G.R. & Lamb, D.R. Indomethacin suppresses the coronary flow response to hypoxia in exercise trained and sedentary rats. *Cardiovasc Res.* **24**, 733–736 (1990).
42. Heyman, S.N., Goldfarb, M., Darmon, D. & Brezis, M. Tissue oxygenation modifies nitric oxide bioavailability. *Microcirculation* **6**, 199–203 (1999).
43. de Belder, A.J., MacAllister, R., Radomski, M.W., Moncada, S. & Vallance, P.J. Effects of S-nitroso-glutathione in the human forearm circulation: evidence for selective inhibition of platelet activation. *Cardiovasc Res.* **28**, 691–694 (1994).
44. Blitzer, M.L., Loh, E., Roddy, M.A., Stamler, J.S. & Creager, M.A. Endothelium-derived nitric oxide regulates systemic and pulmonary vascular resistance during acute hypoxia in humans. *J. Am. Coll. Cardiol.* **28**, 591–596 (1996).
45. Wu, W.C., Rathore, S.S., Wang, Y., Radford, M.J. & Krumholz, H.M. Blood transfusion in elderly patients with acute myocardial infarction. *N. Engl. J. Med.* **345**, 1230–1236 (2001).

APPENDIX B

UV/VIS DECOMPOSITION IN MATHEMATICA®

```
<< LinearAlgebra`MatrixManipulation`
<< Graphics`MultipleListPlot`
<< Graphics`Colors`
<< Statistics`
A1 =
  ReadList["/Users/luchsing/Desktop/BPLDJS nitrite+deoxypaper 9−26−03/467−700
      w:aux smooth−derivative/deoxyb4NO2− 12−20.txt", Number]; A = A1;

Dim = Dimensions[A]
DIM = Dim[[1]]
W = IdentityMatrix[DIM];
exp = 0;
                 total heme;                                  oxy;
W[[DIM − 5, DIM − 5]] = 10^(exp); W[[DIM − 4, DIM − 4]] = 10^(exp);
               deoxy;                                  met;
W[[DIM − 3, DIM − 3]] = 10^(exp); W[[DIM − 2, DIM − 2]] = 10^(exp);
               IINO;                                IIINO;
W[[DIM − 1, DIM − 1]] = 10^(exp); W[[DIM, DIM]] = 10^(exp);
EPS =
   Import["/Applications9X/ Research useful apps/Mathematica 2.2.2/7−12−01 e=
       deriv w ferricNOsvd2.txt", "Table"];
Dimensions[EPS]
SPE = Transpose[EPS];
g = SPE.W.EPS;
Dimensions[g]
G = Inverse[g];
c = G.SPE.W.A;
Dimensions[c];

Q = Part[c, 1] * 10000000;
R = Part[c, 2] * 10000000;
S = Part[c, 3] * 10000000;
T = Part[c, 4] * 10000000;
U = Part[c, 5] * 10000000;
V = Part[c, 6] * 1;

Z = Q + R + S + T + U;
q = Q / Z * 100;
r = R / Z * 100;
s = S / Z * 100;
t = T / Z * 100;
u = U / Z * 100;
ABSTH = EPS.c;
DELTA = A − ABSTH;
Fdelta = DELTA / A;
WSQDEV = DELTA.W.DELTA
WRMSDEV = (WSQDEV / (DIM))^(1 / 2);

Sd11 = 100 * (WSQDEV * G[[1, 1]])^(1 / 2);
Sd22 = 100 * (WSQDEV * G[[2, 2]])^(1 / 2);
```

```
Sd33 = 100 * (WSQDEV * G[[3, 3]]) ^ (1 / 2);
Sd44 = 100 * (WSQDEV * G[[4, 4]]) ^ (1 / 2);
Sd55 = 10000 * (WSQDEV * G[[5, 5]]) ^ (1 / 2);
Sdtot = (((Sd11) ^ 2 + (Sd22) ^ 2 + (Sd33) ^ 2 + (Sd44) ^ 2) ^ (1 / 2) + (Sd55) ^ 2) ^ (1 / 2);
Sdp1 = 100 * (((Sd11) ^ 2 + (q * Sdtot / 100) ^ 2) ^ (1 / 2)) / Z;
Sdp2 = 100 * (((Sd22) ^ 2 + (r * Sdtot / 100) ^ 2) ^ (1 / 2)) / Z;
Sdp3 = 100 * (((Sd33) ^ 2 + (s * Sdtot / 100) ^ 2) ^ (1 / 2)) / Z;
Sdp4 = 100 * (((Sd44) ^ 2 + (t * Sdtot / 100) ^ 2) ^ (1 / 2)) / Z;
Sdp5 = 100 * (((Sd55) ^ 2 + (u * Sdtot / 100) ^ 2) ^ (1 / 2)) / Z;
Sdptot = (((Sdp1) ^ 2 + (Sdp2) ^ 2 + (Sdp3) ^ 2 + (Sdp4) ^ 2) ^ (1 / 2) + (Sdp5) ^ 2) ^ (1 / 2);
Sdptot % = 100 * Sdtot / Z;

SIM = ColumnForm[ABSTH];
Type["μM Total" Z, "μMoxy" Q, "μMdeoxy" R, "μMmet" S, "μMHbNO" T, "uMFeIIINO" U]
Type["±" Sdtot, "±" Sd11, "±" Sd22, "±" Sd33, "±" Sd44, "±" Sd55]
Type["WSQDEV" WSQDEV, "WRMSDEV" WRMSDEV]
Type["%oxy" q, "%deoxy" r, "%met" s, "%HbNO" t, "%FeIIINO" u, "tot100%"]
Type["±" Sdp1 "%", "±" Sdp2 "%", "±" Sdp3 "%", "±" Sdp4 "%", "±" Sdp5 "%",
  "±" Sdptot "%"]
DELTAPLOT = ListPlot[DELTA];
DELTAPLOT = ListPlot[Fdelta];
DELTAPLOT = ListPlot[A];
DELTAPLOT = ListPlot[ABSTH];

Export["/Users/luchsing/Desktop/BPLDJS nitrite+deoxypaper 9−26−03/467−700 w:
      aux smooth−derivative/deoxyb4NO2− 12−20.txt.fit",
  {"uMTotal" Z, "uMoxy" Q, "uMdeoxy" R, "uMmet" S, "uMHbNO" T, "uMFeIIINO" U,
    "100%Total", "%oxy" q, "%deoxy" r, "%met" s, "%HbNO" t, "%FeIIINO" u,
    "sdTotal±" Sdtot, "uMoxy±" Sd11, "uMdeoxy±" Sd22, "uMmet±" Sd33,
    "uMHbNO±" Sd44, "uMFeIIINO±" Sd55, "%Total±" Sdptot, "%oxy±" Sdp1,
    "%deoxy±" Sdp2, "%met±" Sdp3, "%HbNO±" Sdp4, "%FeIIINO±" Sdp5,
    "offset" V, "WSQDEV" WSQDEV, "WRMSDEV" WRMSDEV, Eigenvalues[G],
    Eigenvectors[G], SIM}, "TABLE"];
```

{234}

234

{234, 6}

{6, 6}

0.0000111294

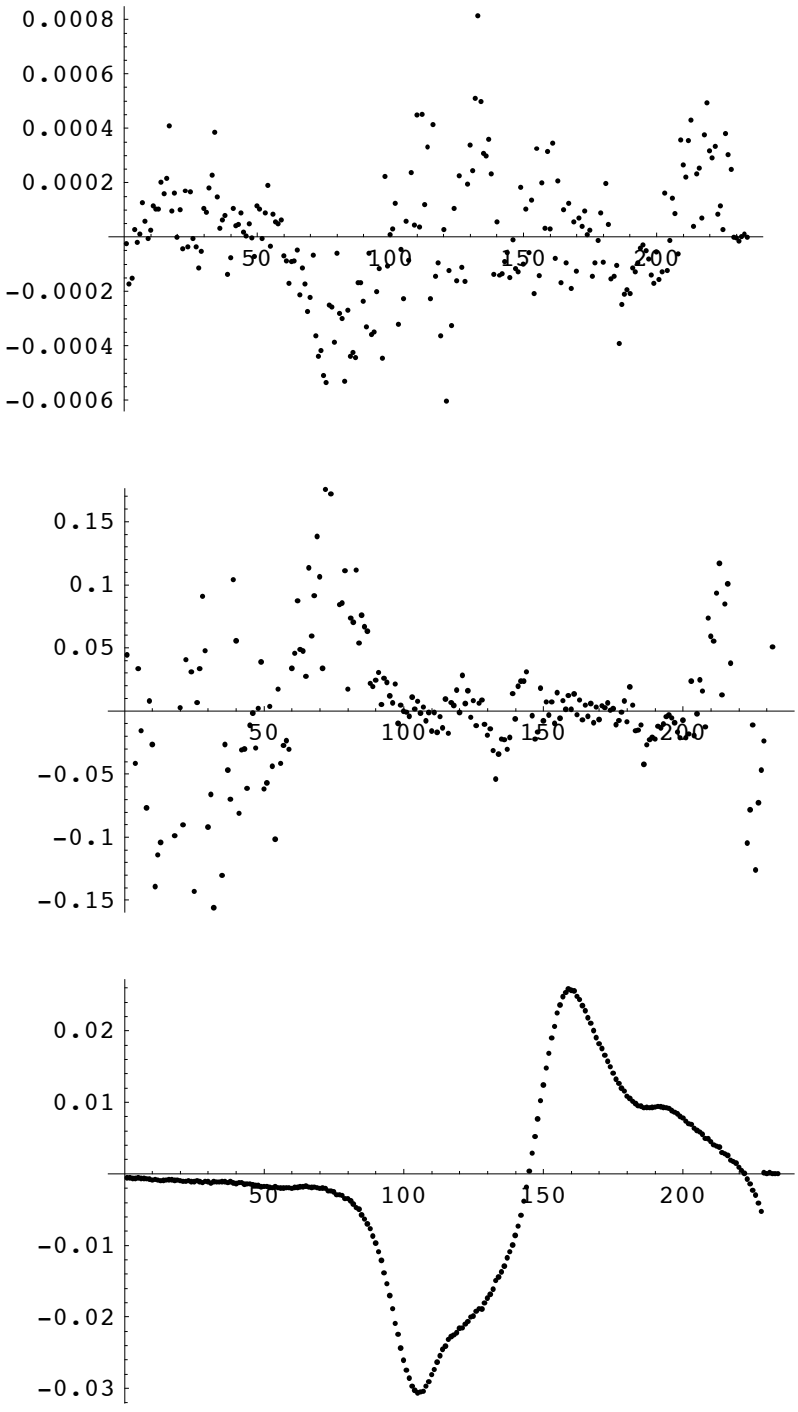
Type[1126.21 μM Total, 42.853 μMoxy, 1010.1 μMdeoxy,
  82.5919 μMmet, −19.0388 μMHbNO, 9.70207 uMFeIIINO]

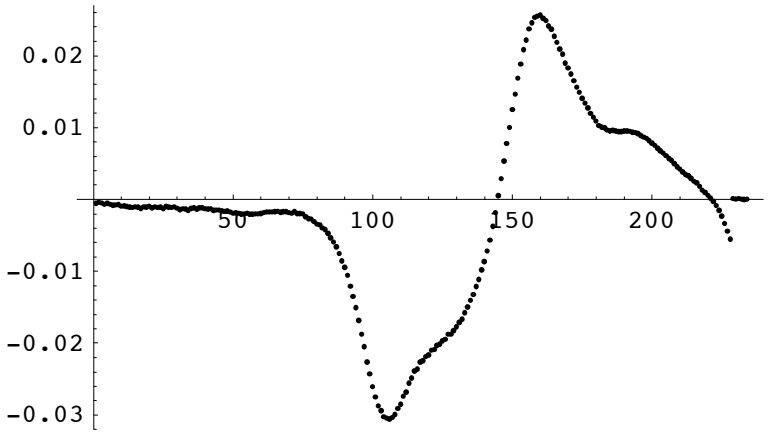
Type[0.0315022 ±, 0.000202922 ±, 0.000360487 ±, 0.000500239 ±, 0.000550778 ±, 0.0118777 ±]

Type[0.0000111294 WSQDEV, 0.000218086 WRMSDEV]

Type[3.80506 %oxy, 89.6904 %deoxy, 7.33361 %met, −1.69052 %HbNO, 0.861478 %FeIIINO, tot100%]

Type[0.000107949 % ±, 0.00250901 % ±,
0.000209888 % ±, 0.0000680279 % ±, 0.00105494 % ±, 0.0502207 % ±]




0.02
0.01
50
100
150
200
-0.01
-0.02
-0.03

APPENDIX C

TARGET FACTOR ANALYSIS IN MATHEMATICA®

```
<< LinearAlgebra`MatrixManipulation`
<< Graphics`MultipleListPlot`
<< Graphics`Colors`
<< Statistics`
EPS817PBS =
    Import["/Users/luchsing/Documents/ Ph.D./All Data&Research/met + NO
        kinetics/ met NO kinetics organization/  with Gepasi kinetic fits/target
        testing all kinetic data/PBS8−17 14x234 input T.csv"];
Dimensions[EPS817PBS];
SPE817PBS = Transpose[EPS817PBS];
g = SPE817PBS.EPS817PBS; Dimensions[g];

SingularValues[EPS817PBS];
{U, s, V'} = %;
Dimensions[V']
Dimensions[U]
Dimensions[s]
U† = Transpose[U];
Dimensions[U†]
S = DiagonalMatrix[s];
Dat = U†.S.V';
Dimensions[Dat]
Export["/Users/luchsing/Documents/Mathematica files/D=U.S.V.txt", Dat,  "Table"];
```

{15, 15}

{15, 234}

{15}

{234, 15}

{234, 15}

```
R = U†.S;
Rt = Transpose[R];
Rr = {Rt[[1]], Rt[[2]], Rt[[3]]};
R̄ = Transpose[Rr];
rr2 = MatrixForm[R̄ ];
Dimensions[R̄ ]
Dimensions[rr2]
Export["/Users/luchsing/Documents/Mathematica files/transR=U.S.txt", R̄ , "Table"];
Export["/Users/luchsing/Documents/Mathematica files/R=U.S.txt", R, "Table"];
metIINO1 = Import["/Users/luchsing/Documents/Mathematica files/metIINO234x1.csv",
      "List"];
metIINO = metIINO1 − .000;
IINO = Import["/Users/luchsing/Documents/Mathematica files/IINO234x1.csv",
      "List"];
IIINO = Import["/Users/luchsing/Documents/Mathematica files/IIINO234x1.csv",
      "List"];
R̄ † = Transpose[R̄ ];
Λ = S^2 ;
(*MultipleListPlot[metIINO];*)
Λ1 = Part[s^2, 1];
Λ2 = Part[s^2, 2];
Λ3 = Part[s^2, 3];
Λ̄ = DiagonalMatrix[{Λ1, Λ2, Λ3}]
Λ⁻ = Inverse[Λ̄]
Dimensions[R̄ †]
Dimensions[Λ⁻]
```

```
{234, 3}

{3, 234}

{3, 3}
```

```
r1 = Table[−j, {j, 0.1 , 8 , 0.1}];  (*Table ramps met percent*)
(*Table Dimension=(Red−Blue+Green)÷Green.Blue is 1 st #,Red is the last #,
  Green is the step−size.*)
dimenNumber817PBS = Dimensions[r1];

Export["/Users/luchsing/Documents/Mathematica files/dimenNumber817PBS.txt",
    dimenNumber817PBS, "Table"];

nnn = Get["/Users/luchsing/Documents/Mathematica files/dimenNumber817PBS.txt"];
(*need Dimension number. Export then Get is the way it worked.*)
```

```
(*middlenumber = nnn− 2*)
r2 = Table[−1, {j, nnn}]; (*Table norms IINO*)

Dimensions[r2];

r3 = Table[5, {j, nnn}]; (*Table norms/scales time series data to cannonical met,IINO*)
Dimensions[r3];
r123 = Table[{r1, r2, r3}]; (*0 th step. making test vector*)
Dimensions[r123]

met = Import["/Users/luchsing/Documents/Mathematica files/met234x1.csv", "List"];

IINO = Import["/Users/luchsing/Documents/Mathematica files/IINO234x1.csv",
       "List"];

Datcol1 = SPE817PBS[[1]]; (*1 st spectrum from time series data*)
Dimensions[Datcol1]
metIINOSPE817PBS = {met, IINO, Datcol1}; (*1 st step. making test vector*)
Dimensions[metIINOSPE817PBS]
metIINOEPS817PBS = Transpose[metIINOSPE817PBS];
(* 234 x3 2 nd step. making test vector*)
Dimensions[metIINOEPS817PBS]
metIINOIIINO1 = metIINOEPS817PBS.r123;
(* 234 x3.r123 3 rd step. making test vector*)
Dimensions[metIINOIIINO1]
metIINOIIINO = Transpose[metIINOIIINO1];
(* 234 x1 4 th step. making test vector*)

IIINO2 = Import["/Users/luchsing/Documents/Mathematica files/IIINOx.txt", "List"];

(*below is equation 3.127 from Factor Analysis in Chemistry, Edmund Malinowski,
  1991*)
metIINOSPE817PBS = {met, IINO};
x̂metIINO = R̄.Λ⁻.R̄†.metIINO;
x̂IIINO1st = R̄.Λ⁻.R̄†.metIINOIIINO[[1]];
(*Blue is predicted vector, Red is test vector*)
x̂2 = R̄.Λ⁻.R̄†.metIINOIIINO[[2]]; (*Blue is predicted vector, Red is test vector*)
x̂3 = R̄.Λ⁻.R̄†.metIINOIIINO[[3]];
x̂4 = R̄.Λ⁻.R̄†.metIINOIIINO[[4]];
x̂5 = R̄.Λ⁻.R̄†.metIINOIIINO[[5]];
x̂6 = R̄.Λ⁻.R̄†.metIINOIIINO[[6]];
x̂7 = R̄.Λ⁻.R̄†.metIINOIIINO[[7]];
x̂8 = R̄.Λ⁻.R̄†.metIINOIIINO[[8]];
x̂9 = R̄.Λ⁻.R̄†.metIINOIIINO[[9]];
```

$$\hat{x}_{10} = \overline{R}.\Lambda^{-}.\overline{R}^{\dagger}.\text{metIINOIIINO}[[10]];$$

$$\hat{x}_{11} = \overline{R}.\Lambda^{-}.\overline{R}^{\dagger}.\text{metIINOIIINO}[[11]];$$
$$\hat{x}_{12} = \overline{R}.\Lambda^{-}.\overline{R}^{\dagger}.\text{metIINOIIINO}[[12]];$$
$$\hat{x}_{13} = \overline{R}.\Lambda^{-}.\overline{R}^{\dagger}.\text{metIINOIIINO}[[13]];$$
$$\hat{x}_{14} = \overline{R}.\Lambda^{-}.\overline{R}^{\dagger}.\text{metIINOIIINO}[[14]];$$
$$\hat{x}_{15} = \overline{R}.\Lambda^{-}.\overline{R}^{\dagger}.\text{metIINOIIINO}[[15]];$$
$$\hat{x}_{16} = \overline{R}.\Lambda^{-}.\overline{R}^{\dagger}.\text{metIINOIIINO}[[16]];$$
$$\hat{x}_{17} = \overline{R}.\Lambda^{-}.\overline{R}^{\dagger}.\text{metIINOIIINO}[[17]];$$
$$\hat{x}_{18} = \overline{R}.\Lambda^{-}.\overline{R}^{\dagger}.\text{metIINOIIINO}[[18]];$$
$$\hat{x}_{19} = \overline{R}.\Lambda^{-}.\overline{R}^{\dagger}.\text{metIINOIIINO}[[19]];$$
$$\hat{x}_{20} = \overline{R}.\Lambda^{-}.\overline{R}^{\dagger}.\text{metIINOIIINO}[[20]];$$

$$\hat{x}_{21} = \overline{R}.\Lambda^{-}.\overline{R}^{\dagger}.\text{metIINOIIINO}[[21]];$$
$$\hat{x}_{22} = \overline{R}.\Lambda^{-}.\overline{R}^{\dagger}.\text{metIINOIIINO}[[22]];$$
$$\hat{x}_{23} = \overline{R}.\Lambda^{-}.\overline{R}^{\dagger}.\text{metIINOIIINO}[[23]];$$
$$\hat{x}_{24} = \overline{R}.\Lambda^{-}.\overline{R}^{\dagger}.\text{metIINOIIINO}[[24]];$$
$$\hat{x}_{25} = \overline{R}.\Lambda^{-}.\overline{R}^{\dagger}.\text{metIINOIIINO}[[25]];$$
$$\hat{x}_{26} = \overline{R}.\Lambda^{-}.\overline{R}^{\dagger}.\text{metIINOIIINO}[[26]];$$
$$\hat{x}_{27} = \overline{R}.\Lambda^{-}.\overline{R}^{\dagger}.\text{metIINOIIINO}[[27]];$$
$$\hat{x}_{28} = \overline{R}.\Lambda^{-}.\overline{R}^{\dagger}.\text{metIINOIIINO}[[28]];$$
$$\hat{x}_{29} = \overline{R}.\Lambda^{-}.\overline{R}^{\dagger}.\text{metIINOIIINO}[[29]];$$
$$\hat{x}_{30} = \overline{R}.\Lambda^{-}.\overline{R}^{\dagger}.\text{metIINOIIINO}[[30]];$$

$$\hat{x}_{31} = \overline{R}.\Lambda^{-}.\overline{R}^{\dagger}.\text{metIINOIIINO}[[31]];$$
$$\hat{x}_{32} = \overline{R}.\Lambda^{-}.\overline{R}^{\dagger}.\text{metIINOIIINO}[[32]];$$
$$\hat{x}_{33} = \overline{R}.\Lambda^{-}.\overline{R}^{\dagger}.\text{metIINOIIINO}[[33]];$$
$$\hat{x}_{34} = \overline{R}.\Lambda^{-}.\overline{R}^{\dagger}.\text{metIINOIIINO}[[34]];$$
$$\hat{x}_{35} = \overline{R}.\Lambda^{-}.\overline{R}^{\dagger}.\text{metIINOIIINO}[[35]];$$
$$\hat{x}_{36} = \overline{R}.\Lambda^{-}.\overline{R}^{\dagger}.\text{metIINOIIINO}[[36]];$$
$$\hat{x}_{37} = \overline{R}.\Lambda^{-}.\overline{R}^{\dagger}.\text{metIINOIIINO}[[37]];$$
$$\hat{x}_{38} = \overline{R}.\Lambda^{-}.\overline{R}^{\dagger}.\text{metIINOIIINO}[[38]];$$
$$\hat{x}_{39} = \overline{R}.\Lambda^{-}.\overline{R}^{\dagger}.\text{metIINOIIINO}[[39]];$$
$$\hat{x}_{40} = \overline{R}.\Lambda^{-}.\overline{R}^{\dagger}.\text{metIINOIIINO}[[40]];$$

$$\hat{x}_{41} = \overline{R}.\Lambda^{-}.\overline{R}^{\dagger}.\text{metIINOIIINO}[[41]];$$
$$\hat{x}_{42} = \overline{R}.\Lambda^{-}.\overline{R}^{\dagger}.\text{metIINOIIINO}[[42]];$$
$$\hat{x}_{43} = \overline{R}.\Lambda^{-}.\overline{R}^{\dagger}.\text{metIINOIIINO}[[43]];$$
$$\hat{x}_{44} = \overline{R}.\Lambda^{-}.\overline{R}^{\dagger}.\text{metIINOIIINO}[[44]];$$

$\hat{x}_{45} = \overline{R}.\Lambda^{-}.\overline{R}^{\dagger}$.metIINOIIINO[[45]];
$\hat{x}_{46} = \overline{R}.\Lambda^{-}.\overline{R}^{\dagger}$.metIINOIIINO[[46]];
$\hat{x}_{47} = \overline{R}.\Lambda^{-}.\overline{R}^{\dagger}$.metIINOIIINO[[47]];
$\hat{x}_{48} = \overline{R}.\Lambda^{-}.\overline{R}^{\dagger}$.metIINOIIINO[[48]];
$\hat{x}_{49} = \overline{R}.\Lambda^{-}.\overline{R}^{\dagger}$.metIINOIIINO[[49]];
$\hat{x}_{50} = \overline{R}.\Lambda^{-}.\overline{R}^{\dagger}$.metIINOIIINO[[50]];

$\hat{x}_{51} = \overline{R}.\Lambda^{-}.\overline{R}^{\dagger}$.metIINOIIINO[[51]];
$\hat{x}_{52} = \overline{R}.\Lambda^{-}.\overline{R}^{\dagger}$.metIINOIIINO[[52]];
$\hat{x}_{53} = \overline{R}.\Lambda^{-}.\overline{R}^{\dagger}$.metIINOIIINO[[53]];
$\hat{x}_{54} = \overline{R}.\Lambda^{-}.\overline{R}^{\dagger}$.metIINOIIINO[[54]];
$\hat{x}_{55} = \overline{R}.\Lambda^{-}.\overline{R}^{\dagger}$.metIINOIIINO[[55]];
$\hat{x}_{56} = \overline{R}.\Lambda^{-}.\overline{R}^{\dagger}$.metIINOIIINO[[56]];
$\hat{x}_{57} = \overline{R}.\Lambda^{-}.\overline{R}^{\dagger}$.metIINOIIINO[[57]];
$\hat{x}_{58} = \overline{R}.\Lambda^{-}.\overline{R}^{\dagger}$.metIINOIIINO[[58]];
$\hat{x}_{59} = \overline{R}.\Lambda^{-}.\overline{R}^{\dagger}$.metIINOIIINO[[59]];
$\hat{x}_{60} = \overline{R}.\Lambda^{-}.\overline{R}^{\dagger}$.metIINOIIINO[[60]];

$\hat{x}_{61} = \overline{R}.\Lambda^{-}.\overline{R}^{\dagger}$.metIINOIIINO[[61]];
$\hat{x}_{62} = \overline{R}.\Lambda^{-}.\overline{R}^{\dagger}$.metIINOIIINO[[62]];
$\hat{x}_{63} = \overline{R}.\Lambda^{-}.\overline{R}^{\dagger}$.metIINOIIINO[[63]];
$\hat{x}_{64} = \overline{R}.\Lambda^{-}.\overline{R}^{\dagger}$.metIINOIIINO[[64]];
$\hat{x}_{65} = \overline{R}.\Lambda^{-}.\overline{R}^{\dagger}$.metIINOIIINO[[65]];
$\hat{x}_{66} = \overline{R}.\Lambda^{-}.\overline{R}^{\dagger}$.metIINOIIINO[[66]];
$\hat{x}_{67} = \overline{R}.\Lambda^{-}.\overline{R}^{\dagger}$.metIINOIIINO[[67]];
$\hat{x}_{68} = \overline{R}.\Lambda^{-}.\overline{R}^{\dagger}$.metIINOIIINO[[68]];
$\hat{x}_{69} = \overline{R}.\Lambda^{-}.\overline{R}^{\dagger}$.metIINOIIINO[[69]];
$\hat{x}_{70} = \overline{R}.\Lambda^{-}.\overline{R}^{\dagger}$.metIINOIIINO[[70]];

$\hat{x}_{71} = \overline{R}.\Lambda^{-}.\overline{R}^{\dagger}$.metIINOIIINO[[71]];
$\hat{x}_{72} = \overline{R}.\Lambda^{-}.\overline{R}^{\dagger}$.metIINOIIINO[[72]];
$\hat{x}_{73} = \overline{R}.\Lambda^{-}.\overline{R}^{\dagger}$.metIINOIIINO[[73]];
$\hat{x}_{74} = \overline{R}.\Lambda^{-}.\overline{R}^{\dagger}$.metIINOIIINO[[74]];
$\hat{x}_{\text{IIINOlast}} = \overline{R}.\Lambda^{-}.\overline{R}^{\dagger}$.metIINOIIINO[[nnn]];
(*Blue is predicted vector, Red is test vector*)
predictedIIINOb = {$\hat{x}_{29}$, $\hat{x}_{30}$, $\hat{x}_{31}$, $\hat{x}_{32}$, $\hat{x}_{33}$, $\hat{x}_{34}$, $\hat{x}_{35}$};
Dimensions[predictedIIINOb];
predictedIIINO = Transpose[predictedIIINOb];
Dimensions[predictedIIINO]
Export[

```
"/Users/luchsing/Documents/ Ph.D./All Data&Research/met + NO kinetics/ met
    NO kinetics organization/  with Gepasi kinetic fits/target testing all kinetic data/
    all 8−17PBS_movie_vary r1&r3/r3=5 #30−35.csv", predictedIIINO,  "CSV"];
```

Null

{3, 80}

{234}

{3, 234}

{234, 3}

{234, 80}

{234, 7}

```
MultipleListPlot[x̂IIINO1st, metIINOIIINO[[1]],
    SymbolStyle → {RGBColor[0.2,  0.2,  0.8], RGBColor[1.,  .1,  .1],
        RGBColor[1.,  0.6,  0.2], RGBColor[0,  0.2,  1.], RGBColor[0.6,  0,  0.8],
        RGBColor[0.8,  0.2,  0.2], RGBColor[0.8,  0.2,  0.4], RGBColor[0.2,  0.2,  0.8],
        RGBColor[0,  0.8,  0.6], RGBColor[0.2,  1.,  0.8]}];
Δ1st = x̂IIINO1st − metIINOIIINO[[1]];
RMS1 st = Mean[Δ1st^2] "RMS 1"
"Blue is predicted vector, Red is test vector"
ListPlot[x̂IIINO1st − metIINOIIINO[[1]]]

MultipleListPlot[x̂5, metIINOIIINO[[5]],
    SymbolStyle → {RGBColor[0.2,  0.2,  0.8], RGBColor[1.,  .1,  .1],
        RGBColor[1.,  0.6,  0.2], RGBColor[0,  0.2,  1.], RGBColor[0.6,  0,  0.8],
        RGBColor[0.8,  0.2,  0.2], RGBColor[0.8,  0.2,  0.4], RGBColor[0.2,  0.2,  0.8],
        RGBColor[0,  0.8,  0.6], RGBColor[0.2,  1.,  0.8]}];
Δ5 = x̂5 − metIINOIIINO[[5]];
RMS1 st = Mean[Δ5^2] "RMS 5"
ListPlot[x̂5 − metIINOIIINO[[5]]]

MultipleListPlot[x̂10, metIINOIIINO[[10]],
    SymbolStyle → {RGBColor[0.2,  0.2,  0.8], RGBColor[1.,  .1,  .1],
        RGBColor[1.,  0.6,  0.2], RGBColor[0,  0.2,  1.], RGBColor[0.6,  0,  0.8],
        RGBColor[0.8,  0.2,  0.2], RGBColor[0.8,  0.2,  0.4], RGBColor[0.2,  0.2,  0.8],
        RGBColor[0,  0.8,  0.6], RGBColor[0.2,  1.,  0.8]}];
Δ10 = x̂10 − metIINOIIINO[[10]];
RMS1 st = Mean[Δ10^2] "RMS 10"
```

```
ListPlot[x̂10 − metIINOIIINO[[10]]]

MultipleListPlot[x̂15, metIINOIIINO[[15]],
    SymbolStyle → {RGBColor[0.2, 0.2, 0.8], RGBColor[1., .1, .1],
        RGBColor[1., 0.6, 0.2], RGBColor[0, 0.2, 1.], RGBColor[0.6, 0, 0.8],
        RGBColor[0.8, 0.2, 0.2], RGBColor[0.8, 0.2, 0.4], RGBColor[0.2, 0.2, 0.8],
        RGBColor[0, 0.8, 0.6], RGBColor[0.2, 1., 0.8]}];
Δ15 = x̂15 − metIINOIIINO[[15]];
RMS1 st = Mean[Δ15^2] "RMS 15"
ListPlot[x̂15 − metIINOIIINO[[15]]]

MultipleListPlot[x̂20, metIINOIIINO[[20]],
    SymbolStyle → {RGBColor[0.2, 0.2, 0.8], RGBColor[1., .1, .1],
        RGBColor[1., 0.6, 0.2], RGBColor[0, 0.2, 1.], RGBColor[0.6, 0, 0.8],
        RGBColor[0.8, 0.2, 0.2], RGBColor[0.8, 0.2, 0.4], RGBColor[0.2, 0.2, 0.8],
        RGBColor[0, 0.8, 0.6], RGBColor[0.2, 1., 0.8]}];
Δ20 = x̂20 − metIINOIIINO[[20]];
RMS1 st = Mean[Δ20^2] "RMS 20"
ListPlot[x̂20 − metIINOIIINO[[20]]]

MultipleListPlot[x̂22, metIINOIIINO[[22]],
    SymbolStyle → {RGBColor[0.2, 0.2, 0.8], RGBColor[1., .1, .1],
        RGBColor[1., 0.6, 0.2], RGBColor[0, 0.2, 1.], RGBColor[0.6, 0, 0.8],
        RGBColor[0.8, 0.2, 0.2], RGBColor[0.8, 0.2, 0.4], RGBColor[0.2, 0.2, 0.8],
        RGBColor[0, 0.8, 0.6], RGBColor[0.2, 1., 0.8]}];
Δ22 = x̂22 − metIINOIIINO[[22]];
RMS1 st = Mean[Δ22^2] "RMS 22"
ListPlot[x̂22 − metIINOIIINO[[22]]]

MultipleListPlot[x̂24, metIINOIIINO[[24]],
    SymbolStyle → {RGBColor[0.2, 0.2, 0.8], RGBColor[1., .1, .1],
        RGBColor[1., 0.6, 0.2], RGBColor[0, 0.2, 1.], RGBColor[0.6, 0, 0.8],
        RGBColor[0.8, 0.2, 0.2], RGBColor[0.8, 0.2, 0.4], RGBColor[0.2, 0.2, 0.8],
        RGBColor[0, 0.8, 0.6], RGBColor[0.2, 1., 0.8]}];
Δ24 = x̂24 − metIINOIIINO[[24]];
RMS1 st = Mean[Δ24^2] "RMS 24"
ListPlot[x̂24 − metIINOIIINO[[24]]]

MultipleListPlot[x̂25, metIINOIIINO[[25]],
    SymbolStyle → {RGBColor[0.2, 0.2, 0.8], RGBColor[1., .1, .1],
        RGBColor[1., 0.6, 0.2], RGBColor[0, 0.2, 1.], RGBColor[0.6, 0, 0.8],
        RGBColor[0.8, 0.2, 0.2], RGBColor[0.8, 0.2, 0.4], RGBColor[0.2, 0.2, 0.8],
```

```
        RGBColor[0, 0.8, 0.6], RGBColor[0.2, 1., 0.8]}];
Δ25 = x̂25 − metIINOIIINO[[25]];
RMS1 st = Mean[Δ25^2] "RMS 25"
ListPlot[x̂25 − metIINOIIINO[[25]]]

MultipleListPlot[x̂27, metIINOIIINO[[27]],
    SymbolStyle → {RGBColor[0.2, 0.2, 0.8], RGBColor[1., .1, .1],
        RGBColor[1., 0.6, 0.2], RGBColor[0, 0.2, 1.], RGBColor[0.6, 0, 0.8],
        RGBColor[0.8, 0.2, 0.2], RGBColor[0.8, 0.2, 0.4], RGBColor[0.2, 0.2, 0.8],
        RGBColor[0, 0.8, 0.6], RGBColor[0.2, 1., 0.8]}];
Δ27 = x̂27 − metIINOIIINO[[27]];
RMS1 st = Mean[Δ27^2] "RMS 27"
ListPlot[x̂27 − metIINOIIINO[[27]]]

MultipleListPlot[x̂28, metIINOIIINO[[28]],
    SymbolStyle → {RGBColor[0.2, 0.2, 0.8], RGBColor[1., .1, .1],
        RGBColor[1., 0.6, 0.2], RGBColor[0, 0.2, 1.], RGBColor[0.6, 0, 0.8],
        RGBColor[0.8, 0.2, 0.2], RGBColor[0.8, 0.2, 0.4], RGBColor[0.2, 0.2, 0.8],
        RGBColor[0, 0.8, 0.6], RGBColor[0.2, 1., 0.8]}];
Δ28 = x̂28 − metIINOIIINO[[28]];
RMS1 st = Mean[Δ28^2] "RMS 28"
ListPlot[x̂28 − metIINOIIINO[[28]]]

MultipleListPlot[x̂29, metIINOIIINO[[29]],
    SymbolStyle → {RGBColor[0.2, 0.2, 0.8], RGBColor[1., .1, .1],
        RGBColor[1., 0.6, 0.2], RGBColor[0, 0.2, 1.], RGBColor[0.6, 0, 0.8],
        RGBColor[0.8, 0.2, 0.2], RGBColor[0.8, 0.2, 0.4], RGBColor[0.2, 0.2, 0.8],
        RGBColor[0, 0.8, 0.6], RGBColor[0.2, 1., 0.8]}];
Δ29 = x̂29 − metIINOIIINO[[29]];
RMS1 st = Mean[Δ29^2] "RMS 29"
ListPlot[x̂29 − metIINOIIINO[[29]]]

MultipleListPlot[x̂30, metIINOIIINO[[30]],
    SymbolStyle → {RGBColor[0.2, 0.2, 0.8], RGBColor[1., .1, .1],
        RGBColor[1., 0.6, 0.2], RGBColor[0, 0.2, 1.], RGBColor[0.6, 0, 0.8],
        RGBColor[0.8, 0.2, 0.2], RGBColor[0.8, 0.2, 0.4], RGBColor[0.2, 0.2, 0.8],
        RGBColor[0, 0.8, 0.6], RGBColor[0.2, 1., 0.8]}];
Δ30 = x̂30 − metIINOIIINO[[30]];
RMS1 st = Mean[Δ30^2] "RMS 30"
"Blue is predicted vector, Red is test vector"
ListPlot[x̂30 − metIINOIIINO[[30]]]
```

```
MultipleListPlot[x̂31, metIINOIIINO[[31]],
    SymbolStyle → {RGBColor[0.2, 0.2, 0.8], RGBColor[1., .1, .1],
        RGBColor[1., 0.6, 0.2], RGBColor[0, 0.2, 1.], RGBColor[0.6, 0, 0.8],
        RGBColor[0.8, 0.2, 0.2], RGBColor[0.8, 0.2, 0.4], RGBColor[0.2, 0.2, 0.8],
        RGBColor[0, 0.8, 0.6], RGBColor[0.2, 1., 0.8]}];
Δ31 = x̂31 − metIINOIIINO[[31]];
RMS1 st = Mean[Δ31^2] "RMS 31"
ListPlot[x̂31 − metIINOIIINO[[31]]]

MultipleListPlot[x̂32, metIINOIIINO[[32]],
    SymbolStyle → {RGBColor[0.2, 0.2, 0.8], RGBColor[1., .1, .1],
        RGBColor[1., 0.6, 0.2], RGBColor[0, 0.2, 1.], RGBColor[0.6, 0, 0.8],
        RGBColor[0.8, 0.2, 0.2], RGBColor[0.8, 0.2, 0.4], RGBColor[0.2, 0.2, 0.8],
        RGBColor[0, 0.8, 0.6], RGBColor[0.2, 1., 0.8]}];
Δ32 = x̂32 − metIINOIIINO[[32]];
RMS1 st = Mean[Δ32^2] "RMS 32"
ListPlot[x̂32 − metIINOIIINO[[32]]]

MultipleListPlot[x̂33, metIINOIIINO[[33]],
    SymbolStyle → {RGBColor[0.2, 0.2, 0.8], RGBColor[1., .1, .1],
        RGBColor[1., 0.6, 0.2], RGBColor[0, 0.2, 1.], RGBColor[0.6, 0, 0.8],
        RGBColor[0.8, 0.2, 0.2], RGBColor[0.8, 0.2, 0.4], RGBColor[0.2, 0.2, 0.8],
        RGBColor[0, 0.8, 0.6], RGBColor[0.2, 1., 0.8]}];
Δ33 = x̂33 − metIINOIIINO[[33]];
RMS1 st = Mean[Δ33^2] "RMS 33"
ListPlot[x̂33 − metIINOIIINO[[33]]]

MultipleListPlot[x̂34, metIINOIIINO[[34]],
    SymbolStyle → {RGBColor[0.2, 0.2, 0.8], RGBColor[1., .1, .1],
        RGBColor[1., 0.6, 0.2], RGBColor[0, 0.2, 1.], RGBColor[0.6, 0, 0.8],
        RGBColor[0.8, 0.2, 0.2], RGBColor[0.8, 0.2, 0.4], RGBColor[0.2, 0.2, 0.8],
        RGBColor[0, 0.8, 0.6], RGBColor[0.2, 1., 0.8]}];
Δ34 = x̂34 − metIINOIIINO[[34]];
RMS1 st = Mean[Δ34^2] "RMS 34"
ListPlot[x̂34 − metIINOIIINO[[34]]]

MultipleListPlot[x̂36, metIINOIIINO[[36]],
    SymbolStyle → {RGBColor[0.2, 0.2, 0.8], RGBColor[1., .1, .1],
        RGBColor[1., 0.6, 0.2], RGBColor[0, 0.2, 1.], RGBColor[0.6, 0, 0.8],
        RGBColor[0.8, 0.2, 0.2], RGBColor[0.8, 0.2, 0.4], RGBColor[0.2, 0.2, 0.8],
        RGBColor[0, 0.8, 0.6], RGBColor[0.2, 1., 0.8]}];
```

```
Δ36 = x̂36 − metIINOIIINO[[36]];
RMS1 st = Mean[Δ36^2] "RMS 36"
ListPlot[x̂36 − metIINOIIINO[[36]]]

MultipleListPlot[x̂37, metIINOIIINO[[37]],
    SymbolStyle → {RGBColor[0.2, 0.2, 0.8], RGBColor[1., .1, .1],
        RGBColor[1., 0.6, 0.2], RGBColor[0, 0.2, 1.], RGBColor[0.6, 0, 0.8],
        RGBColor[0.8, 0.2, 0.2], RGBColor[0.8, 0.2, 0.4], RGBColor[0.2, 0.2, 0.8],
        RGBColor[0, 0.8, 0.6], RGBColor[0.2, 1., 0.8]}];
Δ37 = x̂37 − metIINOIIINO[[37]];
RMS1 st = Mean[Δ37^2] "RMS 37"
ListPlot[x̂37 − metIINOIIINO[[37]]]

MultipleListPlot[x̂39, metIINOIIINO[[39]],
    SymbolStyle → {RGBColor[0.2, 0.2, 0.8], RGBColor[1., .1, .1],
        RGBColor[1., 0.6, 0.2], RGBColor[0, 0.2, 1.], RGBColor[0.6, 0, 0.8],
        RGBColor[0.8, 0.2, 0.2], RGBColor[0.8, 0.2, 0.4], RGBColor[0.2, 0.2, 0.8],
        RGBColor[0, 0.8, 0.6], RGBColor[0.2, 1., 0.8]}];
Δ39 = x̂39 − metIINOIIINO[[39]];
RMS1 st = Mean[Δ39^2] "RMS 39"
ListPlot[x̂39 − metIINOIIINO[[39]]]

MultipleListPlot[x̂40, metIINOIIINO[[40]],
    SymbolStyle → {RGBColor[0.2, 0.2, 0.8], RGBColor[1., .1, .1],
        RGBColor[1., 0.6, 0.2], RGBColor[0, 0.2, 1.], RGBColor[0.6, 0, 0.8],
        RGBColor[0.8, 0.2, 0.2], RGBColor[0.8, 0.2, 0.4], RGBColor[0.2, 0.2, 0.8],
        RGBColor[0, 0.8, 0.6], RGBColor[0.2, 1., 0.8]}];
Δ40 = x̂40 − metIINOIIINO[[40]];
RMS1 st = Mean[Δ40^2] "RMS 40"
ListPlot[x̂40 − metIINOIIINO[[40]]]

MultipleListPlot[x̂41, metIINOIIINO[[41]],
    SymbolStyle → {RGBColor[0.2, 0.2, 0.8], RGBColor[1., .1, .1],
        RGBColor[1., 0.6, 0.2], RGBColor[0, 0.2, 1.], RGBColor[0.6, 0, 0.8],
        RGBColor[0.8, 0.2, 0.2], RGBColor[0.8, 0.2, 0.4], RGBColor[0.2, 0.2, 0.8],
        RGBColor[0, 0.8, 0.6], RGBColor[0.2, 1., 0.8]}];
Δ41 = x̂41 − metIINOIIINO[[41]];
RMS1 st = Mean[Δ41^2] "RMS 41"
ListPlot[x̂41 − metIINOIIINO[[41]]]

MultipleListPlot[x̂43, metIINOIIINO[[43]],
```

```
    SymbolStyle → {RGBColor[0.2, 0.2, 0.8], RGBColor[1., .1, .1],
        RGBColor[1., 0.6, 0.2], RGBColor[0, 0.2, 1.], RGBColor[0.6, 0, 0.8],
        RGBColor[0.8, 0.2, 0.2], RGBColor[0.8, 0.2, 0.4], RGBColor[0.2, 0.2, 0.8],
        RGBColor[0, 0.8, 0.6], RGBColor[0.2, 1., 0.8]}];
Δ43 = x̂43 − metIINOIIINO[[43]];
RMS1 st = Mean[Δ43^2] "RMS 43"
ListPlot[x̂43 − metIINOIIINO[[43]]]

MultipleListPlot[x̂45, metIINOIIINO[[45]],
    SymbolStyle → {RGBColor[0.2, 0.2, 0.8], RGBColor[1., .1, .1],
        RGBColor[1., 0.6, 0.2], RGBColor[0, 0.2, 1.], RGBColor[0.6, 0, 0.8],
        RGBColor[0.8, 0.2, 0.2], RGBColor[0.8, 0.2, 0.4], RGBColor[0.2, 0.2, 0.8],
        RGBColor[0, 0.8, 0.6], RGBColor[0.2, 1., 0.8]}];
Δ35 = x̂45 − metIINOIIINO[[45]];
RMS1 st = Mean[Δ45^2] "RMS 45"
ListPlot[x̂45 − metIINOIIINO[[45]]]

MultipleListPlot[x̂55, metIINOIIINO[[55]],
    SymbolStyle → {RGBColor[0.2, 0.2, 0.8], RGBColor[1., .1, .1],
        RGBColor[1., 0.6, 0.2], RGBColor[0, 0.2, 1.], RGBColor[0.6, 0, 0.8],
        RGBColor[0.8, 0.2, 0.2], RGBColor[0.8, 0.2, 0.4], RGBColor[0.2, 0.2, 0.8],
        RGBColor[0, 0.8, 0.6], RGBColor[0.2, 1., 0.8]}];
Δ55 = x̂55 − metIINOIIINO[[55]];
RMS1 st = Mean[Δ55^2] "RMS 55"
ListPlot[x̂55 − metIINOIIINO[[55]]]

MultipleListPlot[x̂65, metIINOIIINO[[65]],
    SymbolStyle → {RGBColor[0.2, 0.2, 0.8], RGBColor[1., .1, .1],
        RGBColor[1., 0.6, 0.2], RGBColor[0, 0.2, 1.], RGBColor[0.6, 0, 0.8],
        RGBColor[0.8, 0.2, 0.2], RGBColor[0.8, 0.2, 0.4], RGBColor[0.2, 0.2, 0.8],
        RGBColor[0, 0.8, 0.6], RGBColor[0.2, 1., 0.8]}];
Δ65 = x̂65 − metIINOIIINO[[65]];
RMS1 st = Mean[Δ65^2] "RMS 65"
ListPlot[x̂65 − metIINOIIINO[[65]]]

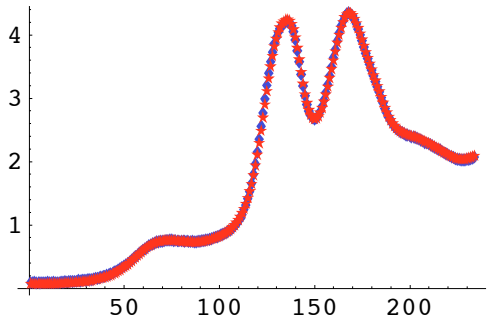
MultipleListPlot[x̂IIINOlast, metIINOIIINO[[nnn]],
    SymbolStyle → {RGBColor[0.2, 0.2, 0.8], RGBColor[1, 0.1, .1],
        RGBColor[1., 0.6, 0.2], RGBColor[0, 0.2, 1.], RGBColor[0.6, 0, 0.8],
        RGBColor[0.8, 0.2, 0.2], RGBColor[0.8, 0.2, 0.4], RGBColor[0.2, 0.2, 0.8],
        RGBColor[0, 0.8, 0.6], RGBColor[0.2, 1., 0.8]}];
Δlast = x̂IIINOlast − metIINOIIINO[[nnn]];
```

$RMS_{last} = Mean\left[\Delta_{last}^{2}\right]$ "RMS last nnn"

"nnn"

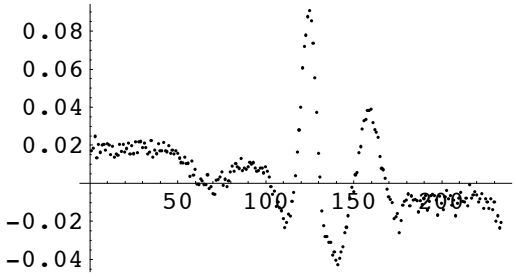
$ListPlot[\hat{x}_{IIINOlast} - metIINOIIINO[[nnn]]]$

Null

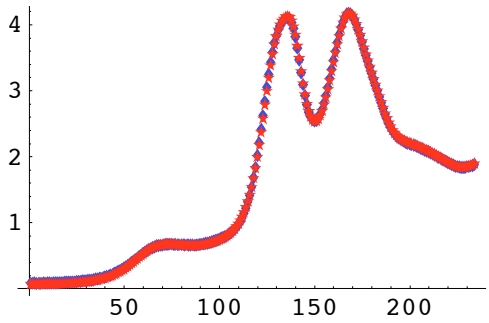


0.000466309 RMS 1

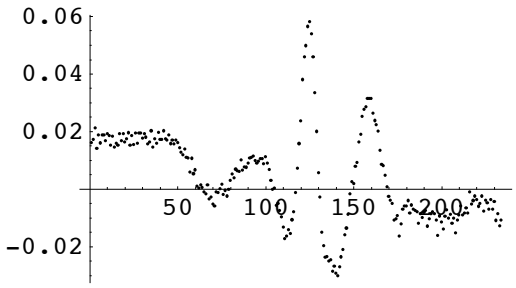
Blue is predicted vector, Red is test vector



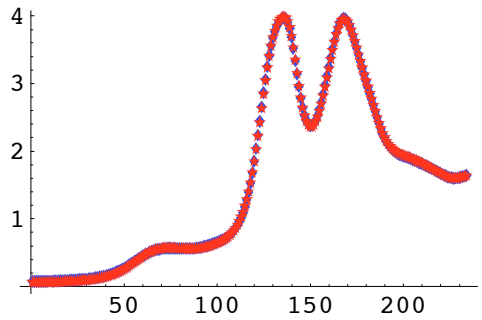
- Graphics -



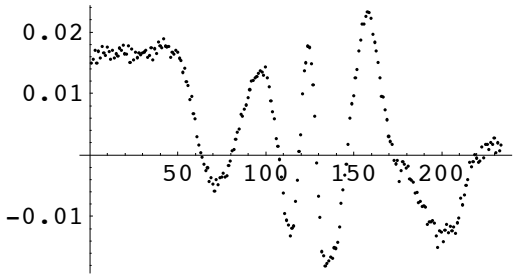
0.000264433 RMS 5



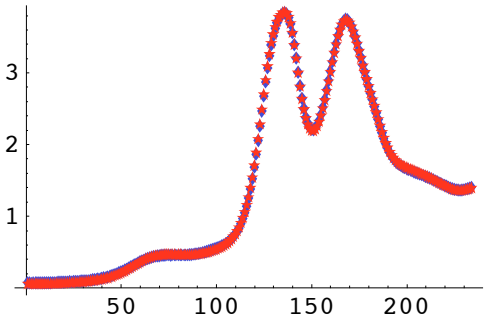
- Graphics -



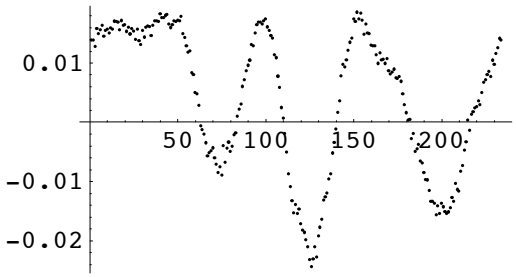
0.000140139 RMS 10



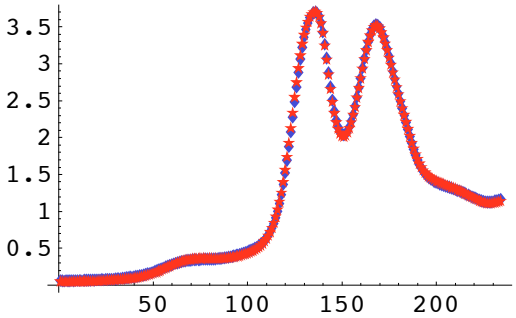
- Graphics -



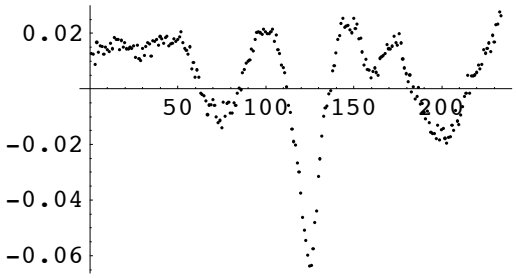
0.000158124 RMS 15



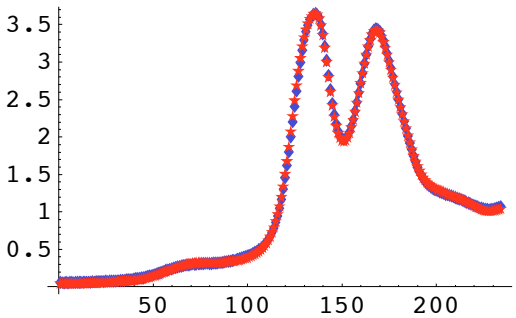
- Graphics -



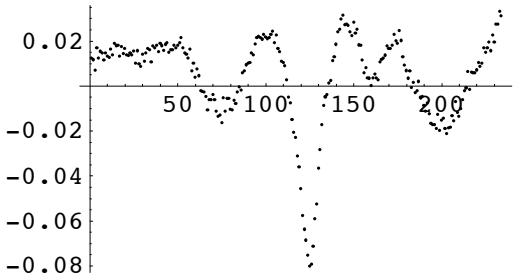
0.000318387 RMS 20



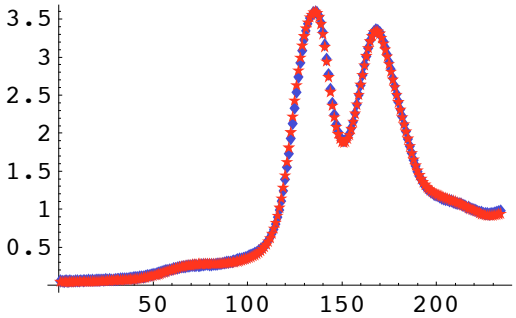
- Graphics -



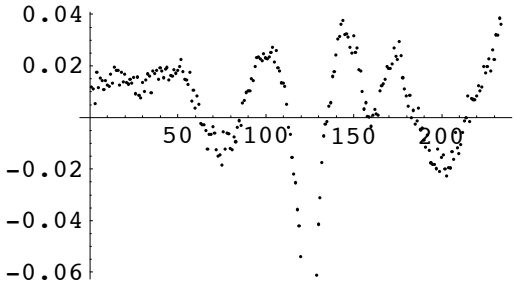
0.00042233 RMS 22



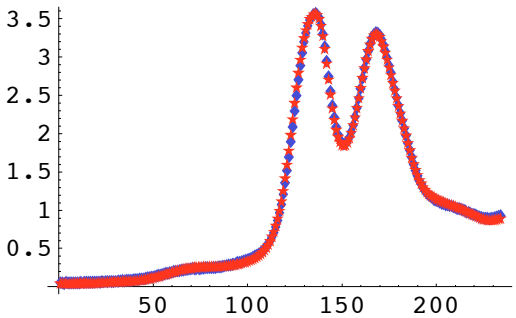
- Graphics -



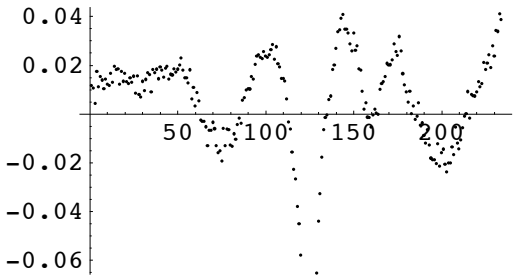
0.000549037 RMS 24



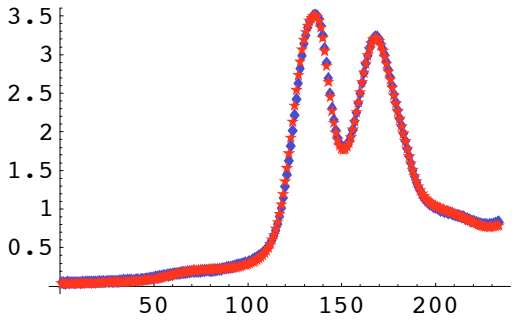
- Graphics -



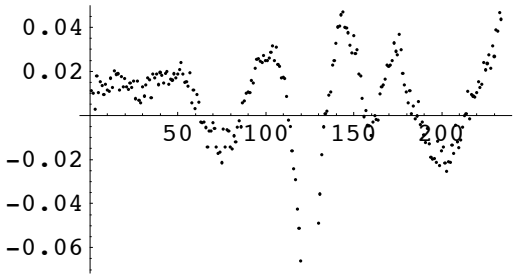
0.000620928 RMS 25



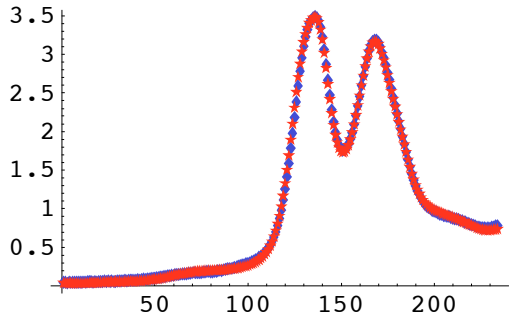
- Graphics -



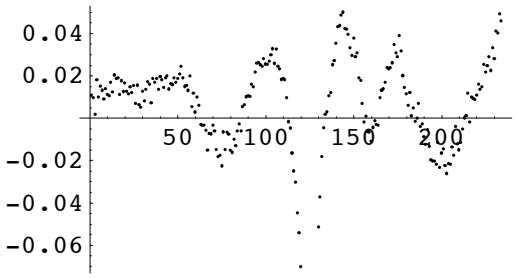
0.000781782 RMS 27



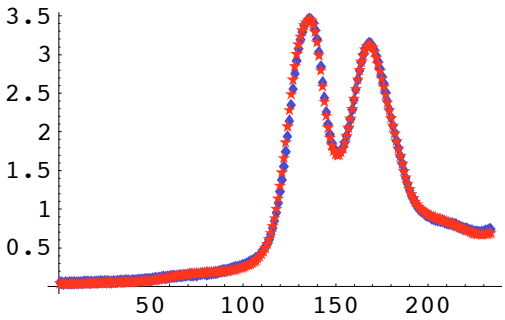
- Graphics -



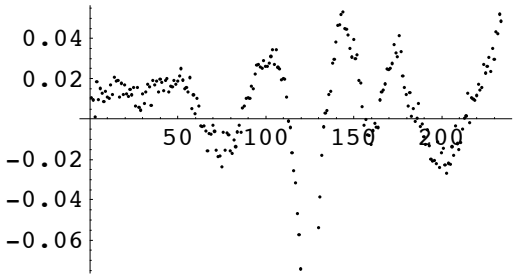
0.000870746 RMS 28



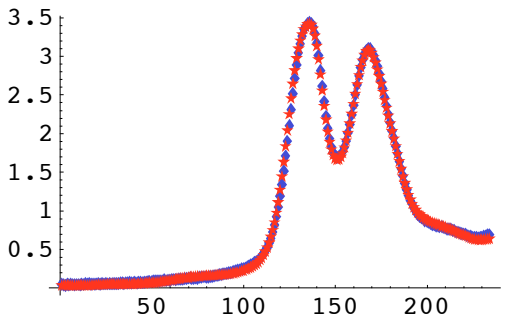
- Graphics -



0.000965401 RMS 29

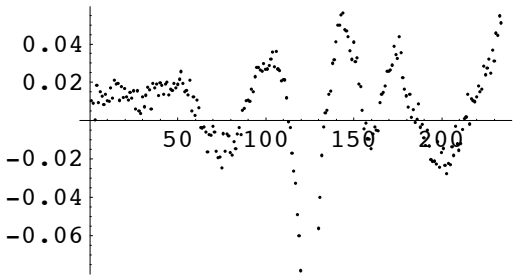


- Graphics -

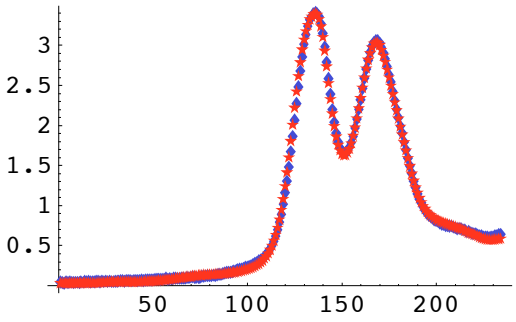


0.00106575 RMS 30

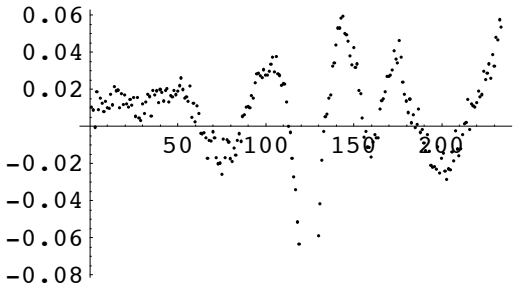
Blue is predicted vector, Red is test vector



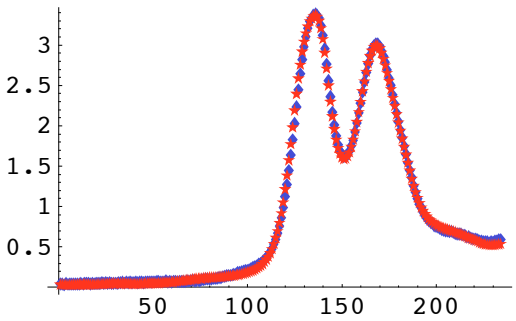
- Graphics -



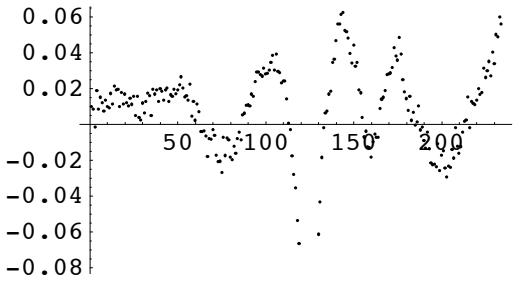
0.00117178 RMS 31



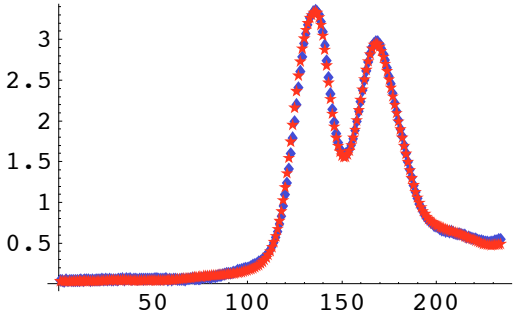
- Graphics -



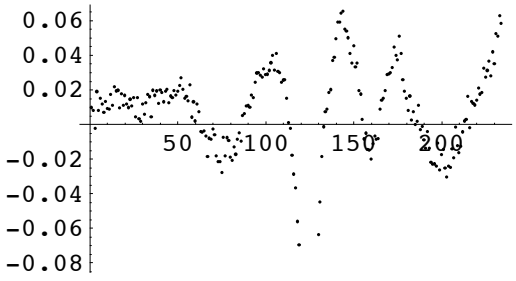
0.00128351 RMS 32



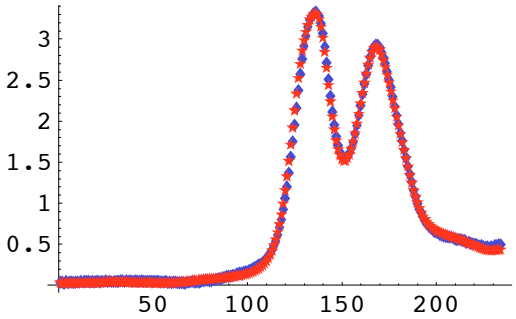
- Graphics -



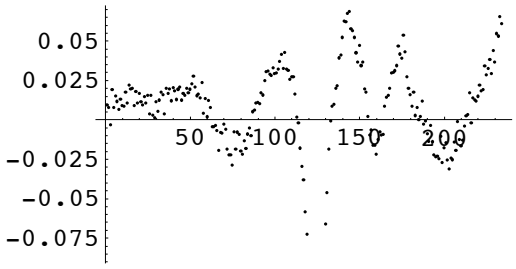
0.00140093 RMS 33



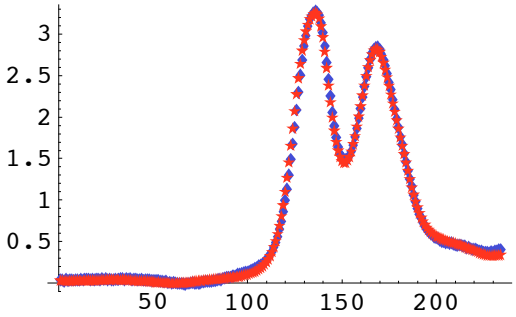
- Graphics -



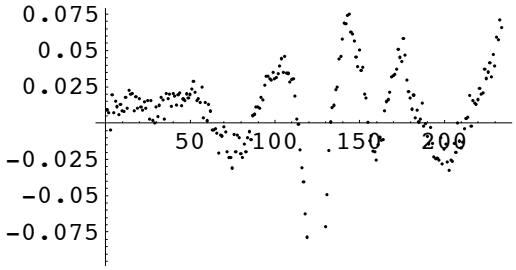
0.00152404 RMS 34



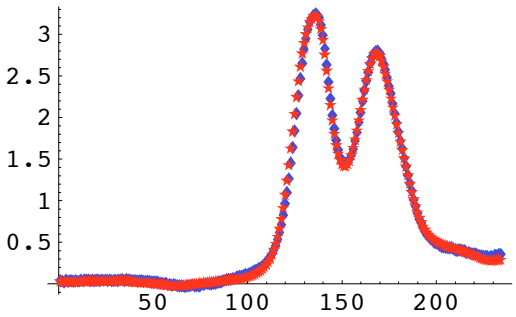
- Graphics -



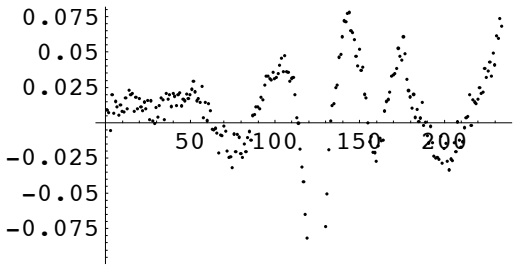
0.00178734 RMS 36



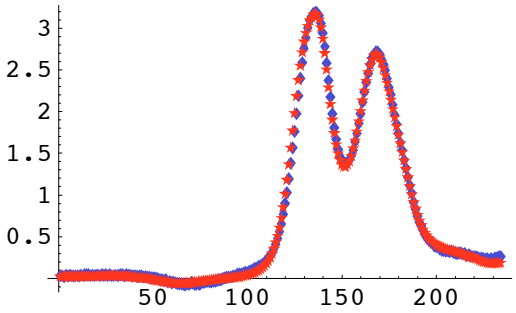
- Graphics -



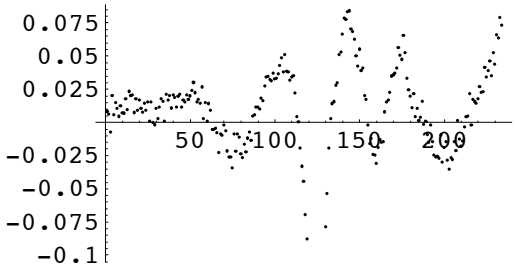
0.00192752 RMS 37



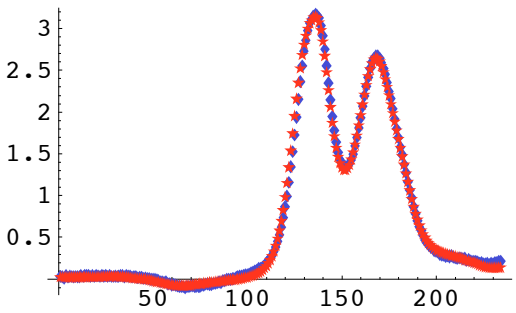
- Graphics -



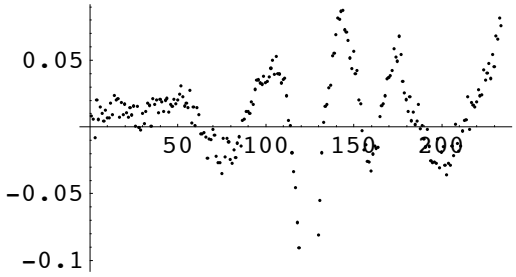
0.00222496 RMS 39



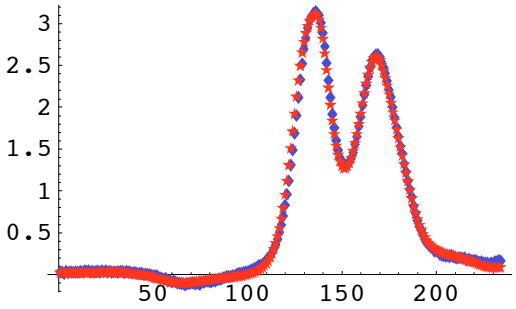
- Graphics -



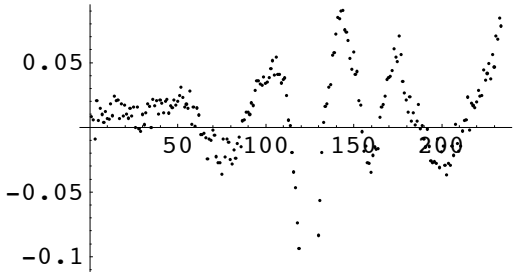
0.00238222 RMS 40



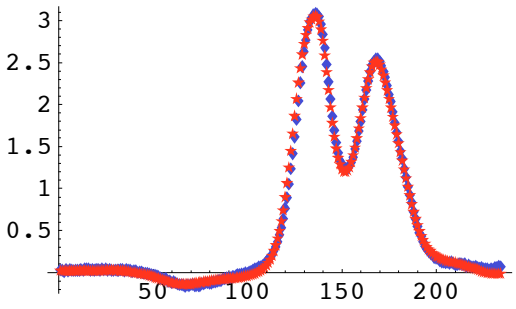
- Graphics -



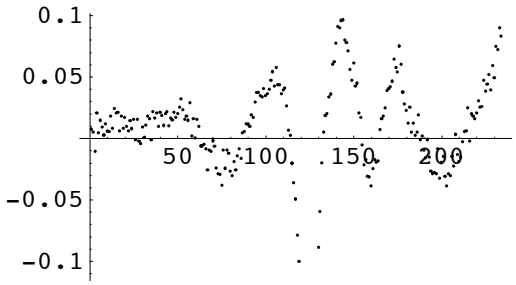
0.00254517 RMS 41



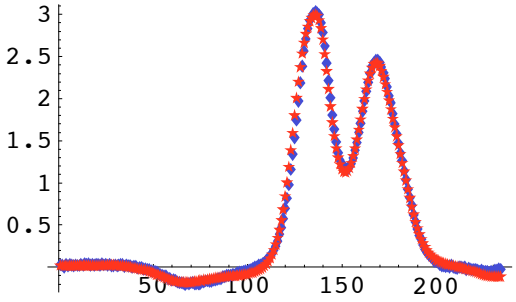
- Graphics -



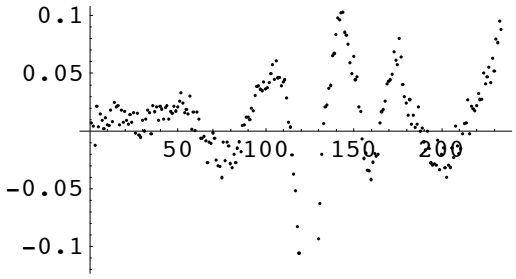
0.00288814 RMS 43



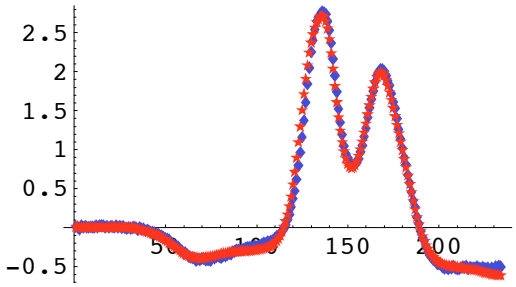
- Graphics -



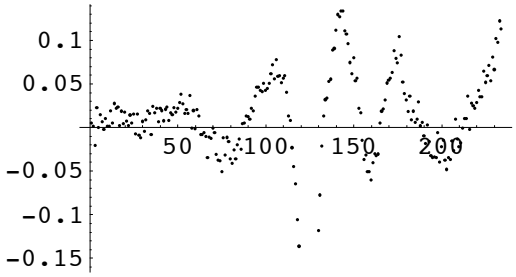
RMS 45 Mean[$\triangle 45^2$]



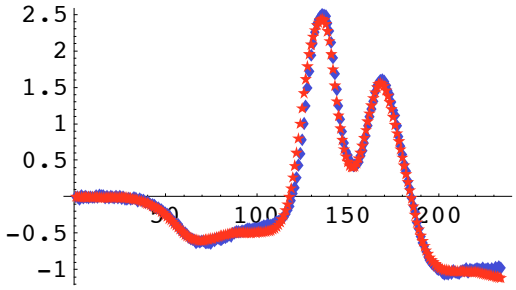
- Graphics -



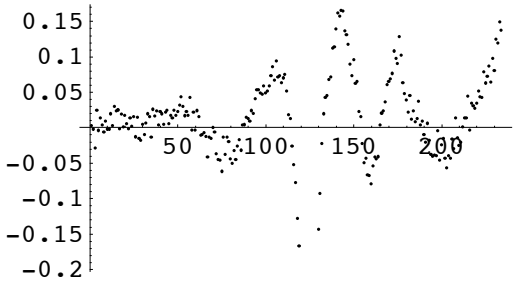
0.00542402 RMS 55



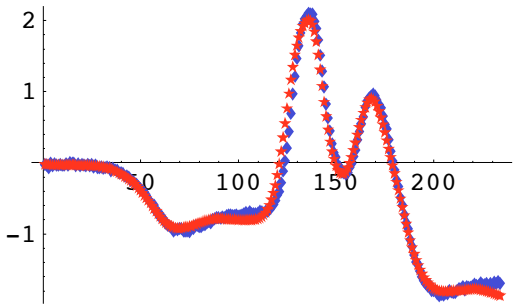
- Graphics -



0.00816328 RMS 65

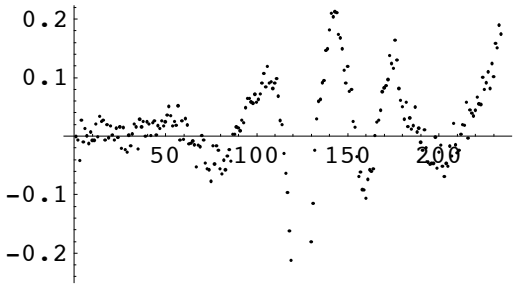


- Graphics -



0.0133393 RMS last nnn

nnn



- Graphics -